JAERI-Research
97-092

DSCu/SS JOINING TECHNIQUES DEVELOPMENT AND TESTING

January 1998

Satoshi SATO, Toshihisa HATANO, Kazuyuki FURUYA,
Toshimasa KURODA, Mikio ENOEDA and Hideyuki TAKATSU

日本原子力研究所
Japan Atomic Energy Research Institute

本レポートは，日本原子力研究所が不定期に公刊している研究報告書です。
入手の問合わせは，日本原子力研究所研究情報部研究情報課（〒319-1195　茨城県那珂郡東海村）あて，お申し越しください。なお，このほかに財団法人原子力弘済会資料センター（〒319-1195　茨城県那珂郡東海村日本原子力研究所内）で複写による実費頒布をおこなっております。

This report is issued irregularly.
Inquiries about availability of the reports should be addressed to Research Information Division, Department of Intellectual Resources, Japan Atomic Energy Research Institute, Tokai-mura, Naka-gun, Ibaraki-ken, 319-1195, Japan.

編集兼発行　日本原子力研究所
印　　刷　いばらき印刷㈱

JAERI-Research 97-092

DSCu/SS Joining Techniques Development and Testing

Satoshi SATO, Toshihisa HATANO, Kazuyuki FURUYA,
Toshimasa KURODA, Mikio ENOEDA and Hideyuki TAKATSU

Department of Fusion Engineering Research
Naka Fusion Research Establishment
Japan Atomic Energy Research Institute
Naka-machi, Naka-gun, Ibaraki-ken

(Received December 2, 1997)

Joining techniques of alumina dispersion strengthened copper alloy (DSCu) and type 316L stainless steel (SS) has been investigated aiming at applying to the fabrication of the ITER first wall/blanket. As the joining method, Hot Isostatic Pressing (HIP) of solid plates and/or blocks has been pursued. By a screening test including HIP temperatures of 980-1050 ℃, it was concluded that the HIP temperature of 1050 ℃ would be optimum for the simultaneous HIPping of DSCu/DSCu, DSCu/SS and SS/SS.

With DSCu/SS joint specimens HIPped at 1050 ℃, tensile, impact, fatigue, crack propagation, and fracture toughness tests were performed as well as mechanical test of structural model with one SS circular tube embedded. Typically, the properties of the joints were almost the same as those of DSCu or SS base metal with the same heat treatment of the HIP process, thus good joints were obtained, though parts of properties were decreased at elevated test temperature. Typical results of the mechanical test of structural mode indicated that a crack initiated at the inner surface of the SS tube under cyclic operation, and the lifetime of the first wall structure could be evaluated by existing SS fatigue data.

Two HIPped first wall panel mock-ups were successfully fabricated with built-in coolant tubes: one was 300 mm long and the other 800 mm long. The former was thermo-mechanically tested with high heat fluxes corresponding to the ITER operation conditions. The mock-up showed

This work is conducted as an ITER Technology R&D and this report corresponds to the 1995 ITER R&D Task (Task No. G16TT65 95-12-15 FJ, ID No. T212, Title : Cu/SS and Cu/Be Joining Techniques Development and Testing).

good heat removal performance during the high heat flux tests. In addition, there were no cracks and delaminations found at HIPped interfaces by microscopic observation after all tests.

Ultrasonic testing have been tried as a non-destructive examination method, and detectable defect size at SS/SS, DSCu/DSCu and DSCu/SS joint interfaces were estimated.

Keywords : ITER, Blanket, First Wall, HIP, Joint, DSCu, High Heat Flux Test, Ultrasonic Testing

DSCu/SUS接合技術の開発及び機械・高熱負荷試験

日本原子力研究所那珂研究所核融合工学部
佐藤　聡・秦野　歳久・古谷　一幸・黒田　敏公
榎枝　幹男・高津　英幸

（1997年12月2日受理）

国際熱核融合実験炉（ＩＴＥＲ）第一壁／ブランケットへの適用を目的に、固相熱間静水圧加圧接合（ＨＩＰ）によるアルミナ分散強化銅（DSCu）とオーステナイトステンレス鋼（SUS316L）の接合技術を開発した。DSCu/DSCu 及び DSCu/SUS、SUS/SUS を同時にＨＩＰ接合することを考慮したスクリーニング試験の結果、ＨＩＰ処理条件としては、温度1050℃が最適であると結論づけられた。

1050℃でＨＩＰした DSCu/SUS 接合片を用いて、引張り、衝撃、疲労、き裂進展、破壊靱性試験を行った。それらの機械特性は、一部、高温の試験条件で特性が下がるものはあるものの、ほぼ母材と同程度の特性であった。加えて、SUS 円管を有する DSCu/SUS 接合モックアップを用いた機械試験を行った。初期き裂はステンレスの冷却管内部に発生し、これは解析において得られた最大歪みの発生位置と一致した。

ＨＩＰ接合により、冷却配管を有する第一壁パネル部分モデルの試作に成功した。二体製作し、一体は300㎜ 長さ、もう一体は800㎜ 長さである。300㎜ 長さの部分モデルを用いて、ＩＴＥＲの運転条件に相当する高熱負荷試験を行った。その結果、熱サイクルによる除熱性能の劣化は確認されなかった。また、ミクロ観察の結果、ＨＩＰ接合面にき裂や剥離等の異常はなく、ＨＩＰ接合面は健全であることが確認された。

ＨＩＰ接合面に対する非破壊検査手法として、超音波探傷試験を試み、検出可能な欠陥の大きさを評価した。

本作業は、国際熱核融合実験炉（International Thermonuclear Experimental Reactor）の工学設計活動として、1995年作業計画（Task No. G16 TT 65 95-12-15 FJ, ID No.T212）に基づいて実施した。
那珂研究所：〒311－0193　茨城県那珂郡那珂町向山801－1

Contents

目　　次

1. Introduction

A shielding blanket integrated with the first wall will be installed during the Basic Performance Phase of ITER. To remove heat loads from the plasma efficiently and, at the same time, to maintain mechanical integrity against huge electromagnetic and thermal loads, the first wall has a structure of Al_2O_3 dispersion strengthened Cu (DSCu) heat sink with built-in coolant tubes of type 316LN stainless steel (SS) and is bonded to a massive SS shield block.

To fabricate the shielding blanket, a Hot Isostatic Pressing (HIP) method has been proposed, especially for the joining of DSCu/DSCu, DSCu/SS and SS/SS at the first wall and the first wall to the shield block [1]. HIP is a non-melting welding method which will realize sufficient mechanical integrity of the joints under the anticipated high neutron and stress fields including the elimination of IASCC concern, high dimensional accuracy, low residual stress during joining process and the joining of three-dimensionally complex structure in comparison with other joining methods, e.g., conventional fusion welding and brazing. Simultaneous HIP bonding of above joints has been pursued so as to minimize thermal effects on the materials, i.e., grain coarsening and degradation of mechanical properties, and also to minimize fabrication steps.

The objective of this study is to develop, characterize and test copper alloy to stainless steel bonding techniques. The objectives can be subdivided into three main areas of investigation;
1) The investigation, development, optimization, and characterization of Cu alloy to stainless steel bonding techniques. Hot Isostatic Pressing (HIP) of solid plates and/or blocks are considered in this study.
2) The confirmation of the bonding techniques by destructive/non-destructive examination methods. These methods will include mechanical testing of bond structure (including tensile tests and low cycle fatigue tests at room and elevated temperatures), examination of the bonding interface structure (microscopic examination) to demonstrate grain boundary configuration, and ultrasonic examination.
3) The demonstration of the fabrication of prototypical size first wall with integral coolant channels.

The materials to be used are alumina dispersion strengthened copper (DSCu), Glidcop Al-25® and annealed type 316LN stainless steel or relevant materials.

2. Screening Tests for HIP Conditions [2, 3]

To avoid or reduce high temperature effects on the microstructure of SS structural material, i.e. grain coarsening and degradation of mechanical properties, and also to simplify manufacturing procedure, thus to reduce manufacturing cost, a simultaneous HIP bonding of DSCu/DSCu, DSCu/SS and SS/SS has been pursued. Optimal conditions for this HIP bonding has been examined using Glidcop Al-15® and Al-25® as DSCu and type 316L stainless steel as SS [4, 5]. Taking into account the optimal HIP temperatures for SS/SS bonding known as about 1050-1100

1. Introduction

A shielding blanket integrated with the first wall will be installed during the Basic Performance Phase of ITER. To remove heat loads from the plasma efficiently and, at the same time, to maintain mechanical integrity against huge electromagnetic and thermal loads, the first wall has a structure of Al_2O_3 dispersion strengthened Cu (DSCu) heat sink with built-in coolant tubes of type 316LN stainless steel (SS) and is bonded to a massive SS shield block.

To fabricate the shielding blanket, a Hot Isostatic Pressing (HIP) method has been proposed, especially for the joining of DSCu/DSCu, DSCu/SS and SS/SS at the first wall and the first wall to the shield block [1]. HIP is a non-melting welding method which will realize sufficient mechanical integrity of the joints under the anticipated high neutron and stress fields including the elimination of IASCC concern, high dimensional accuracy, low residual stress during joining process and the joining of three-dimensionally complex structure in comparison with other joining methods, e.g., conventional fusion welding and brazing. Simultaneous HIP bonding of above joints has been pursued so as to minimize thermal effects on the materials, i.e., grain coarsening and degradation of mechanical properties, and also to minimize fabrication steps.

The objective of this study is to develop, characterize and test copper alloy to stainless steel bonding techniques. The objectives can be subdivided into three main areas of investigation;
1) The investigation, development, optimization, and characterization of Cu alloy to stainless steel bonding techniques. Hot Isostatic Pressing (HIP) of solid plates and/or blocks are considered in this study.
2) The confirmation of the bonding techniques by destructive/non-destructive examination methods. These methods will include mechanical testing of bond structure (including tensile tests and low cycle fatigue tests at room and elevated temperatures), examination of the bonding interface structure (microscopic examination) to demonstrate grain boundary configuration, and ultrasonic examination.
3) The demonstration of the fabrication of prototypical size first wall with integral coolant channels.

The materials to be used are alumina dispersion strengthened copper (DSCu), Glidcop Al-25® and annealed type 316LN stainless steel or relevant materials.

2. Screening Tests for HIP Conditions [2, 3]

To avoid or reduce high temperature effects on the microstructure of SS structural material, i.e. grain coarsening and degradation of mechanical properties, and also to simplify manufacturing procedure, thus to reduce manufacturing cost, a simultaneous HIP bonding of DSCu/DSCu, DSCu/SS and SS/SS has been pursued. Optimal conditions for this HIP bonding has been examined using Glidcop Al-15® and Al-25® as DSCu and type 316L stainless steel as SS [4, 5]. Taking into account the optimal HIP temperatures for SS/SS bonding known as about 1050-1100

℃ [6-8] and DSCu melting point of 1083 ℃, test specimens of HIPped SS316L/DSCu joints at 980-1050 ℃ were fabricated. HIP pressure and holding time were 150 MPa and 2-4 hours, respectively, based on the previous experiences of SS/SS HIP bonding [6-8].

By microscopic and SEM observations, no defects were observed at the HIPped interfaces of all specimens. Figures 2.1 and 2.2 show microscopic images of the SS316L/Al-25 joints at HIPped interfaces. Diffusion and precipitation of SS elements, i.e. Fe and Cr clarified by EPMA, were observed into DSCu up to about 100 μm from the interface. The precipitation increased as the HIP temperature increased. An intermediate layer of < 5-10 μm thickness was formed at the interface, of which composition need to be clarified in detail by further investigation.

Ultimate tensile strength, yield strength, total elongation and reduction of area are shown in Figs. 2.3 - 2.6, respectively, for the HIP bonded SS316L/Al-25 joints fabricated at 980, 1030 and 1050 ℃. Circles, squares and triangles in these figures denote the results for the joints fabricated at 980, 1030 and 1050 ℃, respectively. Remarkable differences were not observed among the tensile properties of these joints, though large elongation and reduction of area of one test piece out of two pieces of the joints fabricated at 1050 ℃ were observed in the case of room temperature tests, as shown in Figs. 3.5 and 3.6.

Results of hardness measurement is shown in Fig. 2.7 for the HIP bonded SS316L/Al-25 joints fabricated at 980, 1030 and 1050 ℃. Significant differences were not observed among the hardness of these joints.

Results of the fatigue tests at room temperature are shown in Fig. 2.8, where the data are plotted in the form of total strain range versus number of cycles to failure for the HIP bonded SS316L/Al-25 joints fabricated at 980, 1030 and 1050 ℃. Fatigue strengths of the HIP bonded SS316L/Al-25 joints fabricated at 1050 ℃ showed slight higher fatigue lifetime compared with those at 980 and 1030 ℃.

Results of Charpy impact tests are shown in Figs. 2.9 - 2.11 for the HIP bonded SS316L/SS316L, SS316L/Al-15 and SS316L/Al-25 joints, respectively. The impact values increased as the HIP temperature increased. The fracture was observed at DSCu base metal in case of SS316L/Al-15 joint HIPped at 1050 ℃. The other joint specimens fractured at HIPped interface.

Based on above results, it was concluded that HIP temperature of 1050 ℃ was an optimal condition for the simultaneous HIP bonding of DSCu/DSCu, SS/DSCu and SS/SS, and to be applied for the mock-ups fabrication.

3. Mechanical Properties of HIPped Joints

3.1Baseline Properties

3.1.1 Experimental procedure

Test blocks for the SS316L/DSCu HIP joint were fabricated by bonding flat plates of SS316L and DSCu (Al-15 and Al-25) under the HIP condition of temperature at 1050 ^{o}C, pressure at 150 MPa and holding time of 2 hours. Rolled directions of both of SS316L and DSCu plates were parallel to the joint interface to be consistent with the fabrication of the first wall structure. Test specimens were made by cutting out of the test blocks with the joint interface at their center. The following mechanical tests were performed:

- Tensile tests at room temperature (RT)-450 ^{o}C,
- Strain controlled fatigue tests with total strain ranges of 0.5-1.2 % with triangular wave form, with strain rate of 0.1%/s, and at RT-400 ^{o}C,
- Charpy impact tests at RT,
- Crack propagation tests by ASTM E647 at RT,
- Fracture toughness tests by ASTM E813 at RT.

3.1.2 Test results

3.1.2.1 Tensile tests

Ultimate tensile strength, yield strength, total elongation and reduction of area are shown in Figs. 3.1.1 - 3.1.4, respectively, for the HIP bonded SS316L/Al-15 [9] and SS316L/Al-25 joints, and the base metals of Al-15 [8] and Al-25 with the same heat treatment of the HIP process. Circles, squares, triangles and lozenges in these figures denote the results of SS316L/Al-15 joints, SS316L/Al-25 joints, Al-15 base metal and Al-25 base metal, respectively. As shown in Figs. 3.1.1 and 3.1.2, ultimate tensile strengths and yield strengths of the HIP bonded SS316L/DSCu joints were nearly equal to those of DSCu base metal. Total elongation and reduction of area of the HIP bonded SS316L/DSCu joints were slightly lower than those of the base metal of DSCu, though very small elongation and reduction of area were observed at test temperatures over 300 ^{o}C, as shown in Figs. 3.1.3 and 3.1.4.

3.1.2.2 Fatigue tests

The results of fatigue tests at room temperature and elevated temperatures are shown in Figs. 3.1.5 and 3.1.6, respectively, where the data are plotted in the form of the total strain range versus the number of cycles to failure. Most of the data of the HIP bonded SS316L/DSCu joints showed slight degradation compared with those of the DSCu base metals.

3.1.2.3 Impact tests

The results of Charpy impact tests are summarized in Table 3.1.1. Both of impact values of the HIP bonded SS316L/Al-15 [7] and SS316L/Al-25 joints were low compared with those of the base metals of Al-15 and Al-25. The impact values of SS316L/Al-15 joints were 27 - 60 % of those of Al-15 base metal [7], and those of Al-25/SS316L joints were 33 - 40 % of those of Al-25 base metal.

3.1.2.4 Crack propagation tests [10]

Crack propagation tests were performed to examine crack behavior of DSCu (Al-25)/SS316L HIPped interface. Two types of test specimens as shown in Fig. 3.1.7 were prepared. One had a notch along the HIPped interface and the other, in DSCu, normal to the interface. Stress ratio and frequency at the tests were 0.1 and 10 cycles per second, respectively.

The crack in the former test specimen propagated along the interface perpendicular to the loading direction during the testing while the crack in the latter specimen propagated in the DSCu also perpendicular to the loading direction, but stopped at the interface, then exfoliated the interface. Thus the crack did not propagated into SS316L in the latter specimen. Evolution of crack length are shown in Fig. 3.1.8. The relationships between ΔK and da/dN are shown in Fig. 3.1.9. The crack along the interface (the former specimen) propagated faster than the crack in DSCu (the latter specimen).

3.1.2.5 Fracture toughness tests

Fracture toughness (J) tests were performed with DSCu(Al-25)/SS316L HIPped joint and DSCu base metal with the same heat treatment as HIP process. Test specimen used are shown in Fig. 3.1.10. Stress ratio and cross head velocity were -1.0 and 1 mm/min., respectively. The J values were evaluated by J-R curve method (power law curve fitting procedure) defined in ASTM-E813 and using Young's modulus and Poisson's ratio of DSCu, i.e. 12000 kgf/mm^2 and 0.3, respectively.

The results of fracture toughness tests are shown in Figs. 3.1.11 and 3.1.12. According to the ASTM-E813, there are a number of criteria for validating the data including the following:

- One point must lie between the 0.15 mm exclusion line and a parallel line with an offset of 0.5 mm from the blunting line.
- One point must lie between a line parallel to the blunting line at an offset of 1.0 mm and the 1.5-mm exclusion line.
- At least four points must remain between the minimum crack extension (the intersection of the 0.15 mm exclusion line and the power law regression line) and the maximum crack extension (the intersection of 1.5 mm exclusion line and the power law regression line) and the J_{max}.

Though the data obtained in this test did not fully satisfy above criteria as shown in Figs. 3.1.11 and 3.1.12, some guideline on the J values could be obtained. The J_Q values evaluated with these data were 17.6 kJ/m^2 and 69.5 kJ/m^2 for the HIPped joint and the DSCu base metal.

3.2 Mechanical Test of Structural Model [11]

3.2.1 Fatigue test

Test specimens reflecting the first wall structure, i.e. with one SS cooling tube embedded in DSCu heat sink, as shown in Fig. 3.2.1 were fabricated by HIP. Glidcop Al-25® and type 316L stainless steels were used as DSCu and SS, respectively. Dimensions of the SS tube were 10 mm in inner diameter and 1 mm in thickness. HIP conditions were 1050 ℃, 150 MPa and holding time of two hours.

Tension-compression fatigue tests using these specimens were performed. Test conditions were as follows:

- Temperature : room temperature
- Atmosphere : air
- Loading : strain-controlled
- Wave form : triangular
- Strain velocity : 0.1 %/sec
- Strain ratio : -1
- Total strain range : 1.0, 0.7, 0.5, 0.3 and 0.2 %

Results of fatigue test are summarized in Table 3.2.1. Changes of stress range during the test are shown in Figs. 3.2.2 - 3.2.6. Stress ranges were calculated with a nominal cross section (A) of the test specimen given by:

$A = (D_2 - D) \times t = (20.0 - 10.2) \times 6.0 = 58.8$ mm^2

D : tube inner diameter

D_2 : width of test specimen

t : thickness of test specimen.

The number of cycles to failure was defined as that at the imposed load decreased down to three fourth of the maximum load. Total, elastic and plastic strain ranges as a function of the number of cycles to failure are shown in Table 3.2.1 and Fig. 3.2.7. The fraction of elastic strain range increased as total strain range increased.

Appearances of test specimens after fatigue test are shown in Figs. 3.2.8 and 3.2.9. For test specimens of 1.0 and 0.7 % strain range (Fig. 3.2.8), the tests were stopped when the failure was observed, i.e. the imposed load reduced to three fourth of the maximum load. On the other hand, tests were continued for specimens of 0.5, 0.3 and 0.2 % strain ranges until the specimens were fully ruptured. In all cases, a crack was initiated at the inner surface of SS tube at the angle of 90° or 270° to the loading direction. Then in some cases, a crack was generated in DSCu at the HIPped interface even without the initial crack propagating through the SS tube. The crack in DSCu propagated in the direction perpendicular to the loading direction. Exfoliation of the HIPped interface was also observed following the crack initiation in DSCu.

3.2.2 Elasto-plastic analysis

Elasto-plastic structure analyses were performed to evaluate the failure behavior of the test specimen. The analysis model was 2-D model incorporating one fourth of the test specimen with plane stress condition. The analysis code used was ABAQUS.

Results of elasto-plastic analysis are shown in Fig. 3.2.10 together with fatigue test results of above structural model, SS316 with the same heat treatment of the HIP process, and DSCu/SS316L HIPped joints of round bar specimen. Analysis results indicate local strain ranges at the inner surface of SS cooling tube and in DSCu at HIPped interface based on the same nominal strain range of the structural model test. The maximum local strain in the analysis was obtained at the SS tube inner surface, which is consistent with the location of crack initiation in the test. The numbers of cycles to failure or the total strain ranges for failure of the analysis results are larger than those obtained from the SS316 test with round bar specimens. It is possibly due to non-uniform stress (strain) distribution in the structural model while the stress (strain) distribution is uniform in the round bar specimen. Therefore, by keeping stresses (strains) in the design analysis lower than the data of round specimen test, probably with some safety factors, the component structural integrity can be maintained.

4. Fabrication of DSCu/SS Panels with Built-in Cooling Channels

Based on the results of the screening test described in Chapter 2, first wall mock-ups with

t : thickness of test specimen.

The number of cycles to failure was defined as that at the imposed load decreased down to three fourth of the maximum load. Total, elastic and plastic strain ranges as a function of the number of cycles to failure are shown in Table 3.2.1 and Fig. 3.2.7. The fraction of elastic strain range increased as total strain range increased.

Appearances of test specimens after fatigue test are shown in Figs. 3.2.8 and 3.2.9. For test specimens of 1.0 and 0.7 % strain range (Fig. 3.2.8), the tests were stopped when the failure was observed, i.e. the imposed load reduced to three fourth of the maximum load. On the other hand, tests were continued for specimens of 0.5, 0.3 and 0.2 % strain ranges until the specimens were fully ruptured. In all cases, a crack was initiated at the inner surface of SS tube at the angle of 90° or 270° to the loading direction. Then in some cases, a crack was generated in DSCu at the HIPped interface even without the initial crack propagating through the SS tube. The crack in DSCu propagated in the direction perpendicular to the loading direction. Exfoliation of the HIPped interface was also observed following the crack initiation in DSCu.

3.2.2 Elasto-plastic analysis

Elasto-plastic structure analyses were performed to evaluate the failure behavior of the test specimen. The analysis model was 2-D model incorporating one fourth of the test specimen with plane stress condition. The analysis code used was ABAQUS.

Results of elasto-plastic analysis are shown in Fig. 3.2.10 together with fatigue test results of above structural model, SS316 with the same heat treatment of the HIP process, and DSCu/SS316L HIPped joints of round bar specimen. Analysis results indicate local strain ranges at the inner surface of SS cooling tube and in DSCu at HIPped interface based on the same nominal strain range of the structural model test. The maximum local strain in the analysis was obtained at the SS tube inner surface, which is consistent with the location of crack initiation in the test. The numbers of cycles to failure or the total strain ranges for failure of the analysis results are larger than those obtained from the SS316 test with round bar specimens. It is possibly due to non-uniform stress (strain) distribution in the structural model while the stress (strain) distribution is uniform in the round bar specimen. Therefore, by keeping stresses (strains) in the design analysis lower than the data of round specimen test, probably with some safety factors, the component structural integrity can be maintained.

4. Fabrication of DSCu/SS Panels with Built-in Cooling Channels

Based on the results of the screening test described in Chapter 2, first wall mock-ups with

built-in rectangular cooling channels were fabricated with the selected HIP conditions, i.e. 1050 ℃, 150 MPa and holding time of 2 hours [4]. Glidcop Al-15® and type 316L stainless steel were used as DSCu and SS, respectively, for trial and mock-ups fabrication shown below.

4.1 Trial Fabrication

Prior to the mock-ups fabrication, trial fabrication on a configuration of the bonding assembly was conducted. Two specimens were fabricated; one was with thin (0.5 mm thick) SS liner inserted between DSCu plate and SS rectangular tubes, and another without the SS liner. The purpose of the SS liner insertion was to avoid DSCu intrusion into gaps between SS tubes and a formation of sharp edge that might cause a crack initiation. An appearance of the former specimen and close-up views of coolant channel cross-sections of both specimens are shown in Fig. 4.1. Micro-photographs of sections between coolant channels with and without SS liner are shown in Fig. 4.2. Though both of specimens were successfully joined resulted from metallurgical observations, DSCu intrusion into gaps between coolant channels was observed in case of the specimen without SS liner. Therefore, the insertion of SS liner was effective to prevent DSCu from intruding into the gaps, and it was concluded to adopt the SS liner insertion for the next first wall mock-ups fabrication. It should be also noted that the effect of the DSCu intrusion on the component integrity, e.g. crack initiation and propagation, should be investigated in more detail because the elimination of the SS liner will contribute to reduce the complication in fabrication and thus fabrication cost.

4.2 Fabrication of First Wall Mock-ups

Based on above results, 300 mm long and 800 mm long mock-ups of HIPped first wall were fabricated with built-in rectangular coolant tubes. Figures 4.3 shows the former mock-up. The first wall panel section is about 110 mm wide and 25 mm thick with DSCu thickness of 5 mm. Eight cooling tubes are embedded, of which dimensions are internally 6 x 10 mm and thickness of 1.5 mm. The 0.5 mm thick SS liner is inserted between DSCu and the coolant tube. A DSCu plate, SS liner, SS coolant tubes, and bottom and edge SS plates were HIPped simultaneously under conditions of 1050 °C, 150 MPa and holding time of 2 hours. Then coolant manifolds and supply/return pipes were welded. The latter (800 mm long) mock-up shown in Fig. 4.4 was fabricated similarly but with 12 built-in coolant tubes and the mock-up width of about 160 mm.

Maximum undulation in the former and the latter mock-ups after the HIP process were less than 0.2 mm and 2.5 mm, respectively. Then the latter mock-up was pressed to reform the undulation down to 0.5 mm. When both mock-ups were HIPped, they were made a little wider and longer than above-mentioned final dimensions. After the HIPping, edge parts of each mock-up were cut and microscopically observed. There were no harmful voids found at their HIPped

interfaces by microscopic observation. After the edge parts were removed, both of mock-ups were finally machined, and inlet/outlet coolant headers were welded by TIG welding.

4.3 Conclusions

Conclusions obtained through the fabrication of the first wall mock-ups are summarized as follows:

(1) Simultaneous HIP bonding of DSCu/SS and SS/SS was successfully conducted for fabricating first wall panel mock-ups with built-in coolant tubes.

(2) Insertion of thin SS liner between DSCu and SS rectangular cooling tubes was effective to prevent DSCu from intruding into gaps between coolant tubes, which might cause crack initiation.

(3) The maximum undulations of the 300 long and 800 mm long first wall panel after HIPping were 0.2 mm and 2.5 mm, respectively, of which the latter panel was decreased down to 0.5 mm by pressing after HIPping.

(4) The same technology can be applied to the fabrication of medium scale mock-up.

5. High Heat Flux Tests of DSCu/SS Panel

5.1 Tested First Wall Mock-up and Pre-analysis

The fabricated 300 mm long first wall mock-up shown in Fig. 4.3 was tested with high heat fluxes at PBEF (Particle Beam Engineering Facility) in JAERI [12-14]. The heat flux tests were composed of short term thermal fatigue test with ITER normal operation condition and thermal shock test with disruption conditions. Heat flux loading time for the thermal fatigue test was decided to be one second so as to perform the test efficiently in a shorter time. With this short heat flux loading time, higher heat fluxes than ITER nominal conditions were to be selected so that temperatures and strains at the HIPped interface could simulate those for ITER operation condition.

Thermo-mechanical analyses were performed to determine the test conditions. Analysis model was a 2-dimensional model of one half of the mock-up taking symmetric condition into account as shown in Fig. 5.1. Analysis code used was ABAQUS [15]. Calculated temperatures of DSCu and HIPped interface with one second heat flux loading time are shown in Fig. 5.2 as a function of heat flux. Coolant temperature in the calculation was 30 ℃, which was the same as in the test. Volumetric heating was not considered also to be consistent with the test condition. A steady state temperature at the HIPped interface with heat flux of 0.5 MW/m^2, i.e. ITER normal operation condition, but with coolant temperature of 30 ℃ and without volumetric heating is 110 ℃. Therefore from Fig. 5.2, it can be concluded that a test with the heat flux of about 2.0 MW/m^2 will simulate the temperature at the HIPped interface during ITER normal

interfaces by microscopic observation. After the edge parts were removed, both of mock-ups were finally machined, and inlet/outlet coolant headers were welded by TIG welding.

4.3 Conclusions

Conclusions obtained through the fabrication of the first wall mock-ups are summarized as follows:

(1) Simultaneous HIP bonding of DSCu/SS and SS/SS was successfully conducted for fabricating first wall panel mock-ups with built-in coolant tubes.

(2) Insertion of thin SS liner between DSCu and SS rectangular cooling tubes was effective to prevent DSCu from intruding into gaps between coolant tubes, which might cause crack initiation.

(3) The maximum undulations of the 300 long and 800 mm long first wall panel after HIPping were 0.2 mm and 2.5 mm, respectively, of which the latter panel was decreased down to 0.5 mm by pressing after HIPping.

(4) The same technology can be applied to the fabrication of medium scale mock-up.

5. High Heat Flux Tests of DSCu/SS Panel

5.1 Tested First Wall Mock-up and Pre-analysis

The fabricated 300 mm long first wall mock-up shown in Fig. 4.3 was tested with high heat fluxes at PBEF (Particle Beam Engineering Facility) in JAERI [12-14]. The heat flux tests were composed of short term thermal fatigue test with ITER normal operation condition and thermal shock test with disruption conditions. Heat flux loading time for the thermal fatigue test was decided to be one second so as to perform the test efficiently in a shorter time. With this short heat flux loading time, higher heat fluxes than ITER nominal conditions were to be selected so that temperatures and strains at the HIPped interface could simulate those for ITER operation condition.

Thermo-mechanical analyses were performed to determine the test conditions. Analysis model was a 2-dimensional model of one half of the mock-up taking symmetric condition into account as shown in Fig. 5.1. Analysis code used was ABAQUS [15]. Calculated temperatures of DSCu and HIPped interface with one second heat flux loading time are shown in Fig. 5.2 as a function of heat flux. Coolant temperature in the calculation was 30 ℃, which was the same as in the test. Volumetric heating was not considered also to be consistent with the test condition. A steady state temperature at the HIPped interface with heat flux of 0.5 MW/m^2, i.e. ITER normal operation condition, but with coolant temperature of 30 ℃ and without volumetric heating is 110 ℃. Therefore from Fig. 5.2, it can be concluded that a test with the heat flux of about 2.0 MW/m^2 will simulate the temperature at the HIPped interface during ITER normal

operation. Calculated strains at the HIPped interface with the same calculation conditions as above are shown in Fig. 5.3.
As strains at the HIPped interface with ITER normal operation condition are 4.2 x 10^{-3} (ε_x) and 3.6 x 10^{-3} (ε_y), heat fluxes of 5.0 - 6.0 MW/m^2 can simulate these strains as indicated in the figure.

5.2 Test Conditions

Test conditions selected based on above analyses results are summarized in Table 5.1. Four tests were performed in series. The first two tests are thermal fatigue tests simulating the temperature (No. 1) and the strain (No. 2) at HIPped interface during ITER normal operation. The last two (Nos. 3 and 4) are thermal shock tests corresponding to disruption conditions, i.e. the radial disruption (20 MJ/m^2 x 25 msec) and the vertical displacement event (60 MJ/m^2 x 300 msec), respectively.

Table 5.1 High heat flux testing conditions

No.	heat flux (MW/m2)	heat flux loading time (sec)	number of cycles
1	2.0 - 2.5	1.0	1000
2	5.0 - 6.0	1.0	1000
3	40.0	0.075	2
4	100.0	0.3	1

5.3 Test Results

Typical temperature responses in the thermal fatigue test (No. 1) under heat flux of 2.0 MW/m^2 are shown in Fig. 5.4. Temperature of DSCu were measured by means of a thermocouple at 2 mm deep from the DSCu surface. Temperature responses indicated in Fig. 5.5 are those at 50th and 1000th cycles. Both responses agree well, thus no degradation of thermal performance is observed between 50th and 1000th cycles. In addition, their responses also agree well with the analysis result as shown in the figure.

Temperature responses at the HIPped interface during the second test (No. 2) are shown in Fig. 5.5. In the figure, the analysis result with heat flux of 5.0 MW/m^2 is also shown. The response at 50th cycle agrees well with the analysis results. Temperatures at 1000th cycle are approximately 20 % higher than those at 50th cycle. This is because the heat flux at the 1000th

cycle was unintentionally increased up to about 6.0 MW/m^2, while the heat flux at the 50th cycle was kept at 5.0 MW/m^2. Taking this heat flux increase into account, it can be said that the temperature response at the 1000th cycle agree well with an expected analysis results without any degradation in heat removal performance.

Therefore, it can be concluded from these fatigue test results that the thermo-mechanical integrity of the DSCu/SS HIPped mock-up was confirmed at least up to 2000 thermal cycles.

Temperatures during the third test also agreed well with analysis result. Maximum temperature of DSCu surface was about 360 ℃ in this case. No change was observed in its physical appearance after the test.

In the last test simulating a severe disruption condition with the heat flux of 100 MW/m^2, ejection of small particles from the heated DSCu surface was observed. An appearance of the first wall panel after this test is shown in Fig. 5.6. There are three representative concentric circle patterns, i.e. hoarse, wavy and glossy from the center, on DSCu surface along with the beam power profile.

5.4 Post-mortem Analysis

After all above tests, the first wall panel was cut, and the HIPped interface and the heated surface of DSCu were microscopically observed. Cutting line of the mock-up is shown in Fig. 5.6. A cross section of the cut first wall panel is shown in Fig. 5.7. Close observations of the region indicated by a square in Fig. 5.7 were performed. Figure 5.8 indicates a SEM observation at the HIPped interfaces of DSCu/SS liner, SS liner/SS tube, and SS tube/SS tube. Since no cracks were observed at their interfaces, the integrity of the HIPped joints were confirmed.

A microscopic observation of the DSCu surface at the beam center is shown in Fig. 5.9. Melting zone of thickness about 1.5 mm is observed. There are many fine cracks propagating from the surface into the melting zone. A number of cylindrical voids of about 100 μm in diameter also appeared in the melting zone, which might be due to residual gas release in the DSCu. A SEM observation of DSCu surface at the beam center is shown in Fig. 5.10. Segregations in the size of 10 μm, fine cracks and a dendritic structure are observed. From composite image shown in Fig. 5.11 and EPMA analysis, it was found that these segregations consisted of Al_2O_3 probably from those contained in DSCu.

Further investigation on the effects of Be armor on the first wall thermo-mechanical performance is also needed because it is the material to which the heat flux from plasma is directly subjected.

6. HIP Joint Performance and Applicability of Ultrasonic Testing

6.1 Introduction

Reliability of a structure strongly depends on the size of defect existing in the structure, as well as the design condition, external force, and the environment. There is a possibility that HIP joints in the first wall structure have interfacial voids. To assure the reliability of the HIP joints, therefore, it is quite important to clarify the minimum defect size that can be detected by NDT.

In this study, HIP joints were made by using type 316L stainless steel (SS316L) and Glidcop Al-25® (DSCu) as base materials. In addition to metallurgical observations and tensile tests of the joints, the maximum echo amplitude from the joint interface and the maximum noise echo amplitude from base metal were investigated. Based on these results and calculations, the minimum detectable defect sizes were estimated for the joints of above material combinations.

6.2 Manufacturing of HIP Joints

In a HIP trial, a couple of 26 mm thick blocks were joined. Three types of material combinations, i.e. SS316L/SS316L, DSCu/DSCu, and SS316L/DSCu were selected. In the HIP procedure, there are three main factors that affect the quality of the joint, i.e. the temperature, the atmospheric pressure, and the roughness of surface to be bonded. Among these factors, the temperature and the pressure are accurately and automatically controlled during the bonding process. On the other hand, generally, it is difficult to make the surface roughness uniform in whole area to be bonded, especially when a large components are assembled. From the viewpoint of the joint quality, finely polished surface is desirable. However, considering the manufacturing cost and the aberration in practice, allowing rough surface preparation (up to 25 μm in Rz) would be requested. From this standpoint, test blocks of three different surface roughness levels, 2 μm, 10 μm and 40 μm in Rz, were prepared for each material combination mentioned above. Table 6.1 shows the surface roughness of test blocks measured prior to the bonding.

6.3 Sampling of Test Specimens

Figure 6.1 shows sampling locations of specimens from the bonded block. The design thickness indicated in the figure expresses the actual beam path distance of UT based on the

Further investigation on the effects of Be armor on the first wall thermo-mechanical performance is also needed because it is the material to which the heat flux from plasma is directly subjected.

6. HIP Joint Performance and Applicability of Ultrasonic Testing

6.1 Introduction

Reliability of a structure strongly depends on the size of defect existing in the structure, as well as the design condition, external force, and the environment. There is a possibility that HIP joints in the first wall structure have interfacial voids. To assure the reliability of the HIP joints, therefore, it is quite important to clarify the minimum defect size that can be detected by NDT.

In this study, HIP joints were made by using type 316L stainless steel (SS316L) and Glidcop Al-25® (DSCu) as base materials. In addition to metallurgical observations and tensile tests of the joints, the maximum echo amplitude from the joint interface and the maximum noise echo amplitude from base metal were investigated. Based on these results and calculations, the minimum detectable defect sizes were estimated for the joints of above material combinations.

6.2 Manufacturing of HIP Joints

In a HIP trial, a couple of 26 mm thick blocks were joined. Three types of material combinations, i.e. SS316L/SS316L, DSCu/DSCu, and SS316L/DSCu were selected. In the HIP procedure, there are three main factors that affect the quality of the joint, i.e. the temperature, the atmospheric pressure, and the roughness of surface to be bonded. Among these factors, the temperature and the pressure are accurately and automatically controlled during the bonding process. On the other hand, generally, it is difficult to make the surface roughness uniform in whole area to be bonded, especially when a large components are assembled. From the viewpoint of the joint quality, finely polished surface is desirable. However, considering the manufacturing cost and the aberration in practice, allowing rough surface preparation (up to 25 μm in Rz) would be requested. From this standpoint, test blocks of three different surface roughness levels, 2 μm, 10 μm and 40 μm in Rz, were prepared for each material combination mentioned above. Table 6.1 shows the surface roughness of test blocks measured prior to the bonding.

6.3 Sampling of Test Specimens

Figure 6.1 shows sampling locations of specimens from the bonded block. The design thickness indicated in the figure expresses the actual beam path distance of UT based on the

present design of the first wall. Tensile test specimens of base metal were collected in the direction parallel to the joint surface, due to insufficient thickness of available base material at that time (30 mm).

6.4 Cross Sectional Observation of Joints

6.4.1 SS316L/SS316L joints

Figure 6.2 shows macrostructures of the cross sections of SS316L/SS316L joints. Slight grain growth due to dynamic recrystallization was observed in the joint of roughest surface preparation. However, for all surface roughness conditions, defects were not observed at joint interfaces. Moreover, as shown in Fig. 6.3, even a fine defect was not seen, either, from the observation of the microstructure.

6.4.2 DSCu/DSCu joints

Macrostructures and microstructures of the cross sections of DSCu/DSCu joints are shown in Figs. 6.4 and 6.5, respectively. From these observations, joint interface lines were clearly identified in all joints because of the existence of grain boundaries. However, a defect was not observed in the joints for all surface roughness conditions.

6.4.3 SS316L/DSCu joints

Macrostructures and microstructures of the cross sections of SS316L/DSCu joints are shown in Figs. 6.6 and 6.7, respectively. In all joint interfaces, a transition zone was not formed, and a defect was not observed.

6.5 Tensile Test Results

Figure 6.8 shows the relationship between the proof stress of joints and surface roughness conditions, for three types of material combinations. Results of the base metal are also shown in the figure. From these results, it was confirmed that change of the surface roughness from 2 to 40 μm in Rz did not affect the proof stress of HIP joint for all material combinations. Proof stresses of HIP joints were slightly lower than that of base metal. The reason of this is considered to be the difference of sampling direction of test pieces between HIP joint and base metal. On SS316L/DSCu combination, necking and fracture occurred at DSCu base metal, and therefore, proof stress of the joint met the value of DSCu base metal. The tensile strength of the HIP joints and base metals (Fig. 6.9) showed the same tendency as the proof stress.

Figs. 6.10 and 6.11 show the influence of the surface roughness on the elongation and the reduction of area (RA) of the HIP joints, respectively. In the combination of DSCu/DSCu and DSCu/SS316L, the elongation and RA of the joints did not change at different surface roughness conditions. However, in comparison with base metal, those joints showed a decline especially in RA. As for SS316L/SS316L joints, both of the elongation and RA slightly decreased at the surface roughness of 40 μm.

6.6 Ultrasonic Testing

6.6.1 Automatic ultrasonic testing

Figure 6.12 shows an example of a top view result of SS316L/SS316L joints by UT. All joints were examined at 1 mm scanning pitch with an automatic UT system of immersion type. Applied frequency was 5 MHz and 10 MHz. In the figure, colors express the echo amplitude from the joint interface. Eighty-percent-color-echo level was adjusted to be 48 dB higher level than that from wide plane. A quite high sensitivity was adopted for this test because a flaw echo was not obtained when normal sensitivity was applied. Therefore, the difference of the sensitivity among colors were very small, and defects were not detected by UT.

6.6.2 Estimation of detectable defect size

To estimate the detectable defect size by UT, a noise echo from the base metal that disturb the distinction of the defect echo has to be taken into account. Based on the results of above tests, Figs. 6.13 and 6.14 show the estimation of detectable defect size in SS316L/SS316L joints by UT at the frequency of 5 MHz and 10 MHz, respectively. In the figure, solid line shows the result of the calculation on the relationship between the echo amplitude and the diameter of circular defects. Horizontal broken and dash-dotted lines show the maximum echo amplitude from the joint interface and the maximum noise echo amplitude from base metal. The minimum detectable defect size is expressed by the cross point of higher horizontal line and the calculation curve.

From these figures, detectable defect size is expected to be 0.9 mm in diameter at 5 MHz, and 1.8 mm at 10 MHz. In case that there are a number of small defects within a ultrasonic beam size, the area of small defects should be summed up and dealt as a single circular defect of the same area. Based on above idea, the minimum detectable sizes of the defects are expected to be 0.35 mm for DSCu/DSCu joints (Figs. 6.15 and 6.16), and 1.4 mm for DSCu/SS316L joints (Figs. 6.17 and 6.18).

6.7 Summary

The results of this study are summarized as follows;

(1) HIP joints were made with different surface roughness levels for the material combinations of SS316L/SS316L, SS316L/DSCu and DSCu/DSCu.
(2) At joint interfaces of all HIP joints, a defect was not observed by cross sectional observation of macro and microstructure.
(3) Proof stress and tensile strength of HIP joints was not influenced by the difference of surface roughness in the range from 2 to 40 μm in Rz.
(4) SS316L/SS316L joint showed a slight decrease of the elongation and RA under the surface roughness condition of 40 μm in Rz.
(5) Defects were not detected by UT in all HIP joints made in this study.
(6) From the results of the estimation by using calculations, the minimum detectable defects are expected to be 0.9 mm, 0.35 mm, and 1.4 mm in diameter on SS316L/SS316L, DSCu/DSCu, and SS316L/DSCu joints, respectively.

The following further investigations are necessary to confirm above estimations and optimization of inspection conditions:

(1) Confirmation of the minimum detectable defect size through experiments,
(2) Determination of the inspection condition for the structure of actual size and geometry.

7. Summary

Joining techniques of alumina dispersion strengthened copper alloy (DSCu) and type 316L stainless steel (SS) has been investigated aiming at applying to the fabrication of the ITER first wall/blanket. As the joining method, Hot Isostatic Pressing (HIP) of solid plates and/or blocks has been pursued. For applying this method, a simultaneous HIPping of three types of joints included in the first wall/blanket structure, DSCu/DSCu, DSCu/SS and SS/SS, has been considered in order to avoid or reduce high temperature effects on the SS structural material, e.g. grain coarsening and degradation of mechanical properties, and also to simplify manufacturing procedure, thus to reduce manufacturing cost. Starting from the optimization study of the HIP condition, characterization, especially by mechanical tests, of the HIPped joints, the fabrication of first wall mock-ups, high heat flux tests of the mock-ups, and examination of applicable non-destructive testing method have been performed.

From a screening test for HIP temperatures of 980-1050 ℃, it was concluded that the HIP temperature of 1050 ℃ would be optimum for the simultaneous HIPping because the DSCu/SS joint specimen made at 1050 ℃ showed higher impact values and fatigue properties than DSCu/SS

The results of this study are summarized as follows;

(1) HIP joints were made with different surface roughness levels for the material combinations of SS316L/SS316L, SS316L/DSCu and DSCu/DSCu.
(2) At joint interfaces of all HIP joints, a defect was not observed by cross sectional observation of macro and microstructure.
(3) Proof stress and tensile strength of HIP joints was not influenced by the difference of surface roughness in the range from 2 to 40 μm in Rz.
(4) SS316L/SS316L joint showed a slight decrease of the elongation and RA under the surface roughness condition of 40 μm in Rz.
(5) Defects were not detected by UT in all HIP joints made in this study.
(6) From the results of the estimation by using calculations, the minimum detectable defects are expected to be 0.9 mm, 0.35 mm, and 1.4 mm in diameter on SS316L/SS316L, DSCu/DSCu, and SS316L/DSCu joints, respectively.

The following further investigations are necessary to confirm above estimations and optimization of inspection conditions:

(1) Confirmation of the minimum detectable defect size through experiments,
(2) Determination of the inspection condition for the structure of actual size and geometry.

7. Summary

Joining techniques of alumina dispersion strengthened copper alloy (DSCu) and type 316L stainless steel (SS) has been investigated aiming at applying to the fabrication of the ITER first wall/blanket. As the joining method, Hot Isostatic Pressing (HIP) of solid plates and/or blocks has been pursued. For applying this method, a simultaneous HIPping of three types of joints included in the first wall/blanket structure, DSCu/DSCu, DSCu/SS and SS/SS, has been considered in order to avoid or reduce high temperature effects on the SS structural material, e.g. grain coarsening and degradation of mechanical properties, and also to simplify manufacturing procedure, thus to reduce manufacturing cost. Starting from the optimization study of the HIP condition, characterization, especially by mechanical tests, of the HIPped joints, the fabrication of first wall mock-ups, high heat flux tests of the mock-ups, and examination of applicable non-destructive testing method have been performed.

From a screening test for HIP temperatures of 980-1050 ℃, it was concluded that the HIP temperature of 1050 ℃ would be optimum for the simultaneous HIPping because the DSCu/SS joint specimen made at 1050 ℃ showed higher impact values and fatigue properties than DSCu/SS

specimens made at other temperature conditions. DSCu/SS joint specimens for further mechanical tests and mock-ups were fabricated at this HIP temperature.

The following baseline mechanical properties of the DSCu/SS joints were obtained as a function test temperature:

- tensile
- impact
- fatigue
- crack propagation
- fracture toughness.

Typically, the properties of the joints were almost the same as those of DSCu or SS base metal with the same heat treatment of the HIP process, thus good joints were obtained. However, reduction of area in tensile test and fatigue lifetime of the joints were decreased at elevated test temperature, e.g. over 300 ℃. The behavior of the joints under elevated temperatures needs to be investigated in more detail as well as operation temperatures at the DSCu/SS joints.

Mechanical test of first wall structural model including one SS circular tube embedded in DSCu were also performed. Typical results of this test indicated that a crack initiated at the inner surface of the SS tube under cyclic operation, and the lifetime of the first wall structure could be evaluated by existing SS fatigue data.

Two HIPped first wall panel mock-ups were successfully fabricated with built-in coolant tubes: one was 300 mm long and the other 800 mm long. The former was thermo-mechanically tested with high heat fluxes corresponding to the ITER normal operation (short term thermal fatigue tests) and disruption conditions (thermal shock tests). During the tests, temperature responses in DSCu and at HIPped interface were agreed well with analysis results, thus no degradation in heat removal performance. In addition, there were no cracks and delaminations found at HIPped interfaces in microscopic observation after all above tests.

As for non-destructive testing method, ultrasonic testing were investigated. Based on the results of trial testing of HIPped specimens of SS/SS, DSCu/DSCu and DSCu/SS, detectable defect size at their joint interfaces were estimated.

Acknowledgment

The authors would like to express their sincere appreciation to Drs. M. Ohta, T. Nagashima and S. Matsuda for their continuous guidance and encouragement. They also would like to acknowledge all the members who supported this work.

specimens made at other temperature conditions. DSCu/SS joint specimens for further mechanical tests and mock-ups were fabricated at this HIP temperature.

The following baseline mechanical properties of the DSCu/SS joints were obtained as a function test temperature:

- tensile
- impact
- fatigue
- crack propagation
- fracture toughness.

Typically, the properties of the joints were almost the same as those of DSCu or SS base metal with the same heat treatment of the HIP process, thus good joints were obtained. However, reduction of area in tensile test and fatigue lifetime of the joints were decreased at elevated test temperature, e.g. over 300 ℃. The behavior of the joints under elevated temperatures needs to be investigated in more detail as well as operation temperatures at the DSCu/SS joints.

Mechanical test of first wall structural model including one SS circular tube embedded in DSCu were also performed. Typical results of this test indicated that a crack initiated at the inner surface of the SS tube under cyclic operation, and the lifetime of the first wall structure could be evaluated by existing SS fatigue data.

Two HIPped first wall panel mock-ups were successfully fabricated with built-in coolant tubes: one was 300 mm long and the other 800 mm long. The former was thermo-mechanically tested with high heat fluxes corresponding to the ITER normal operation (short term thermal fatigue tests) and disruption conditions (thermal shock tests). During the tests, temperature responses in DSCu and at HIPped interface were agreed well with analysis results, thus no degradation in heat removal performance. In addition, there were no cracks and delaminations found at HIPped interfaces in microscopic observation after all above tests.

As for non-destructive testing method, ultrasonic testing were investigated. Based on the results of trial testing of HIPped specimens of SS/SS, DSCu/DSCu and DSCu/SS, detectable defect size at their joint interfaces were estimated.

Acknowledgment

The authors would like to express their sincere appreciation to Drs. M. Ohta, T. Nagashima and S. Matsuda for their continuous guidance and encouragement. They also would like to acknowledge all the members who supported this work.

References

[1] K. Ioki, ITER Joint Central Team and Home Teams, ITER Blanket System Design, Proc. 19th Symp. Fusion Technol., Lisbon, 1996, to appear.

[2] S. Sato, et al., "Development of First Wall/Blanket Structure by HIP in JAERI", to be published as Proc. 4th Int. Symp. on Fusion Technol., Tokyo, 1997.

[3] S. Sato, et al., "Optimization of HIP Bonding Conditions for ITER Shielding Blanket/First Wall Made from Austenitic Stainless Steel and Dispersion Strengthened Copper Alloy", to be published as Proc. 8th Int. Confe. on Fusion Reactor Mat., Sendai, 1997.

[4] S. Sato et al., "Fabrication of HIPped First Wall Panel for Fusion Experimental reactor and Preliminary Analysis for Its Thermo-mechanical Test", Proc. 16th IEEE/NPSS Symp. on Fusion Eng., Champaign, USA(1995)202-205.

[5] T. Kuroda et al., Proc. 4th Japan-China Symp. on Materials for Advanced Energy Systems and Fission and Fusion Engineering and 10th Japan-China Symp. of JCSTEA Series, Sapporo, Japan(1996).

[6] K. Mohri, et al., Fusion Eng. **9**(1989) 159-165.

[7] S. Sato et al., "Fabrication of HIPped First Wall Panel for Fusion Experimental Reactor and Preliminary Analyses for Its Thermo-mechanical Test", Proc. 15th IEEE/NPSS Symp. on Fusion Eng., Cape Cod, USA (1993)259-262.

[8] K. Mohri, et al., Fusion Eng. **27**(1995) 438-443.

[9] S. Sato et al., J. Nucl. Mater. **233-237**(1996)940-944.

[10] T. Hatano et al., "Fracture strengths of HIPed DS-Cu/SS Joints for ITER Shielding Blanket/First Wall", , to be published as Proc. 8th Int. Confe. on Fusion Reactor Mat., Sendai, 1997.

[11] T. Hatano et al., submitted to J. Nuclear Science and Technology.

[12] T. Hatano et al., Fusion Technology **30**(1996)752-756.

[13] T. Hatano et al., "Post-mortem Analysis of HIP Bonded First Wall Panel Made from SS316 and DS-Cu after High Heat Flux Testing", Proc. 19th Symp. on Fusion Technology, Lisbon, Portugal(1996).

[14] T. Hatano et al., JAERI-Research 97-017(1996).

[15] ABAQUS USER'S MANUAL, Ver. 5.4, Hibbitt, Karlson & Sorenssen, Inc. (1995).

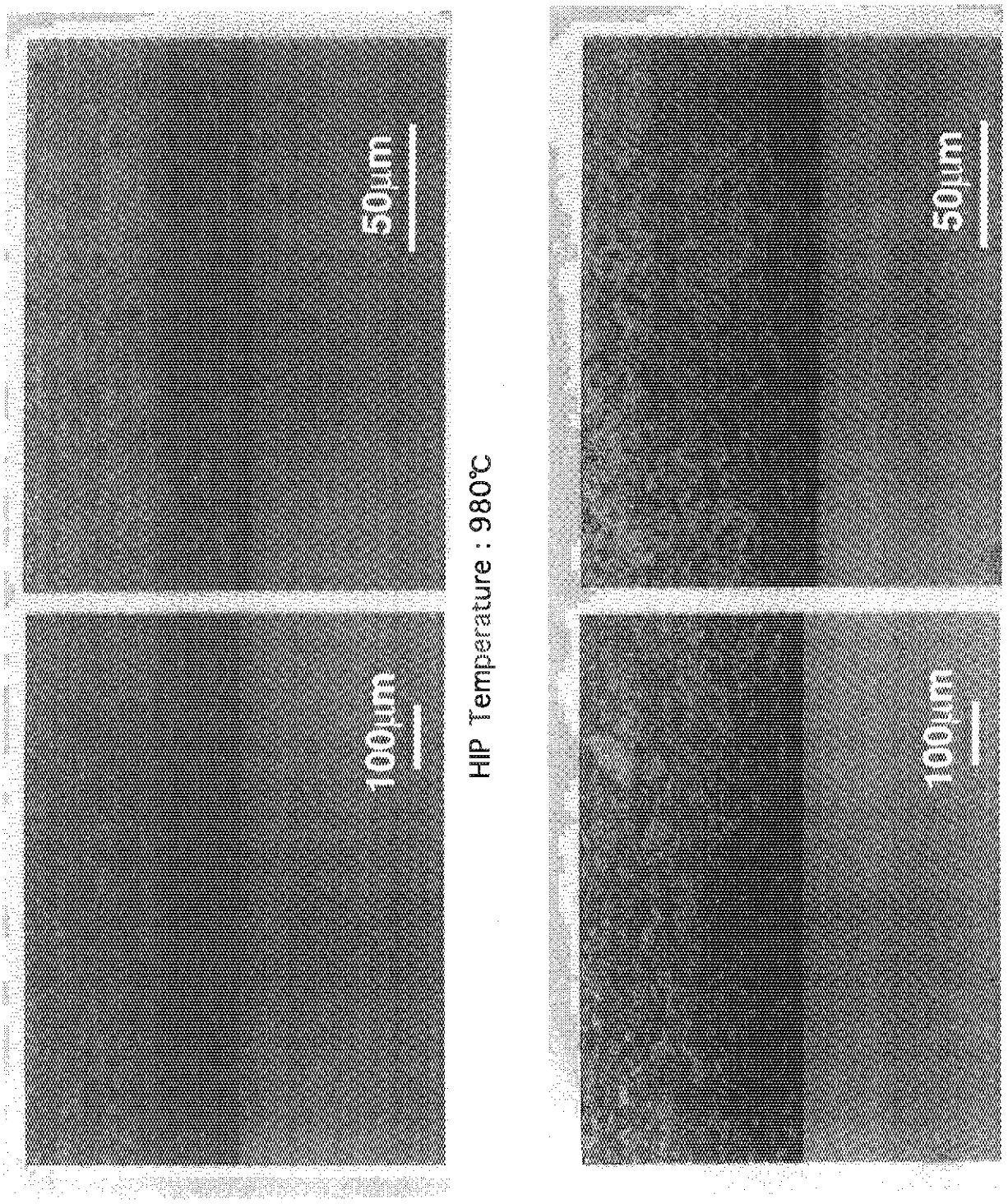

Fig. 2.1 Microscopic image of HIPed SS316L/Al-25 interface (Etched for Al-25)

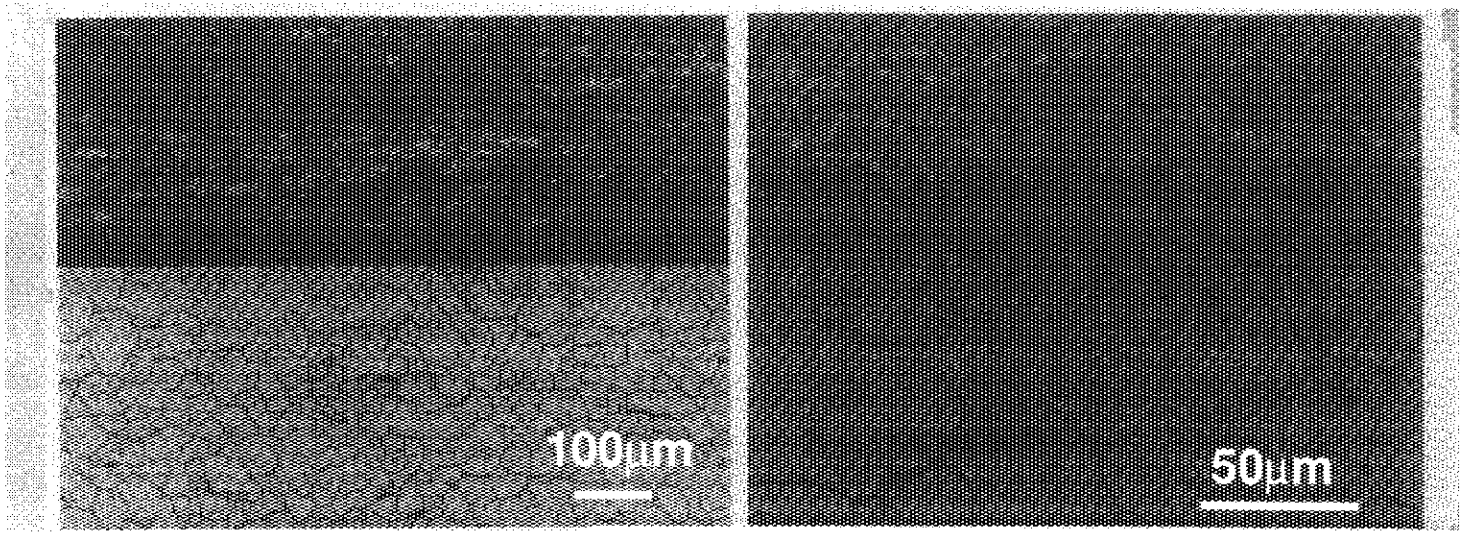

Fig. 2.2 Microscopic image of HIPed SS316L/Al-25 interface (Etched for SS316L)

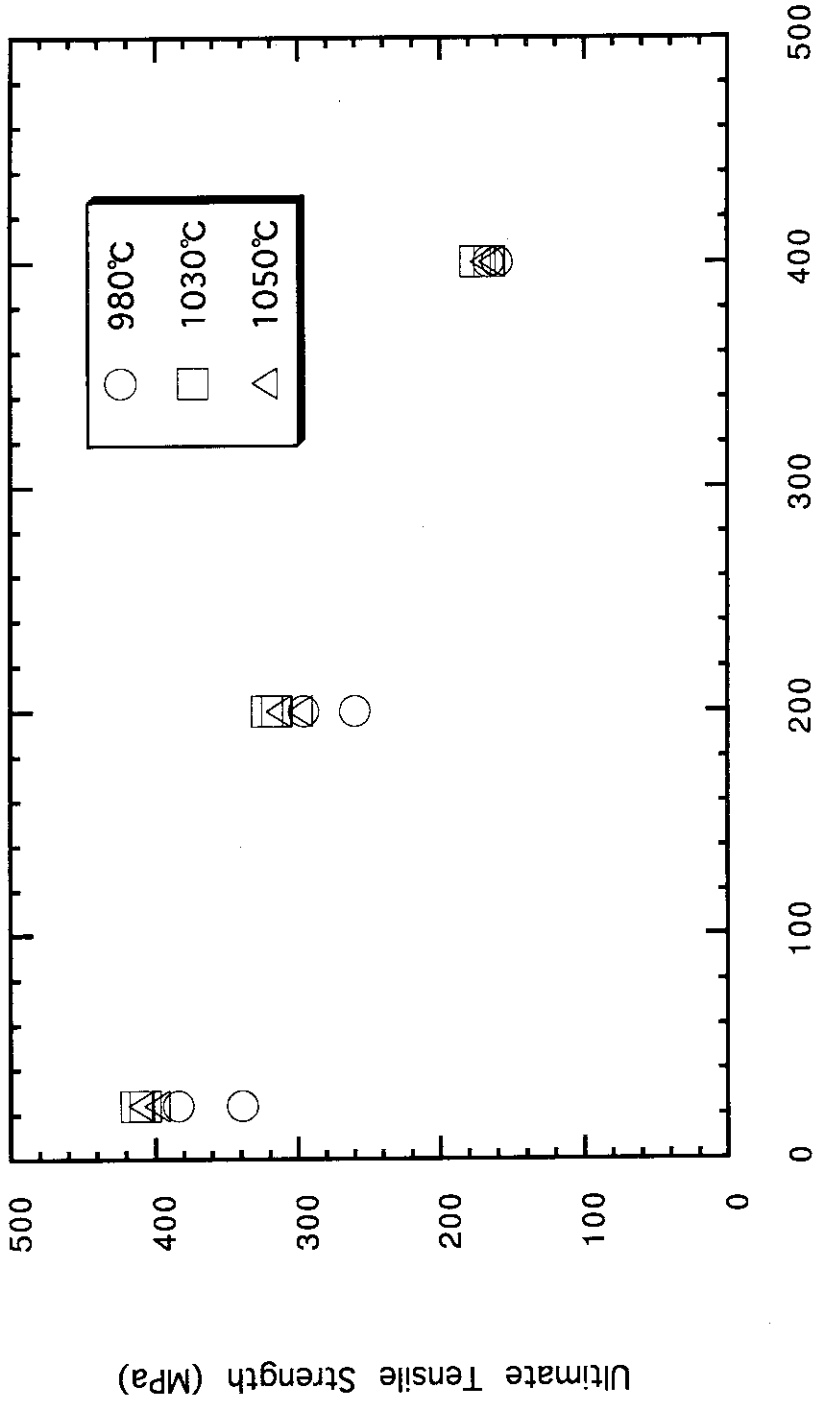

Fig. 2.3 Ultimate tensile strength of HIP bonded SS316L/Al-25 joints (HIP temperature : 980℃, 1030℃, 1050℃)

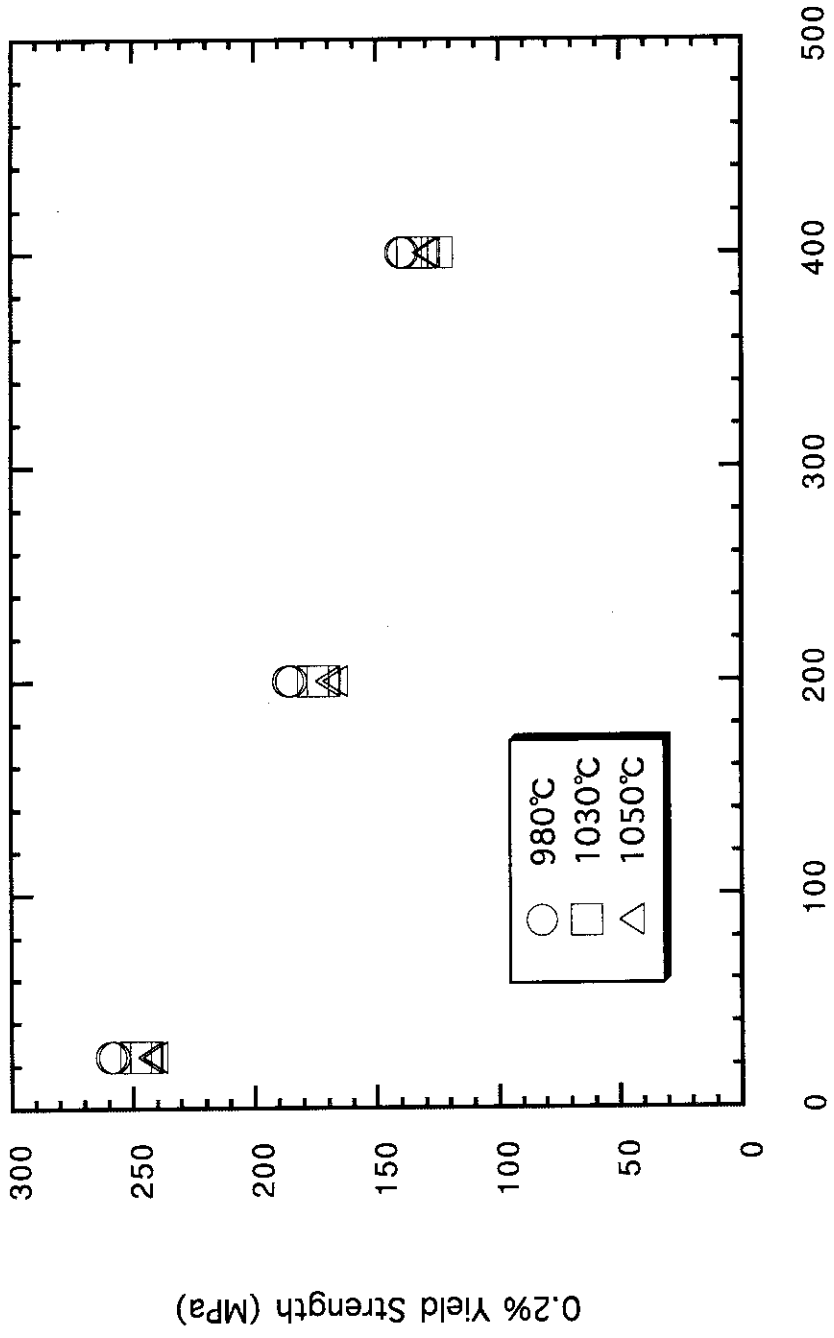

Fig. 2.4 0.2% yield strength of HIP bonded SS316L/Al-25 joints (HIP temperature : 980℃, 1030℃, 1050℃)

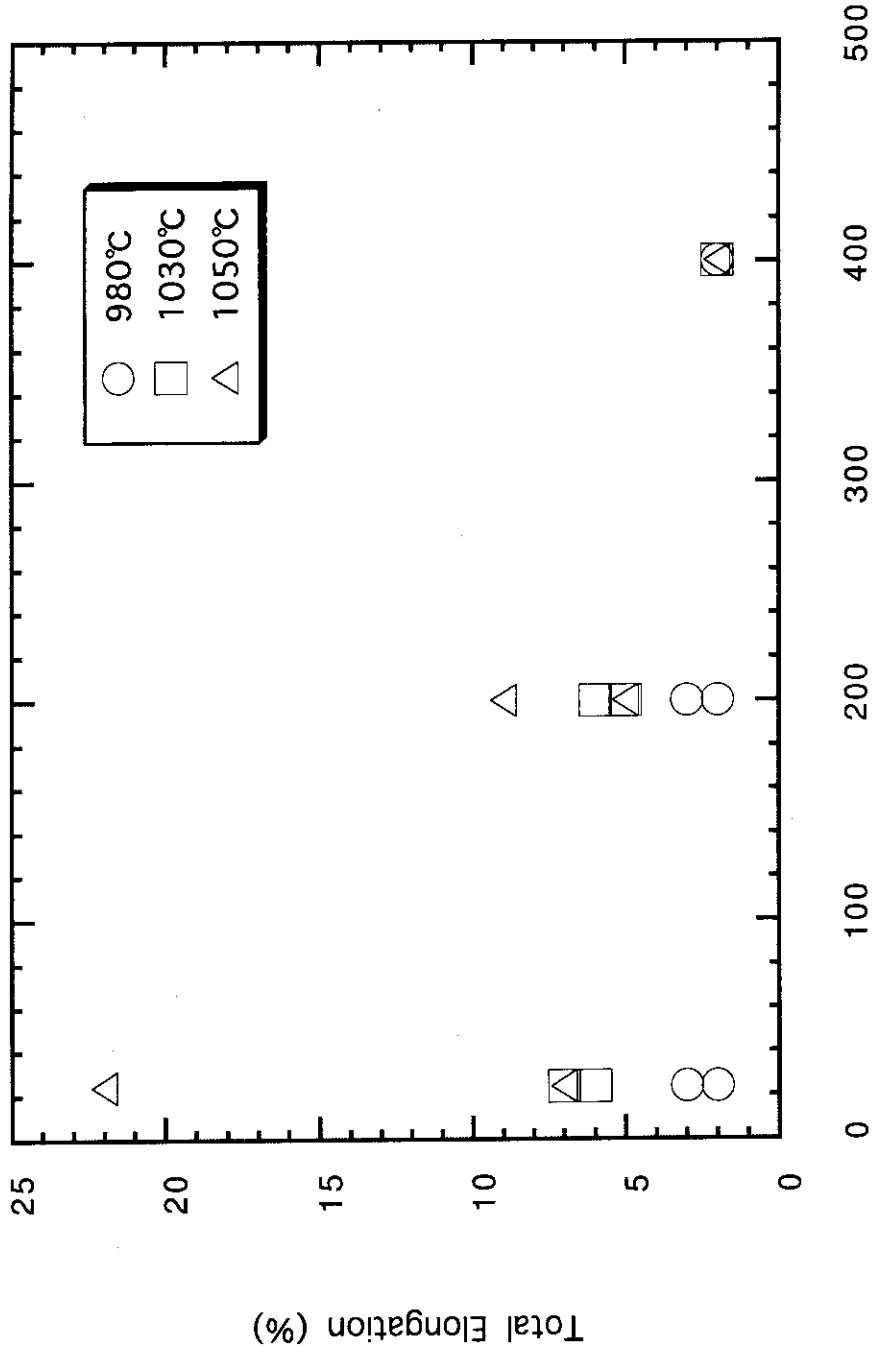

Fig. 2.5 Total elongation of HIP bonded SS316L/Al-25 joints (HIP temperature : 980℃, 1030℃, 1050℃)

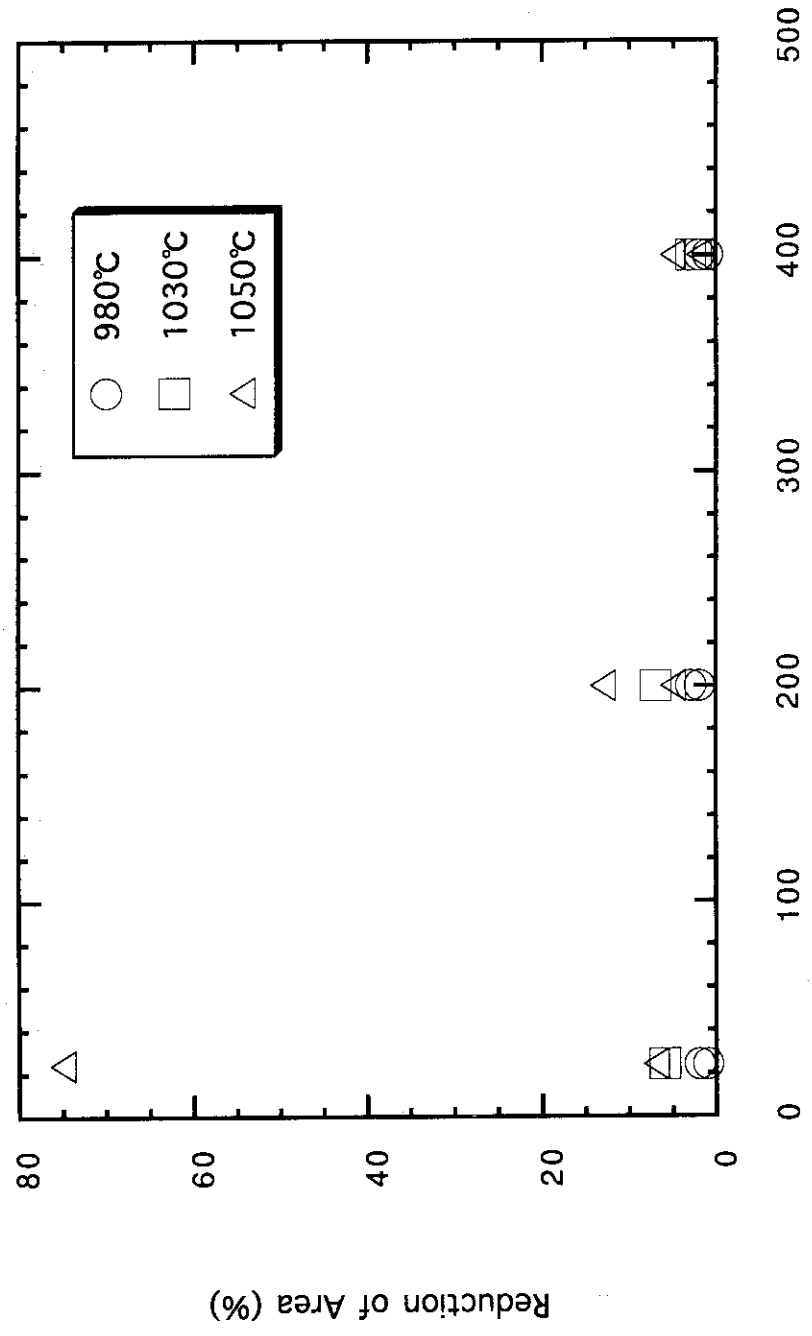

Fig. 2.6 Reduction of area of HIP bonded SS316L/Al-25 joints (HIP temperature : 980℃, 1030℃, 1050℃)

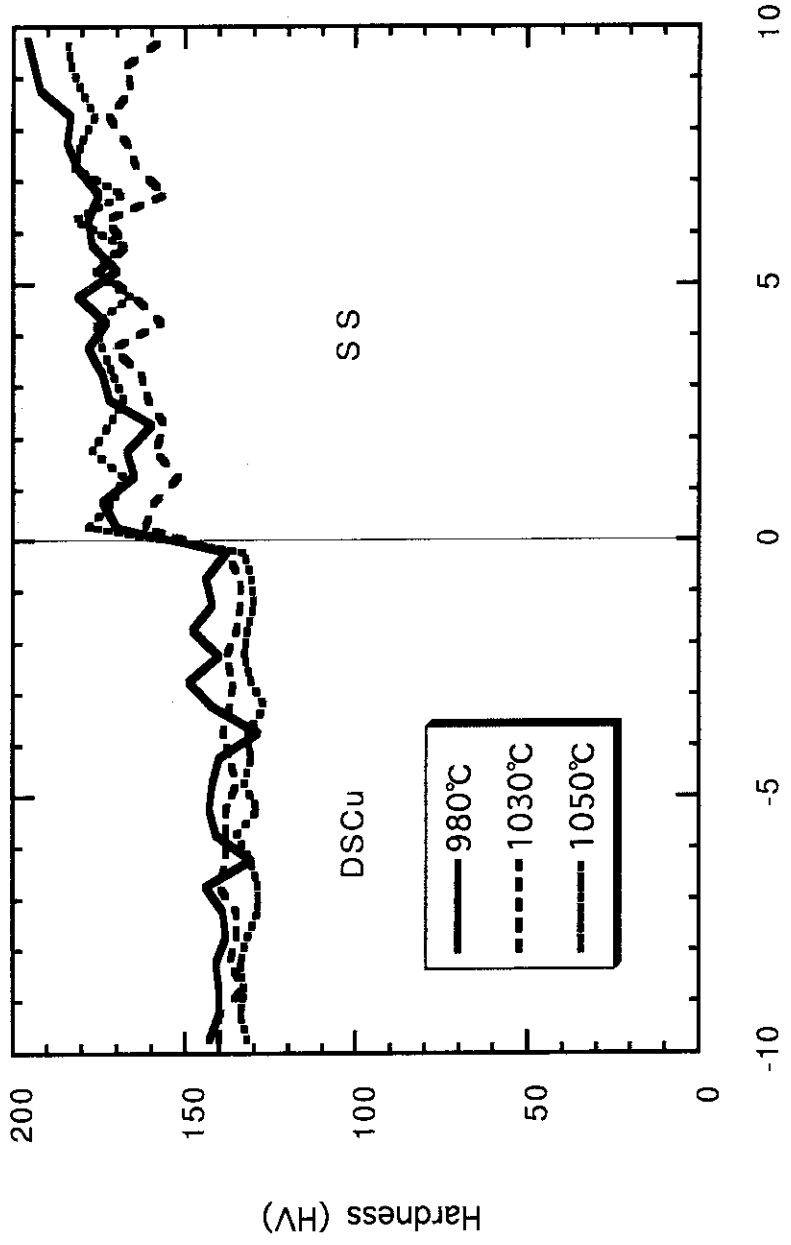

Fig. 2.7 Hardness of area of HIP bonded SS316L/Al-25 joints (HIP temperature : 980℃, 1030℃, 1050℃)

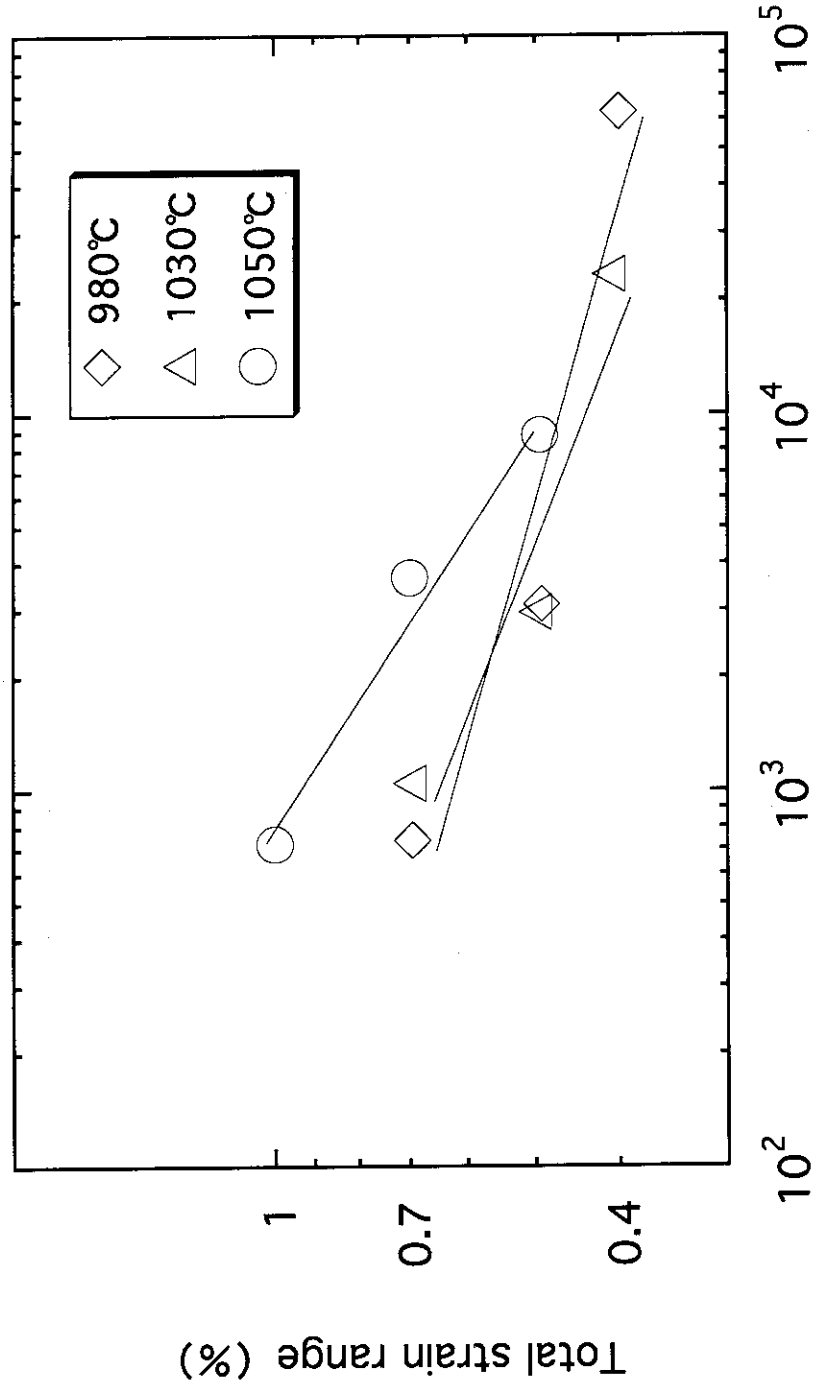

Fig. 2.8 Fatigue properties of HIP bonded SS316L/Al-25 joints (HIP temperature : 980℃, 1030℃, 1050℃)

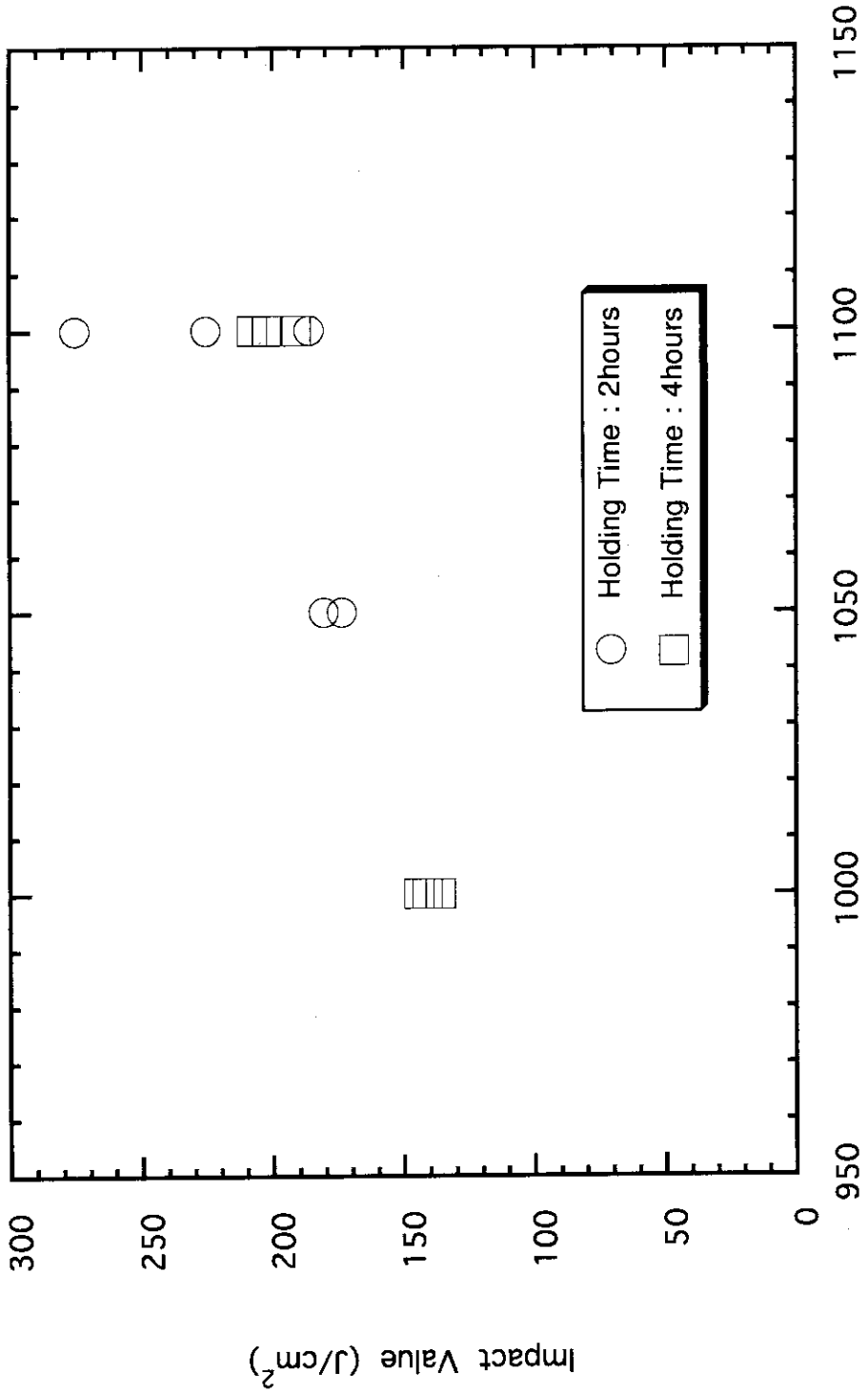

Fig. 2.9 Impact value of HIP bonded SS316L/SS316L joints (HIP temperature : 1000℃, 1050℃, 1100℃)

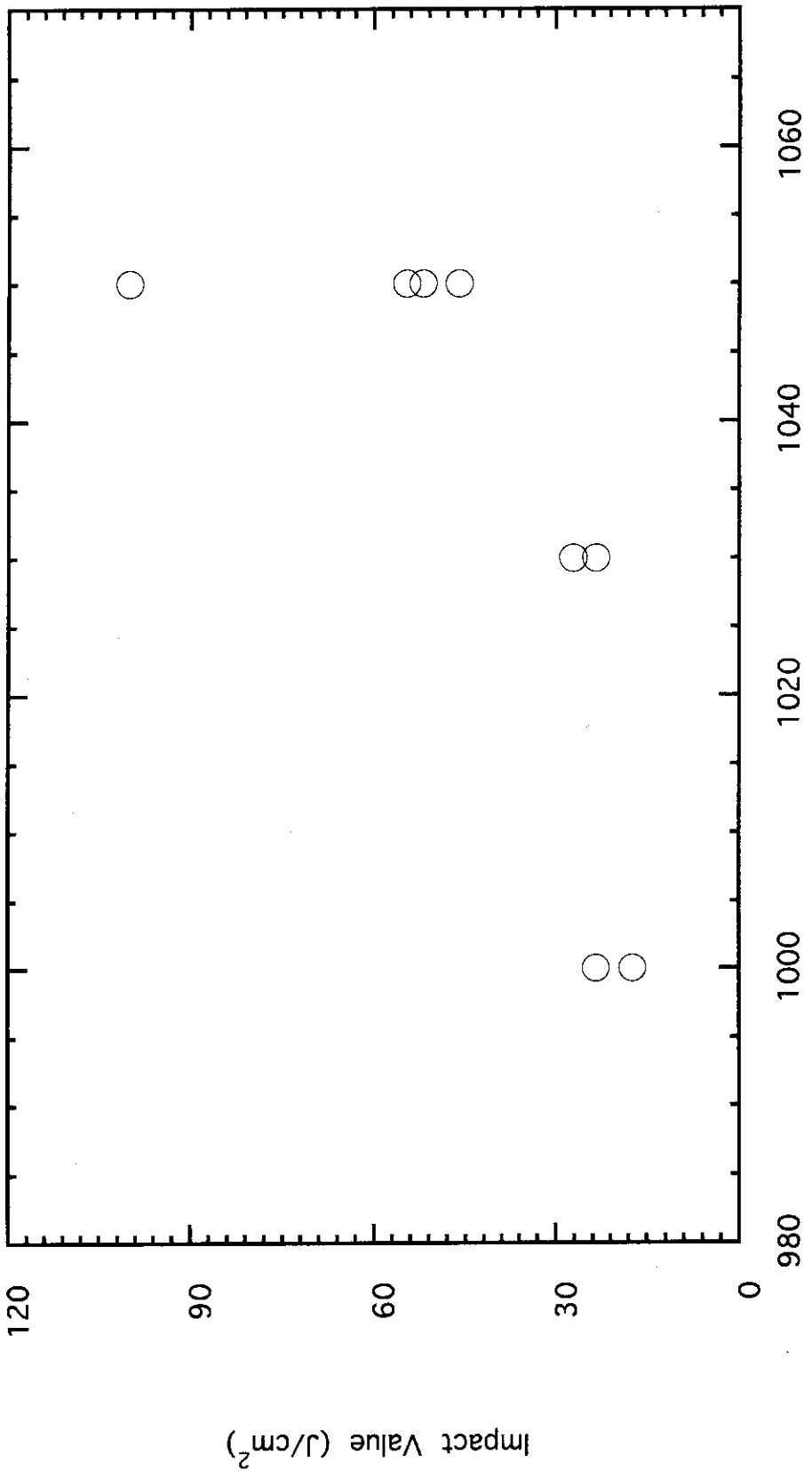

Fig. 2.10 Impact value of HIP bonded SS316L/Al-15 joints (HIP temperature : 1000℃, 1030℃, 1050℃)

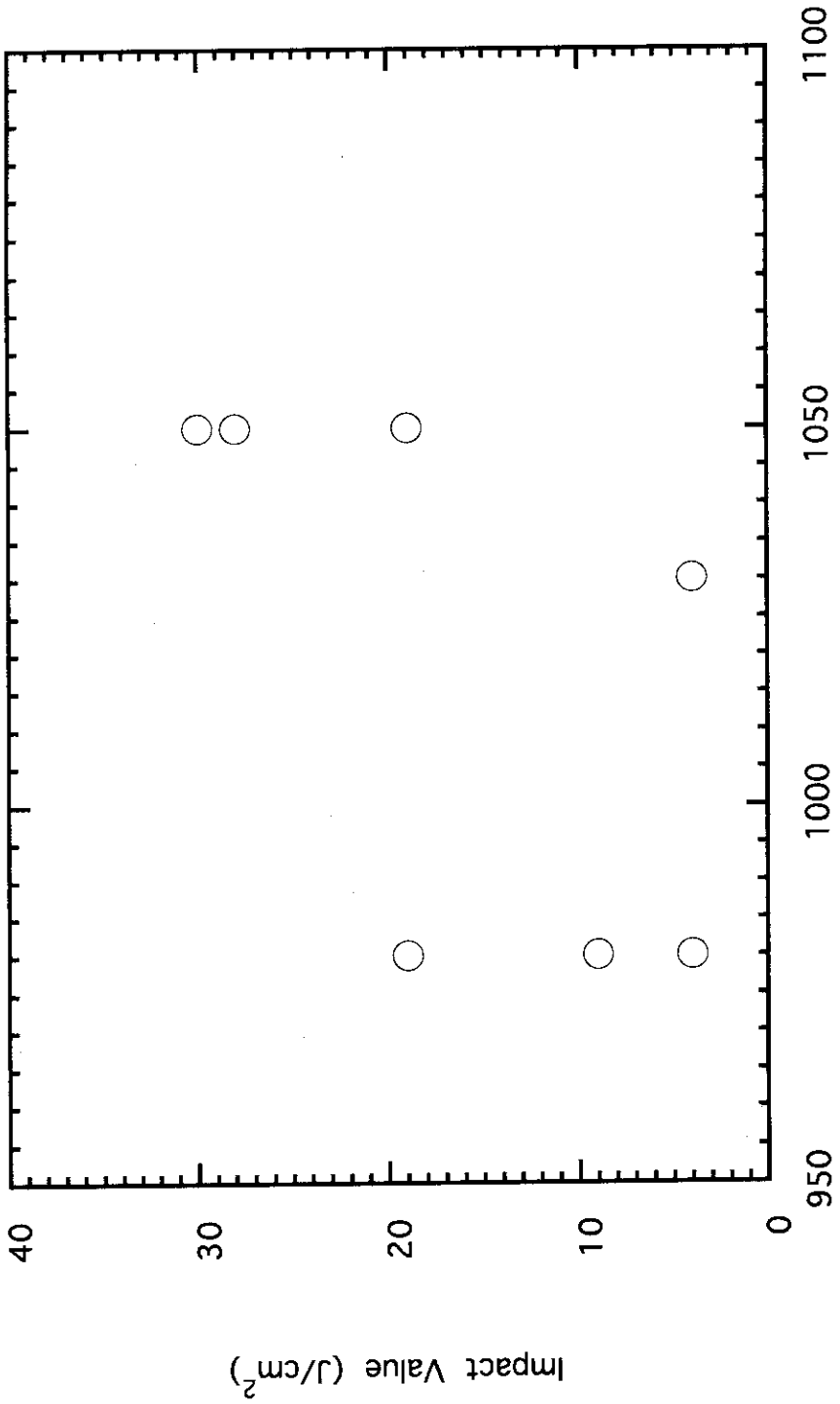

Fig. 2.11 Impact value of HIP bonded SS316L/Al-25 joints (HIP temperature : 980℃, 1030℃, 1050℃)

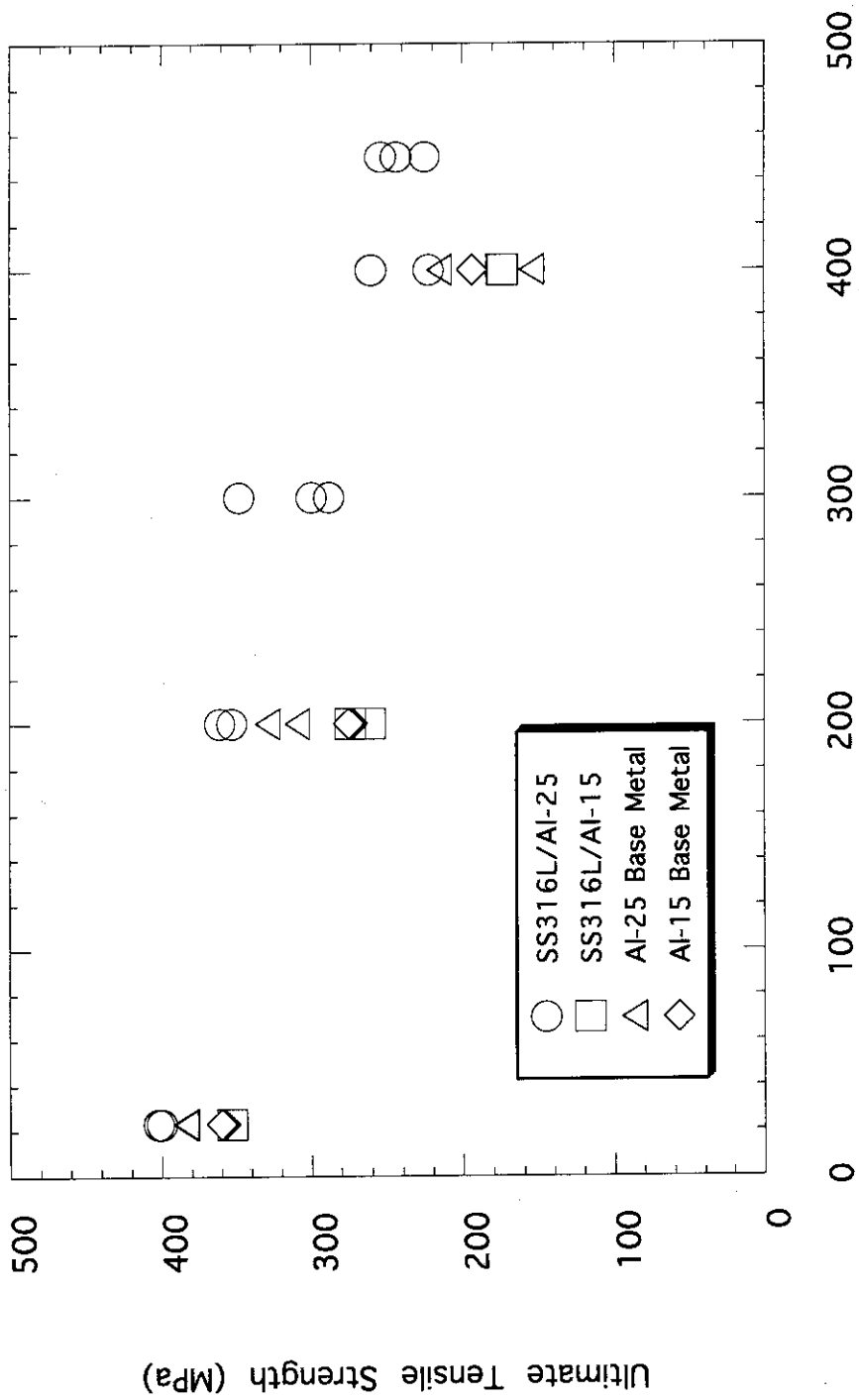

Fig. 3.1.1 Ultimate tensile strength of HIP bonded SS316L/Al-15 and SS316/Al-25, and base metals of Al-15 and Al-25

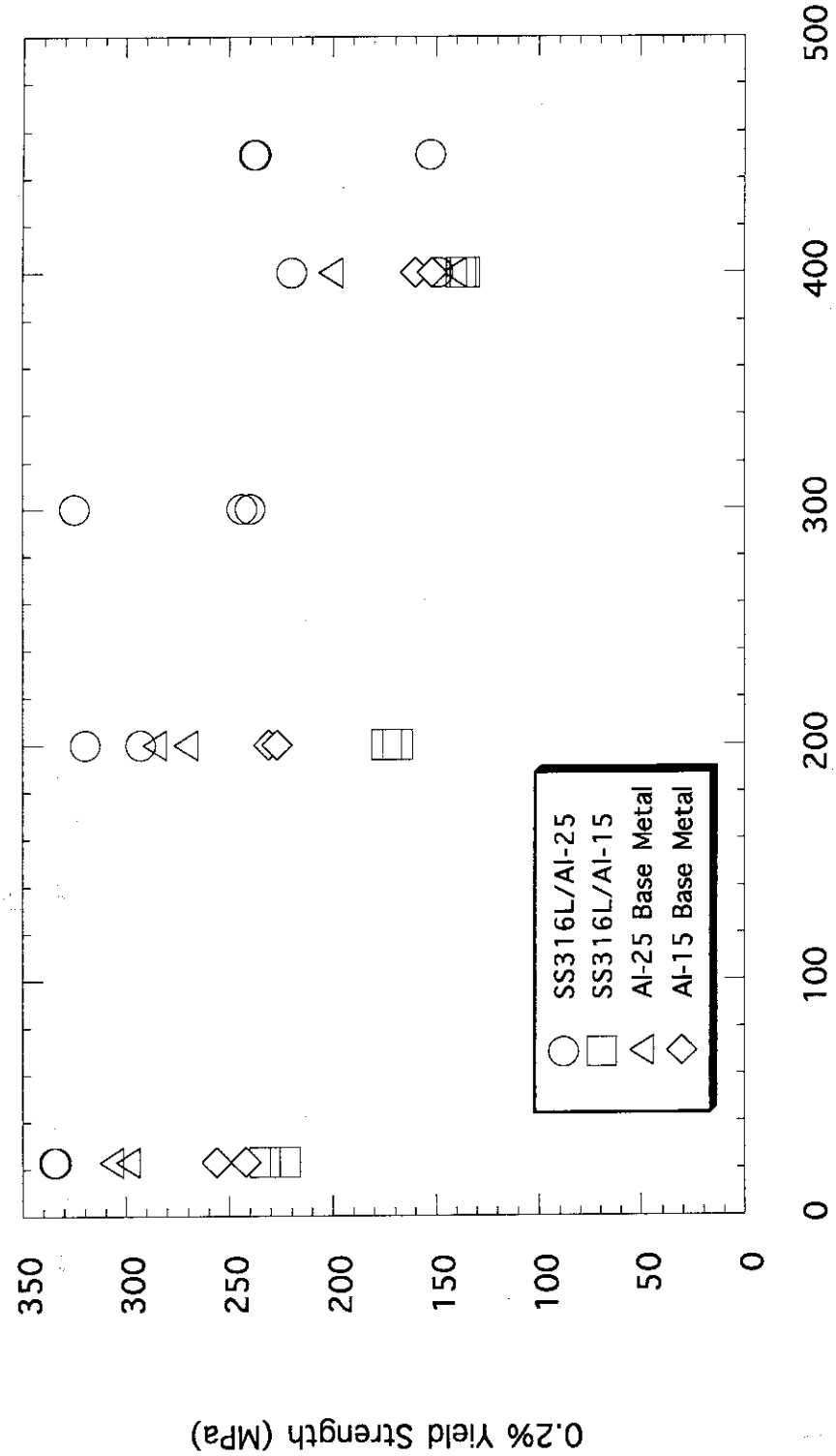

Fig. 3.1.2 0.2% Yield strength of HIP bonded SS316/Al-15 and SS316/Al-25, and base metals of Al-15 and Al-25

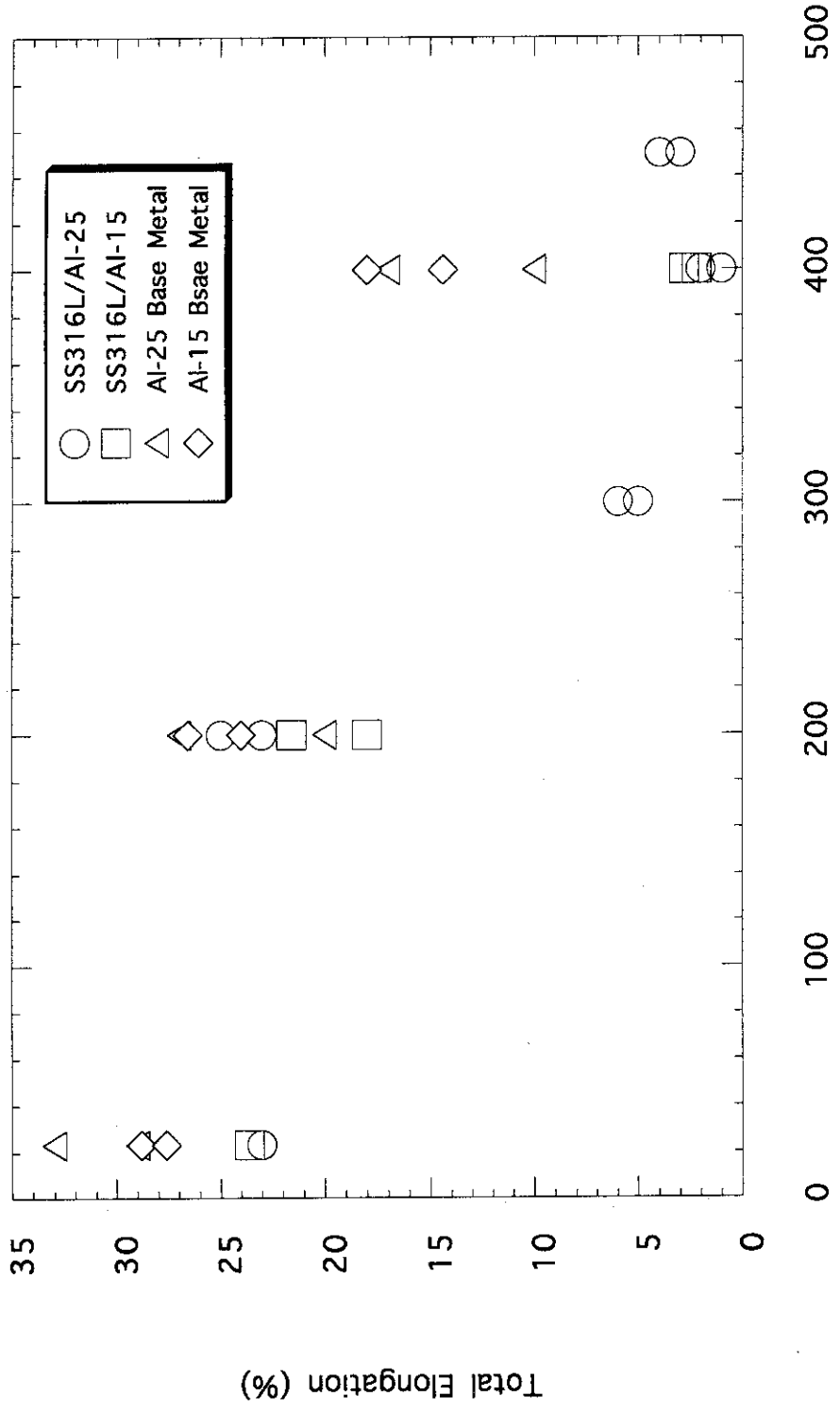

Fig. 3.1.3 Total elongation of HIP bonded SS316L/Al-15 and SS316L/Al-25, and base metals of Al-15 and Al-25

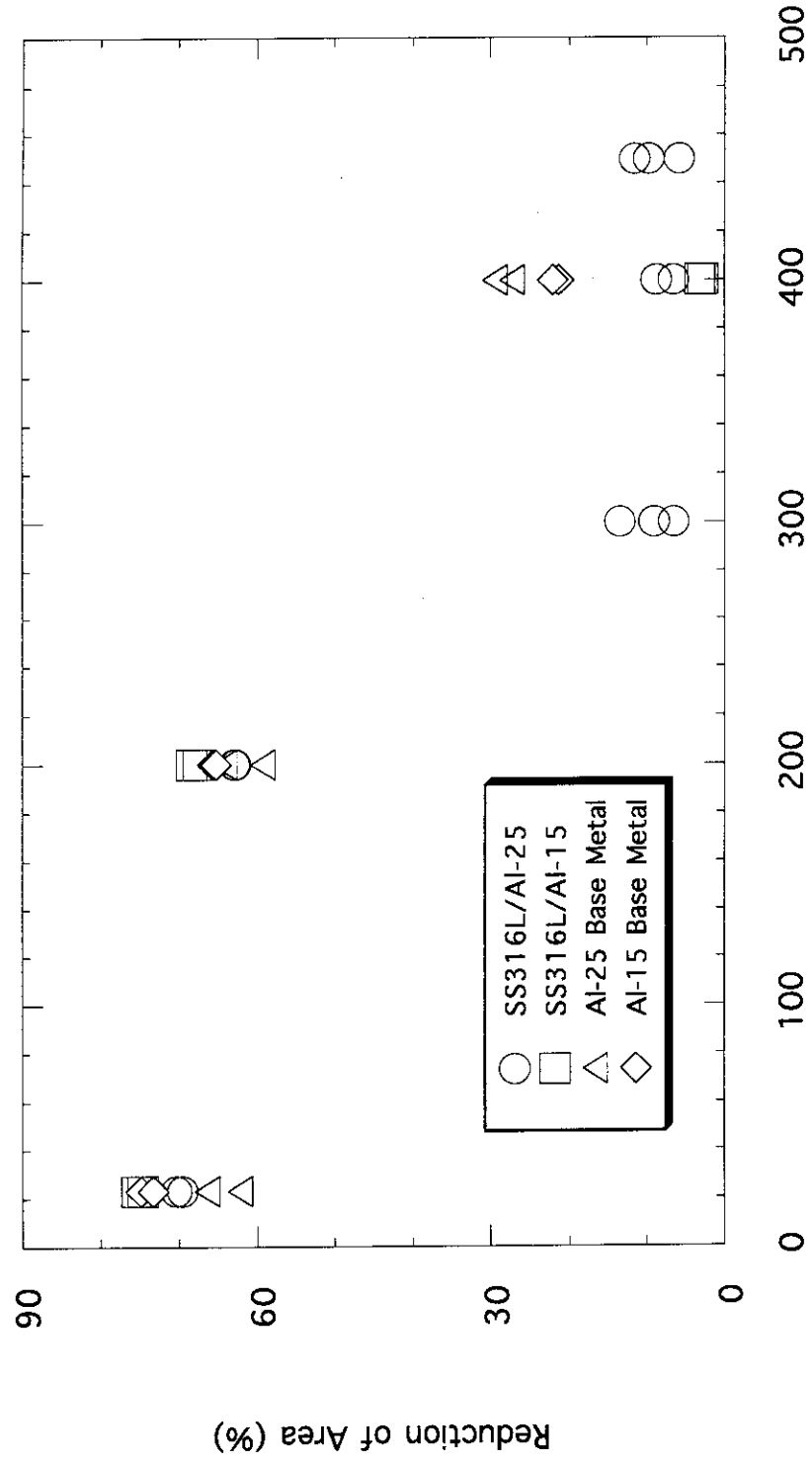

Fig. 3.1.4 Reduction of area of HIP bonded SS316L/Al-15 and SS316L/Al-25, and base metals of Al-15 and Al-25

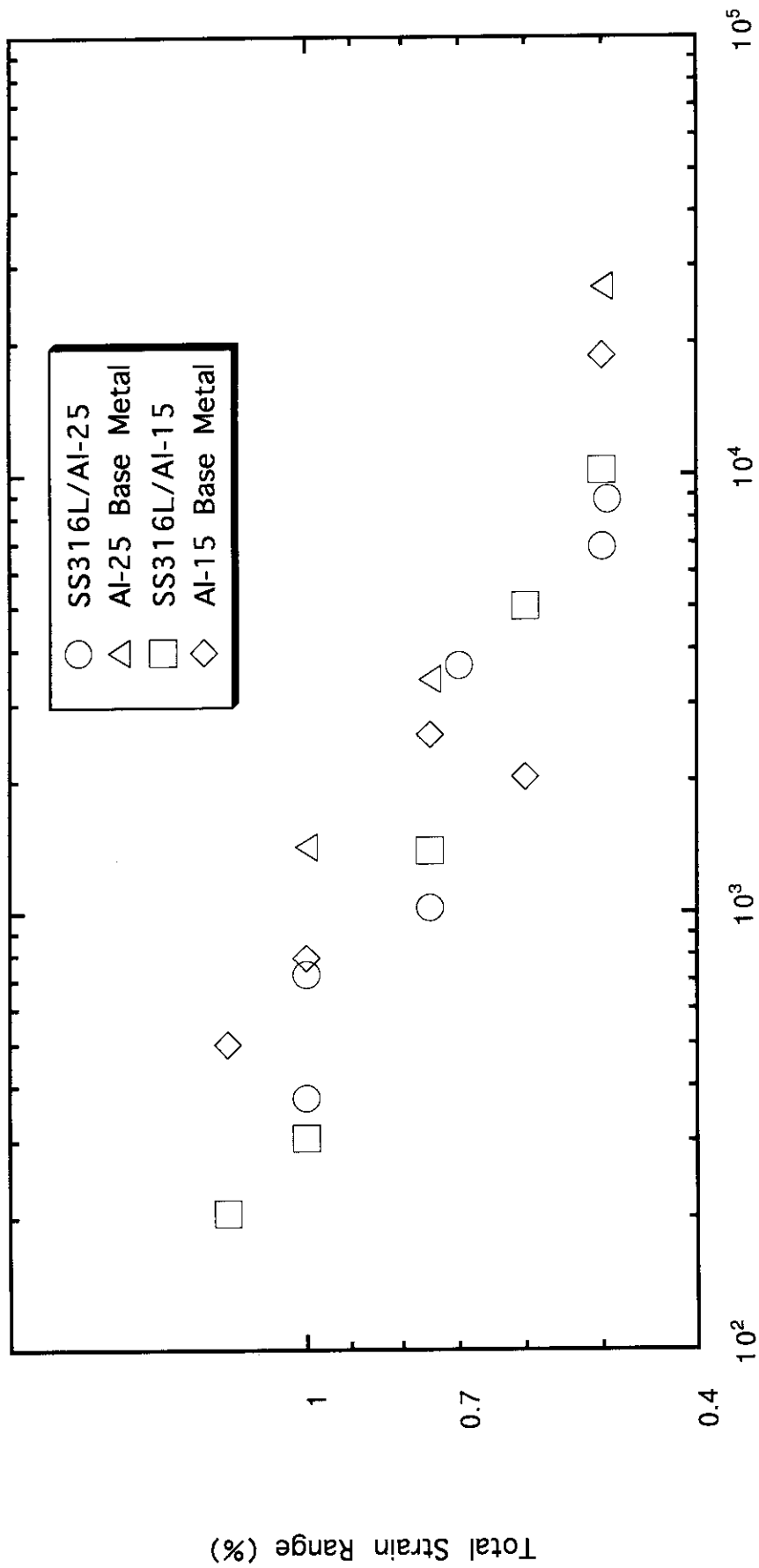

Fig. 3.1.5 Fatigue properties of HIP bonded SS316L/Al-15 and SS316L/Al-25, and base metals of Al-15 and Al-25

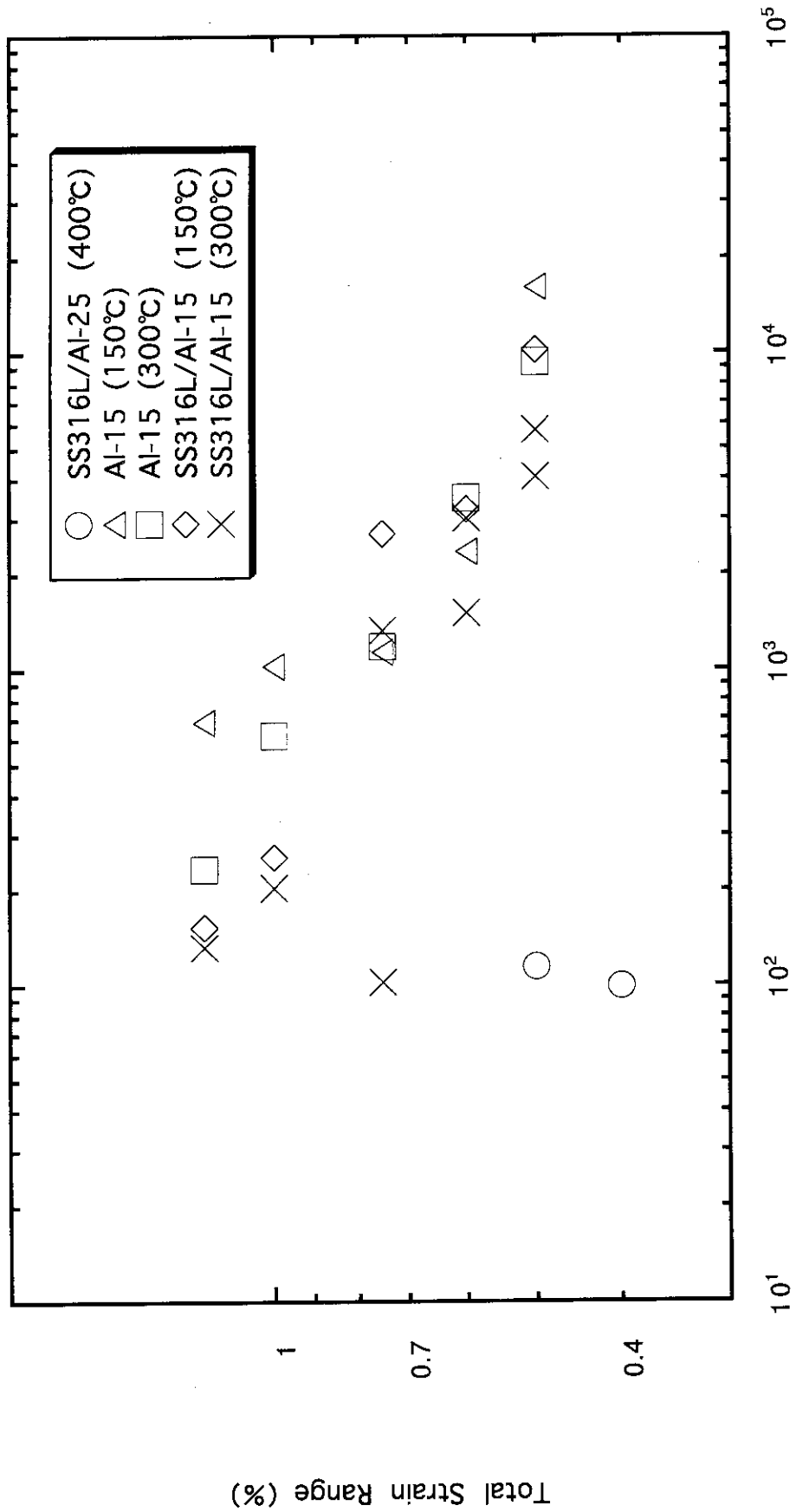

Fig. 3.1.6 Fatigue properties of HIP bonded SS316L/Al-15 and SS316L/Al-25, and base metals of Al-15 and Al-25 (Tested at elevated temperatures)

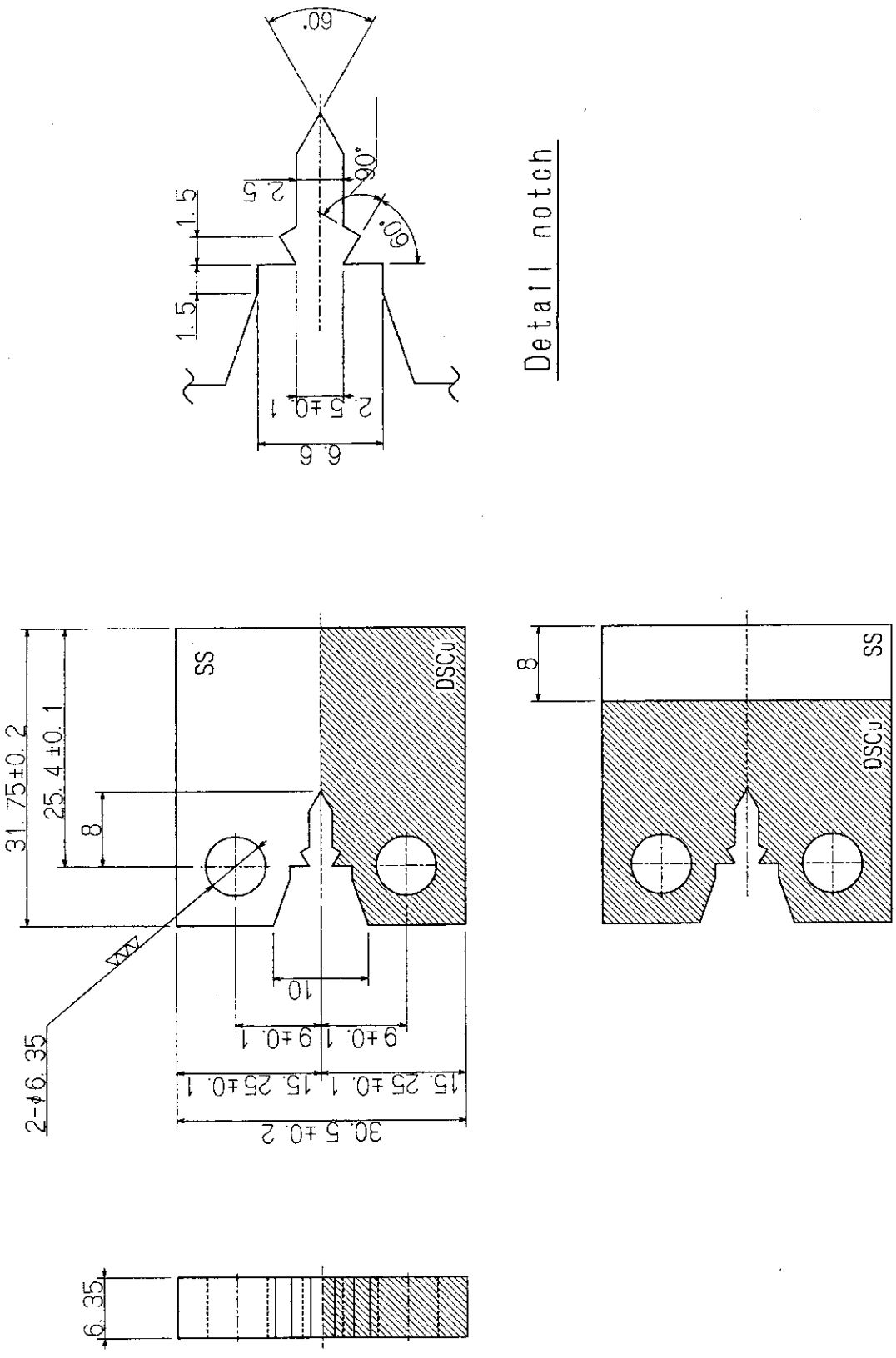

Fig. 3.1.7 Shape of crack propagation test specimen (unit: mm)

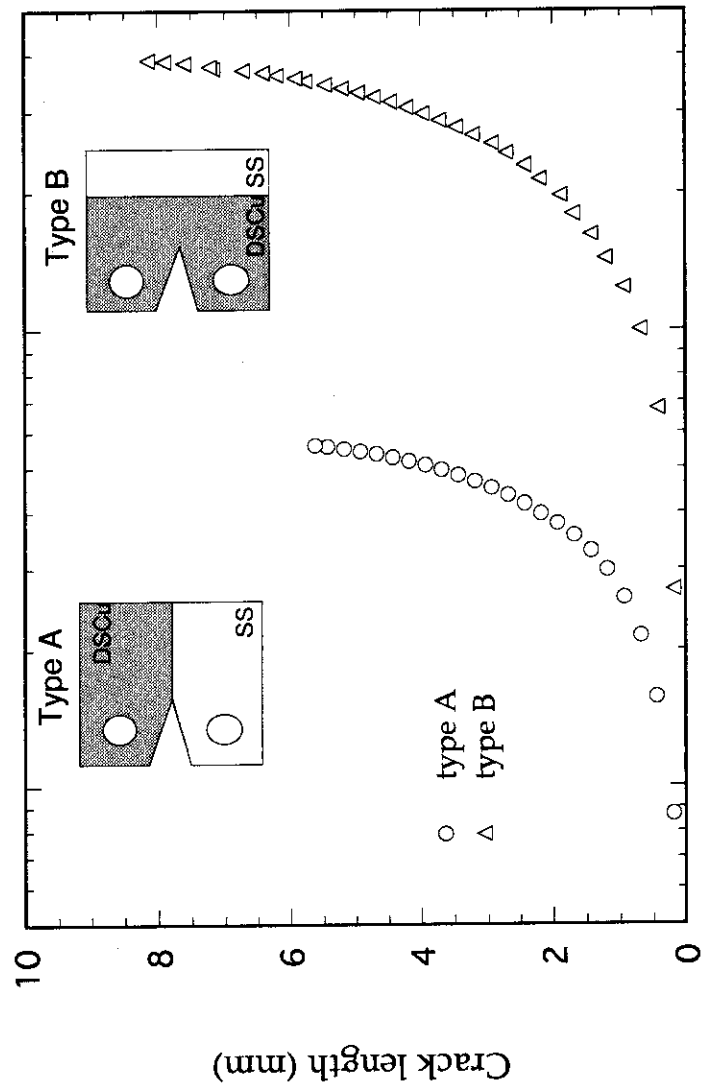

Fig. 3.1.8 Relationship between cycle and crack length

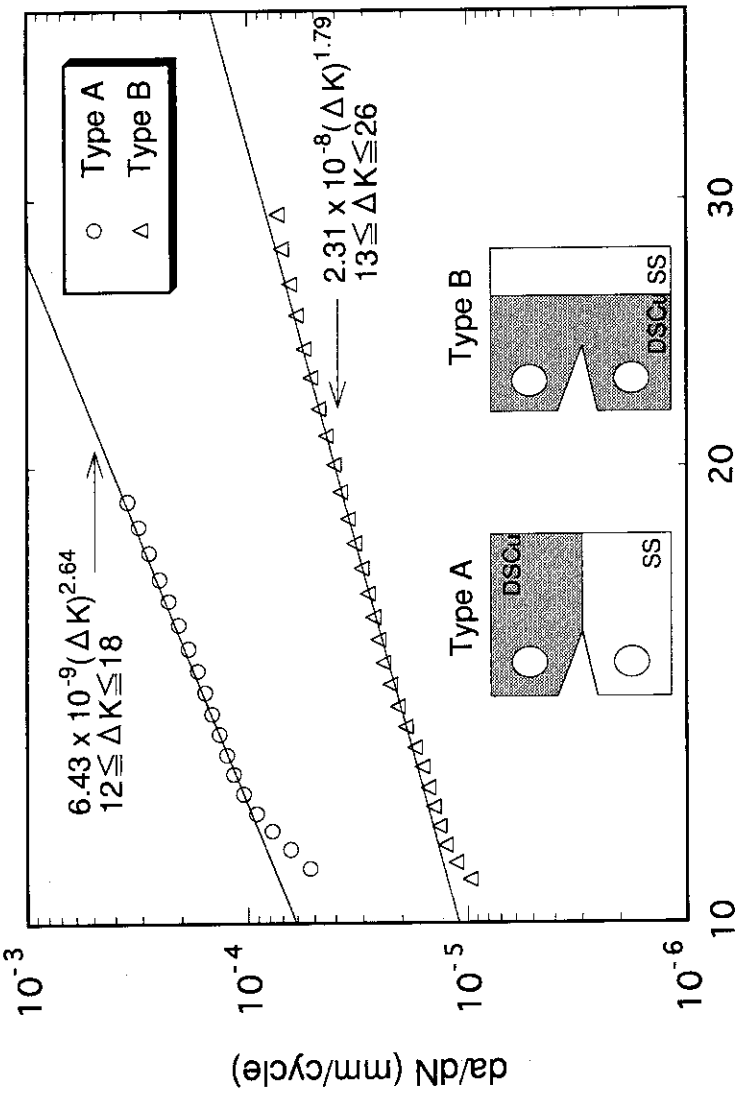

Fig. 3.1.9 da/dN versus ΔK of HIPped joint

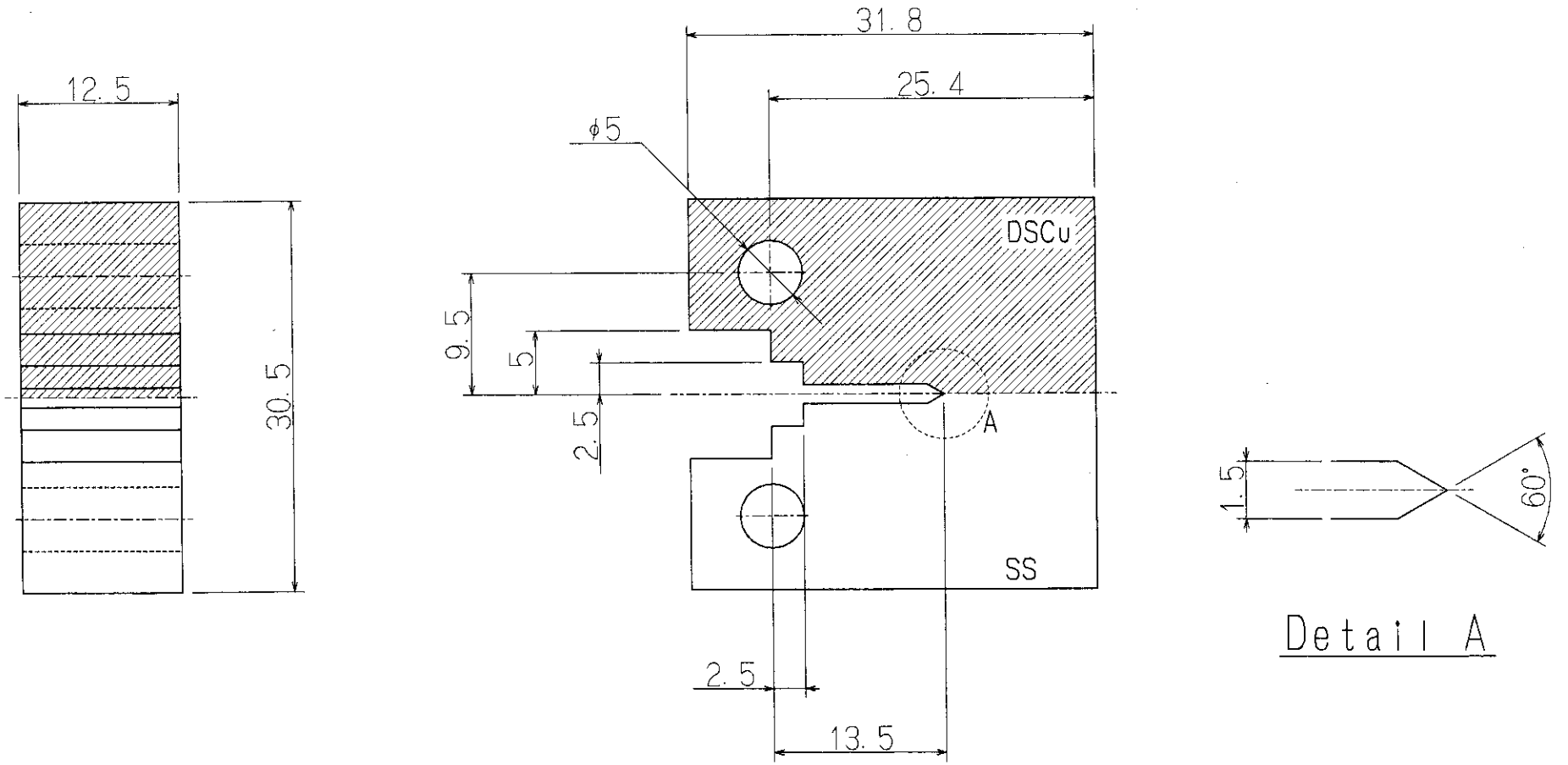

Fig. 3. 1. 10 Shape of fracture toughness test specimen

(unit:mm)

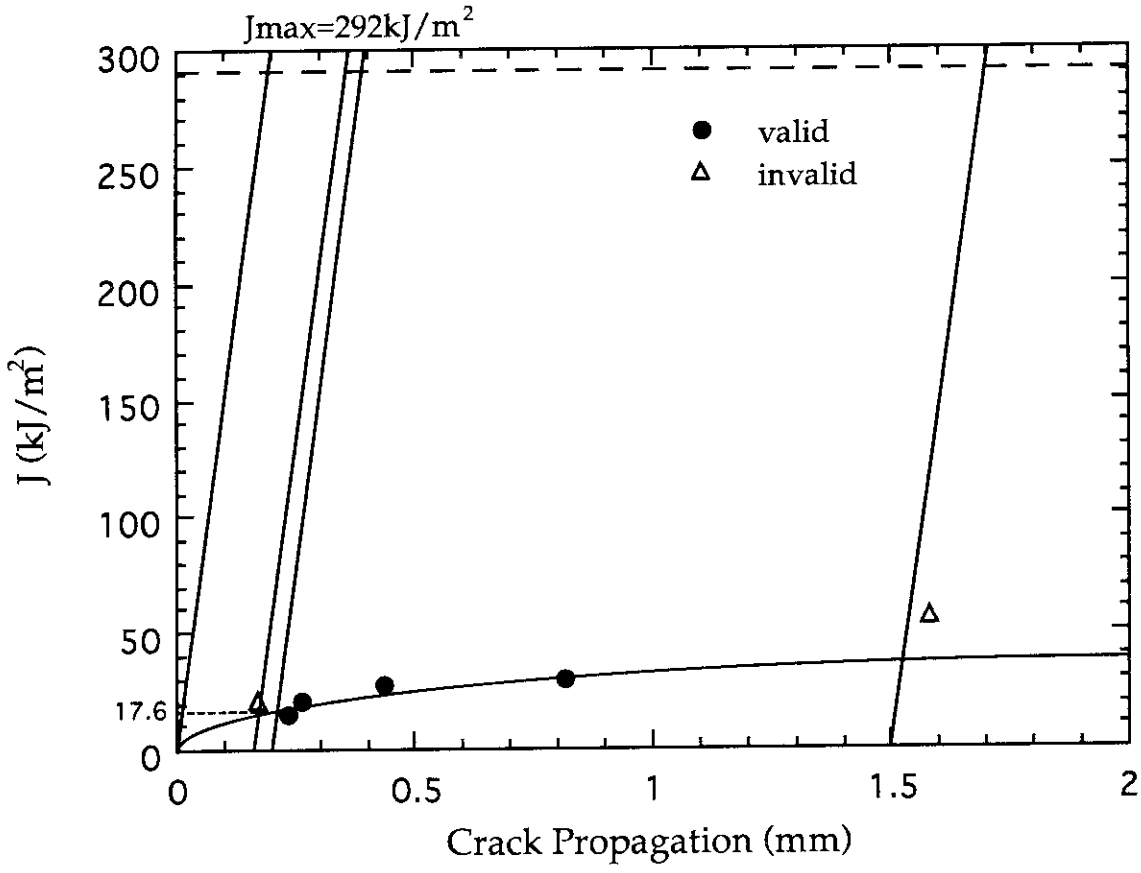

Fig. 3.1.11 J versus crack propagation of HIPped joint

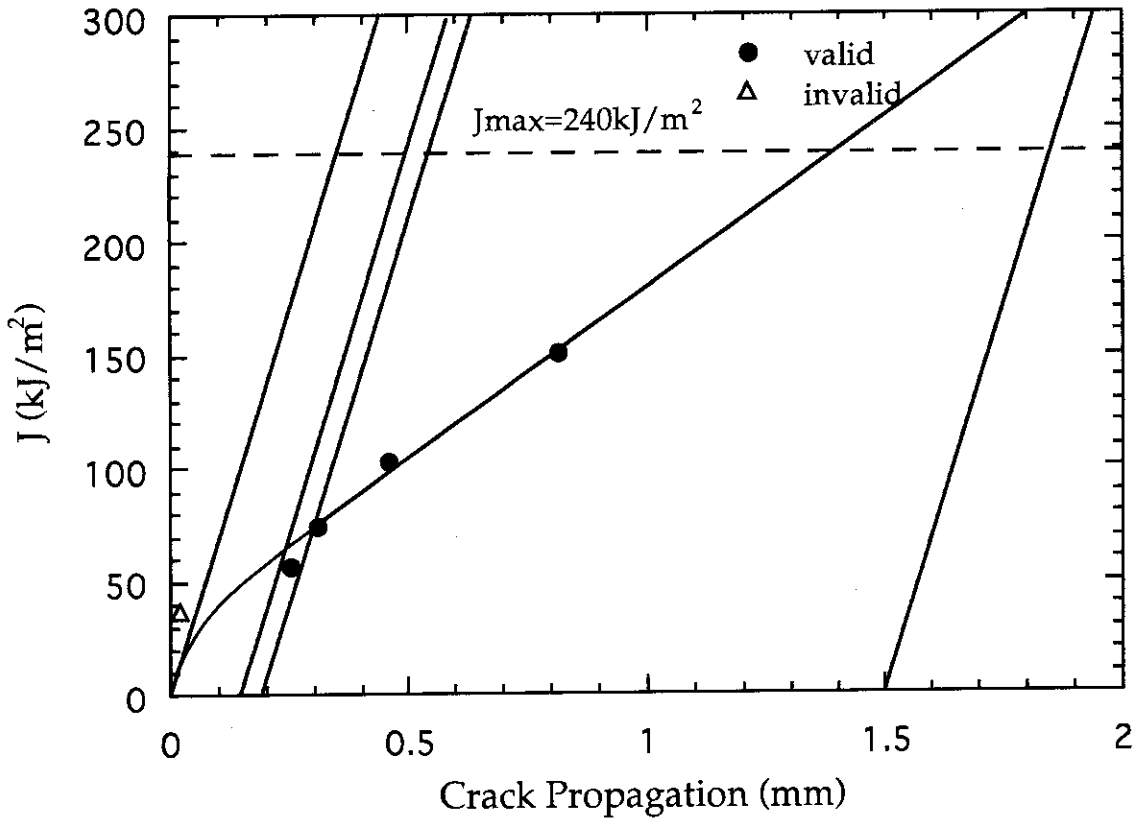

Fig. 3.1.12 J versus crack propagation of DSCu base metal

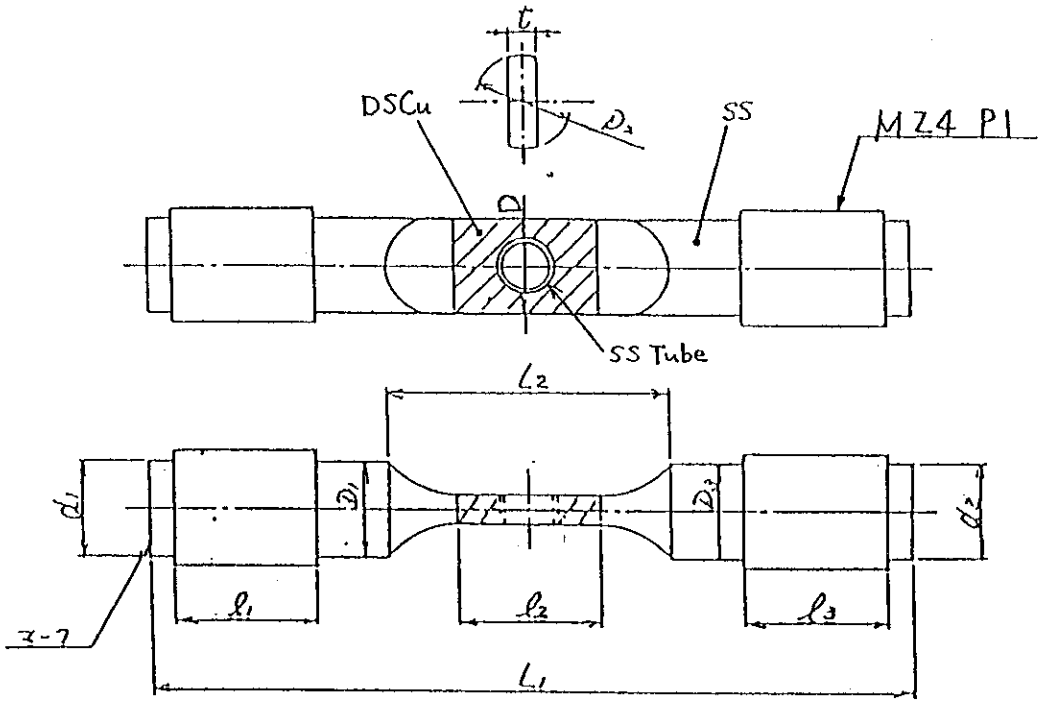

Measurement of test piece

Test piece		L_1	L_2	l_1	l_2	l_3	t	D_1	D_2	D_3	d_1	d_2	D
nominal value		160	60.4	30	30	30	6	20	20	20	19.8	19.8	10
allowable error		±0.2	±0.15	±0.15	±0.15	±0.15	±0.01	±0.01	±0.01	±0.01	0 −0.5	0 −0.5	
Test piece No.	1	160.00	60.41	30.05	30.00	30.06	5.995	19.995	19.995	19.995	19.700	19.770	10.19
	2	160.00	60.40	30.05	30.00	30.08	6.010	20.000	20.000	20.000	19.680	19.710	10.17
	3	160.00	60.40	30.07	30.00	30.02	6.005	20.000	20.000	20.000	19.685	19.665	10.21
	4	159.99	60.40	30.06	30.00	29.99	6.010	20.005	20.005	20.005	19.680	19.670	10.20
	5	160.00	60.40	30.01	30.00	30.05	6.005	20.000	20.000	20.000	19.660	19.665	10.19

Fig. 3.2.1 Shape and result of dimension measurement on test pieces

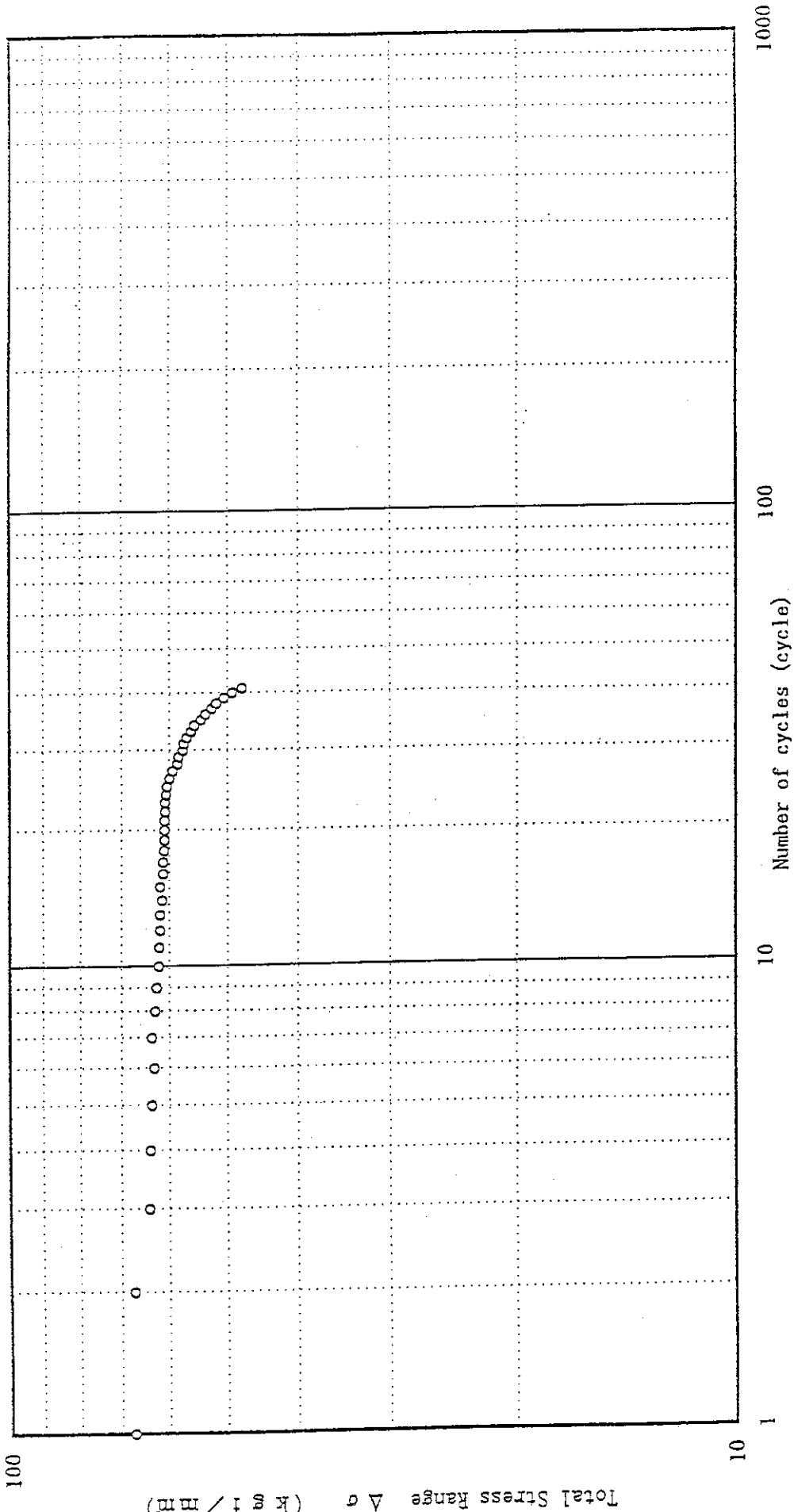

Fig. 3.2.2 Variation of total stress range (Test piece No. 1, $\Delta\varepsilon t = 1.0\%$)

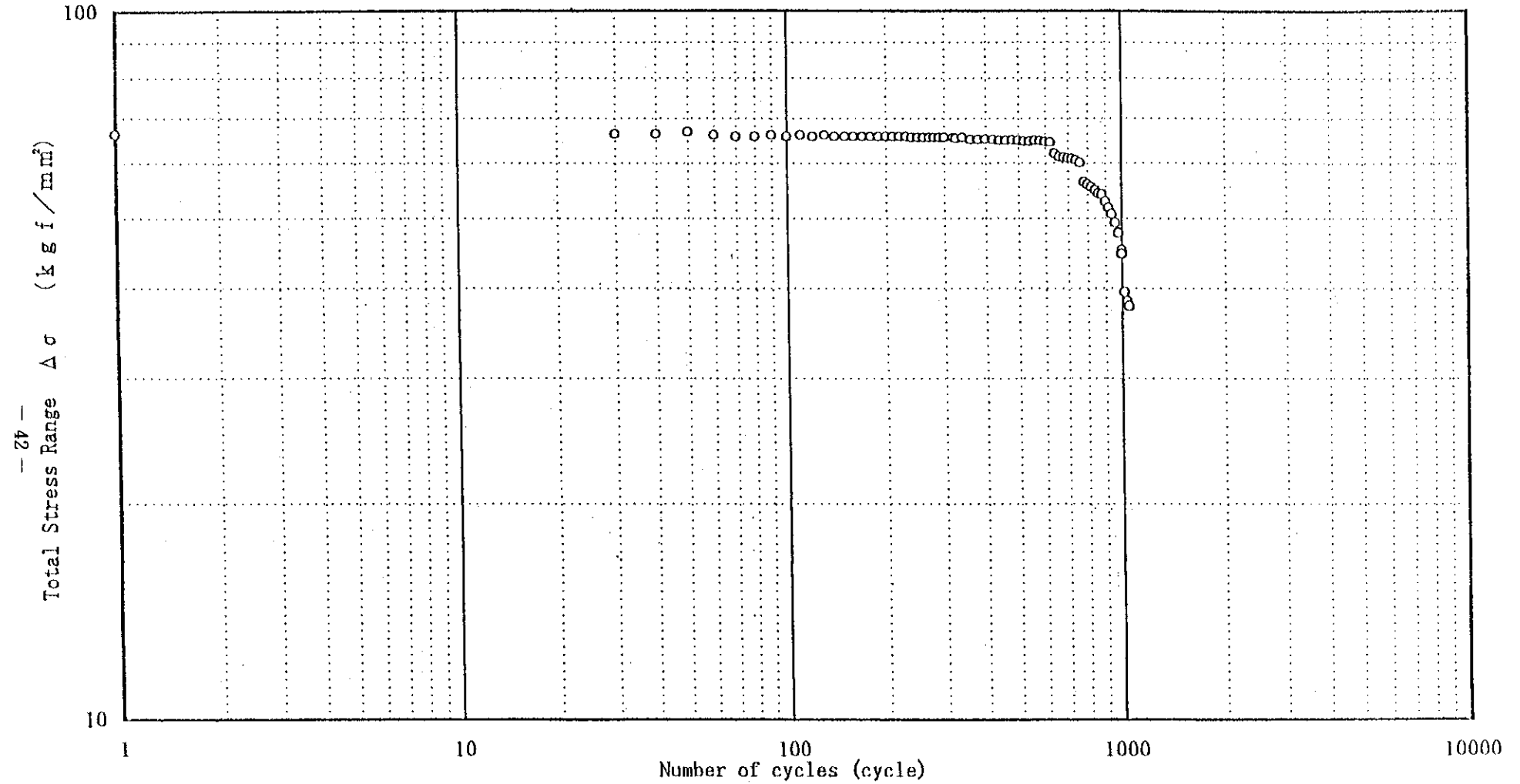

Fig. 3.2.3 Variation of total stress range (Test piece No. 2, $\Delta\varepsilon t = 0.7\%$)

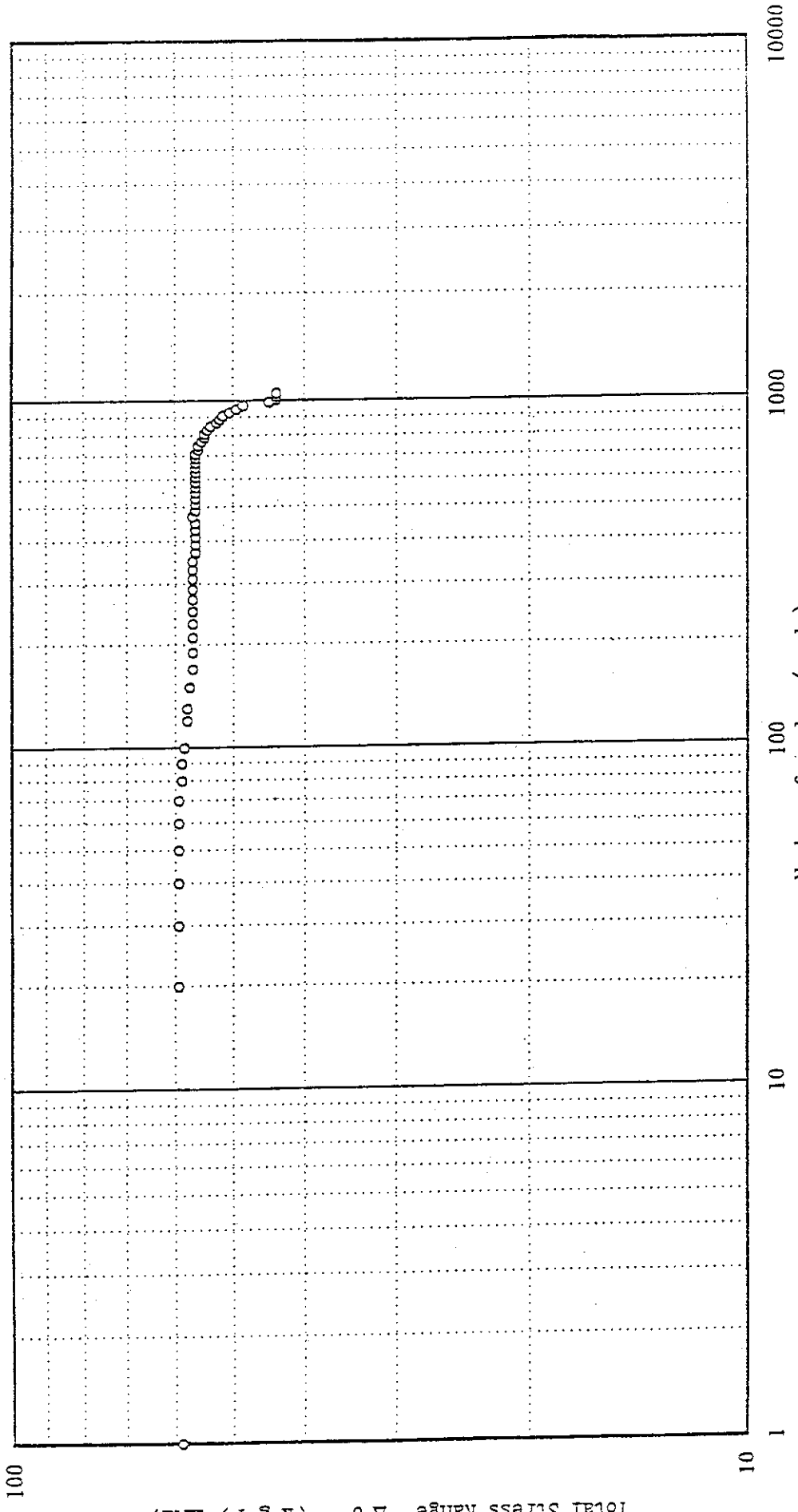

Fig. 3.2.4 Variation of total stress range (Test piece No. 3, $\Delta\varepsilon t = 0.5\%$)

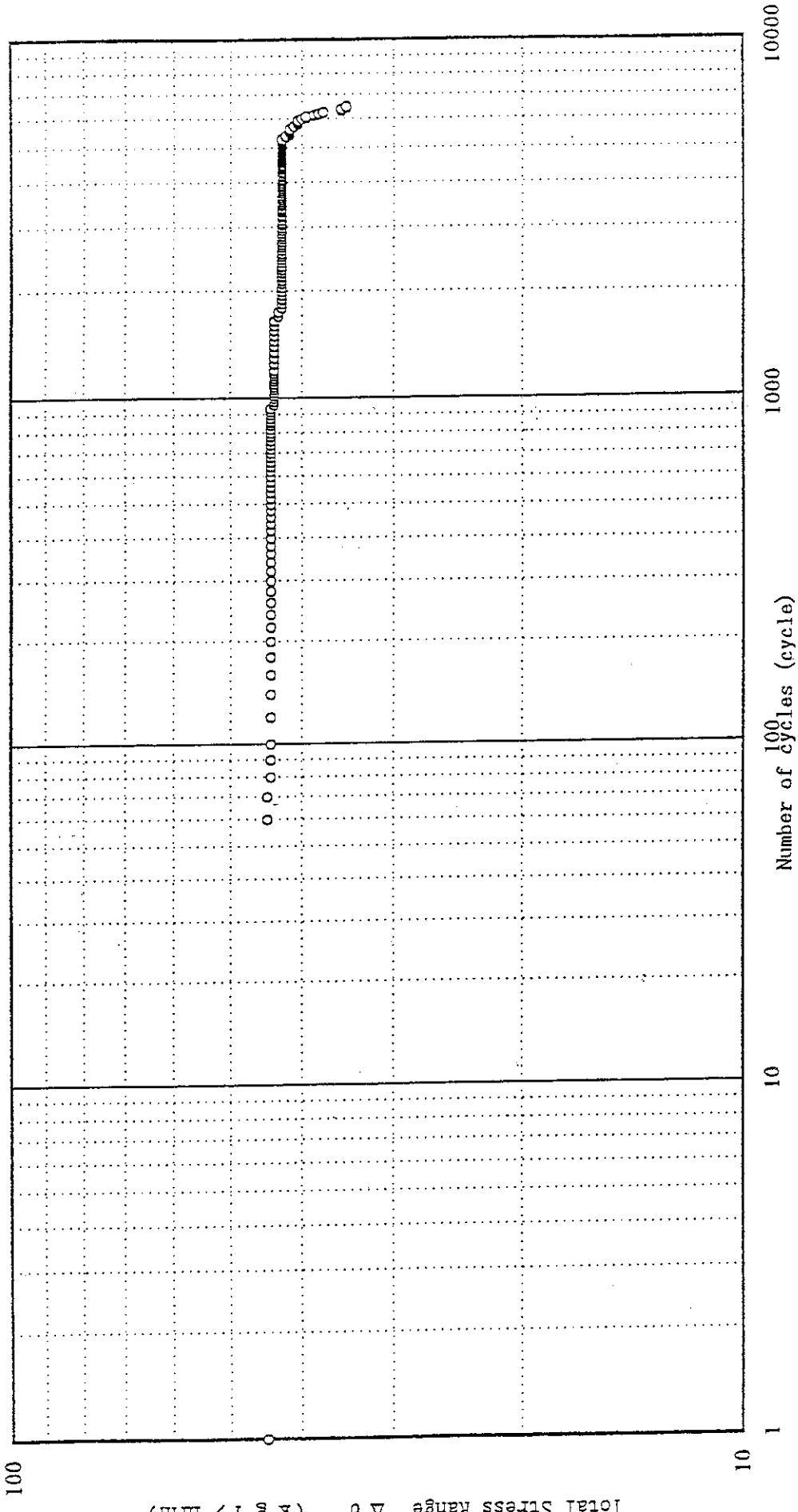

Fig. 3.2.5 Variation of total stress range (Test piece No. 4, $\Delta\varepsilon t = 0.3\%$)

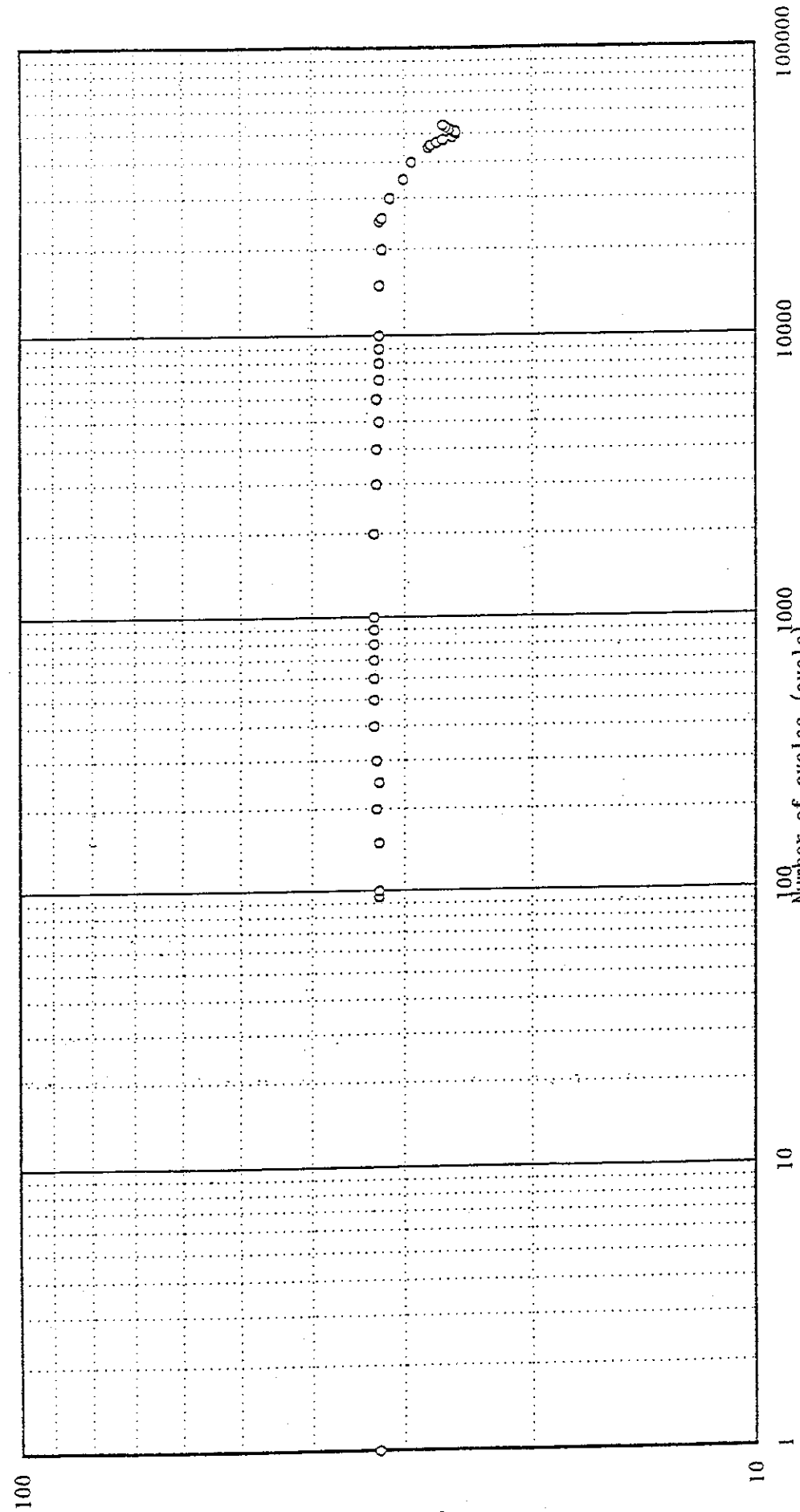

Fig. 3.2.6 Variation of total stress range (Test piece No. 5, $\Delta\varepsilon t = 0.2\%$)

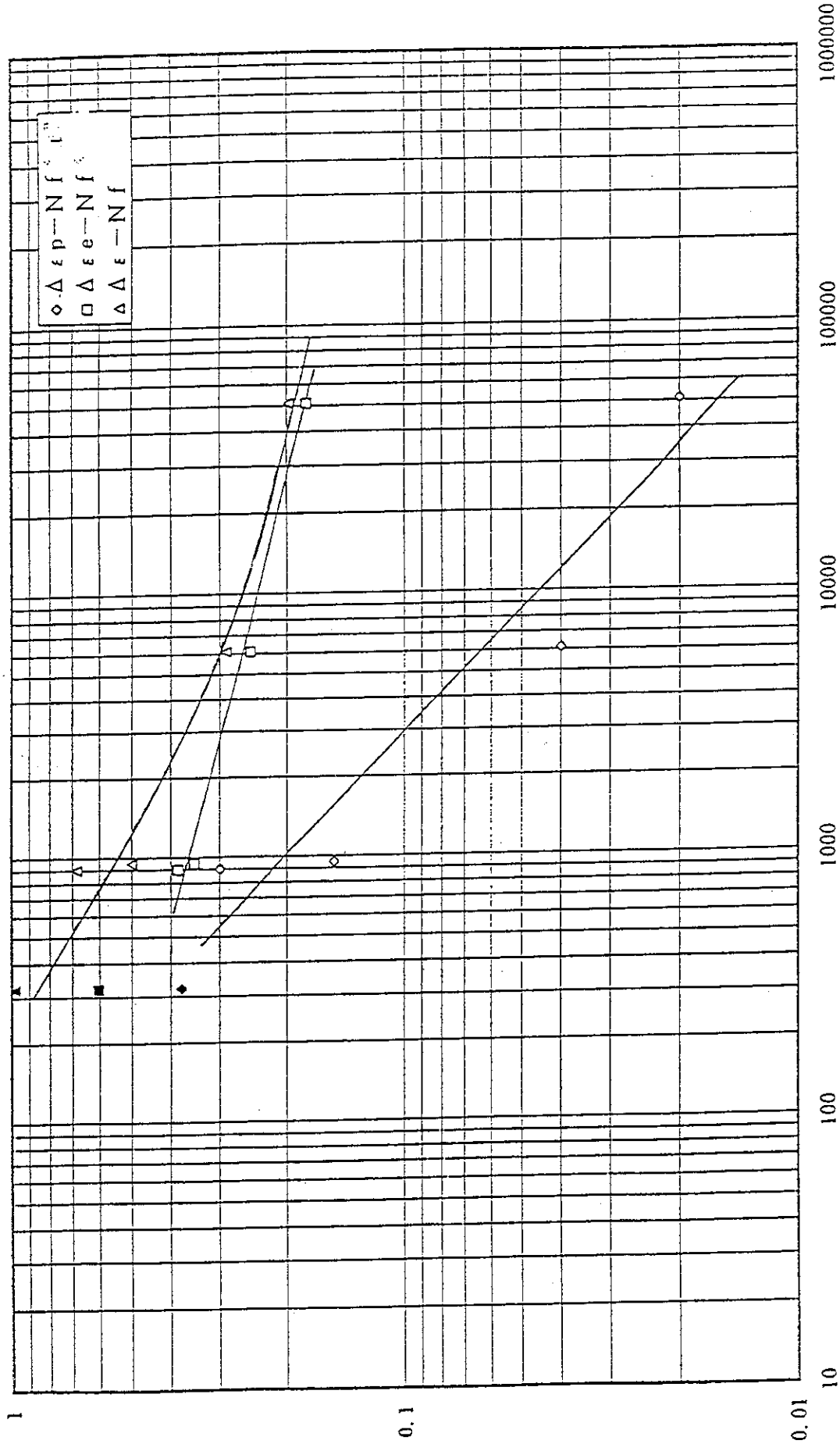

Fig. 3.2.7 Relation between plastic, elastic strain ranges and number of cycles to failure

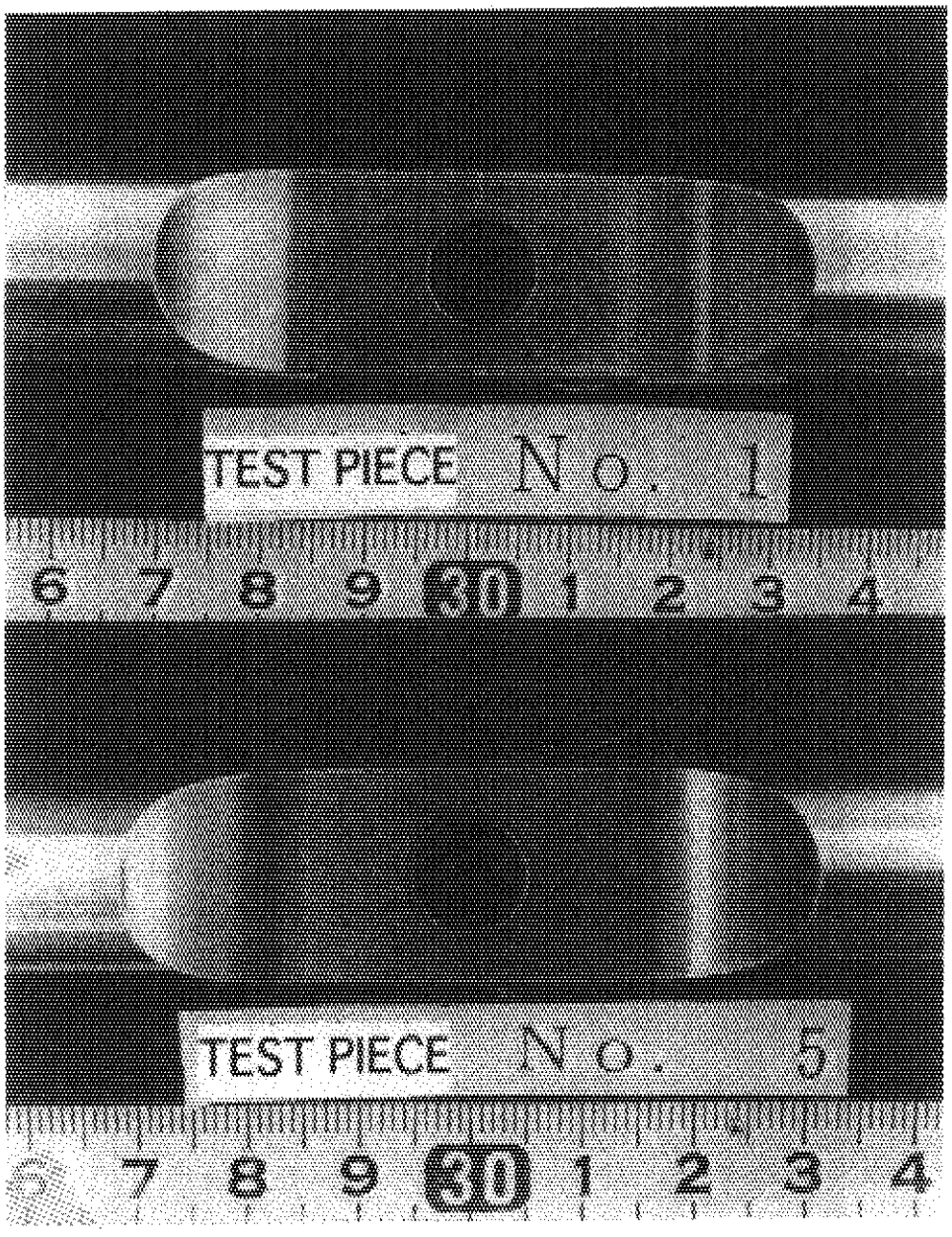

Fig. 3.2.8 The HIPped structural model after fatigue test (1)

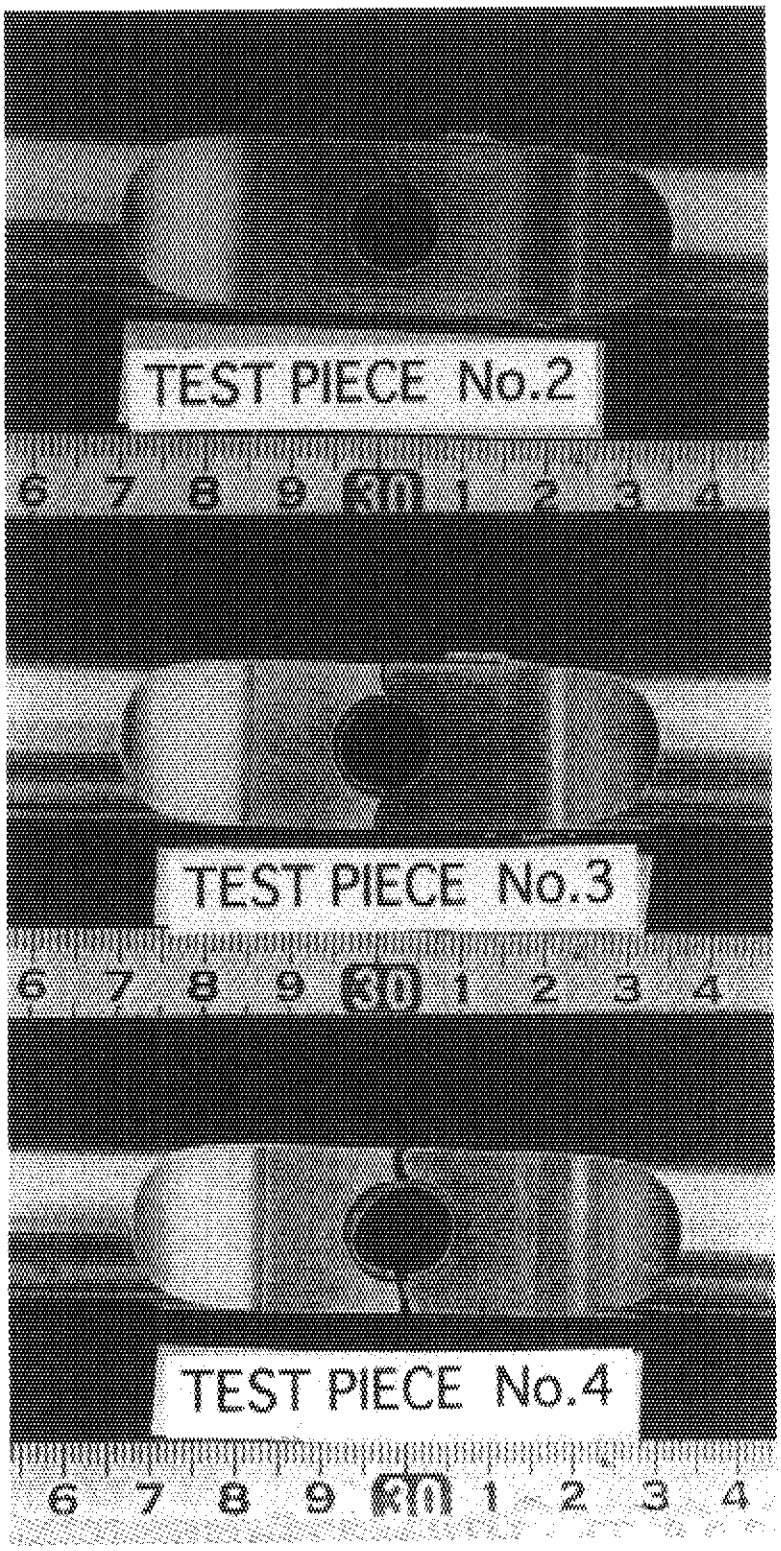

Fig. 3.2.9 The HIPped structural model after fatigue test (2)

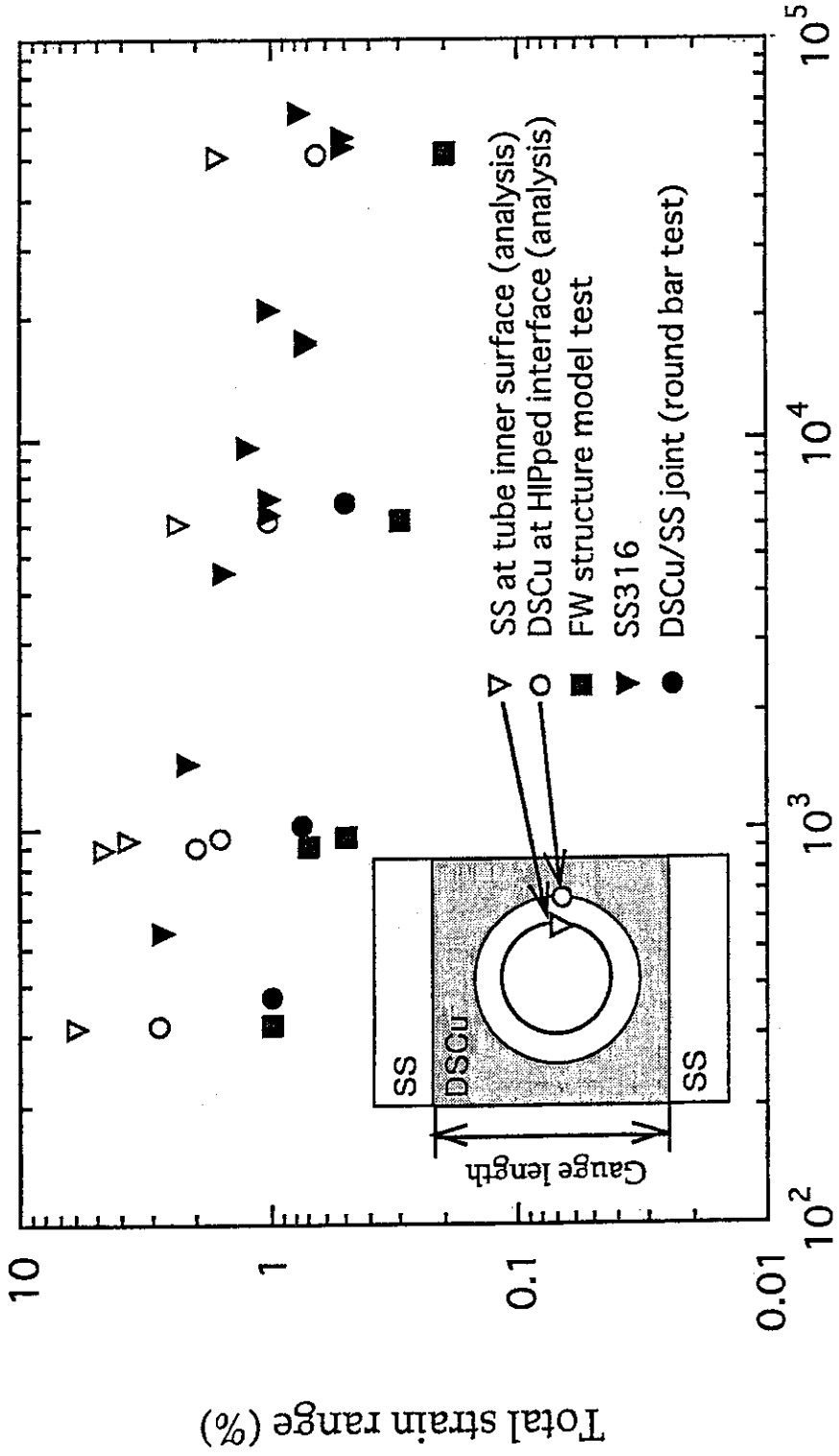

Fig. 3.2.10 Results of analyses and fatigue test

Table 3.1.1 The result of Charpy impact tests

Test Pieace	Impact Value (J/cm^2)
Al-15 Base Metal	167
	167
Al-25 Base Metal	38
	39
	38
SS316L/Al-15 Joint	46
	54.6
	100
	52
SS316L/Al-25 Joint	13
	15
	13

Table 3.2.1 : Result of Low cycle fatigue test

Test piece No.	Total Strain Range (%)	Plastic Strain Range (%)*1	Elastic Strain Range (%)*1	Total Stress Range (MPa) *1	Maximum Stress (MPa) *1	Minimum Stress (MPa) *1	Failure cycles Nf*2	Failure location
1	0.98	0.376	0.604	609	297	-312	320	inner surface*3
2	0.684	0.300	0.384	649	322	-327	900	same
3	0.500	0.152	0.348	562	270	-292	950	same
4	0.290	0.040	0.250	427	208	-219	6100	same
5	0.198	0.020	0.178	322	156	-166	51200	same

*1: Value is defined at the 1/2Nf

*2 : Nf is defined to be the number of cycle at 25% reduction of the maximum load

*3 : inner surface of SS-pipe (or HIP bonding boundary of Cu) at the angle of 90° or 270° against the load direction

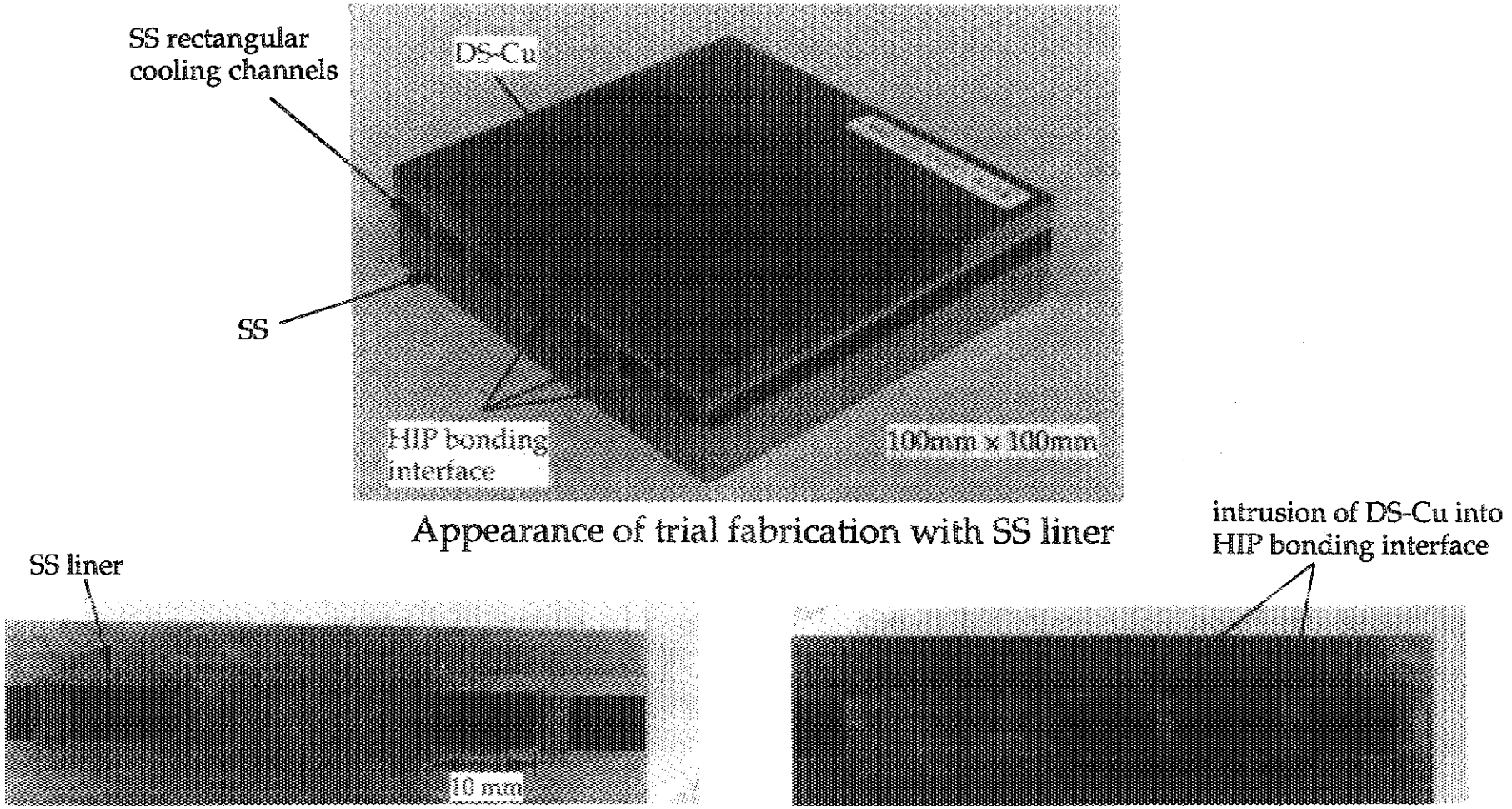

Fig. 4.1 Appearance and Close-up view of trial fabrications

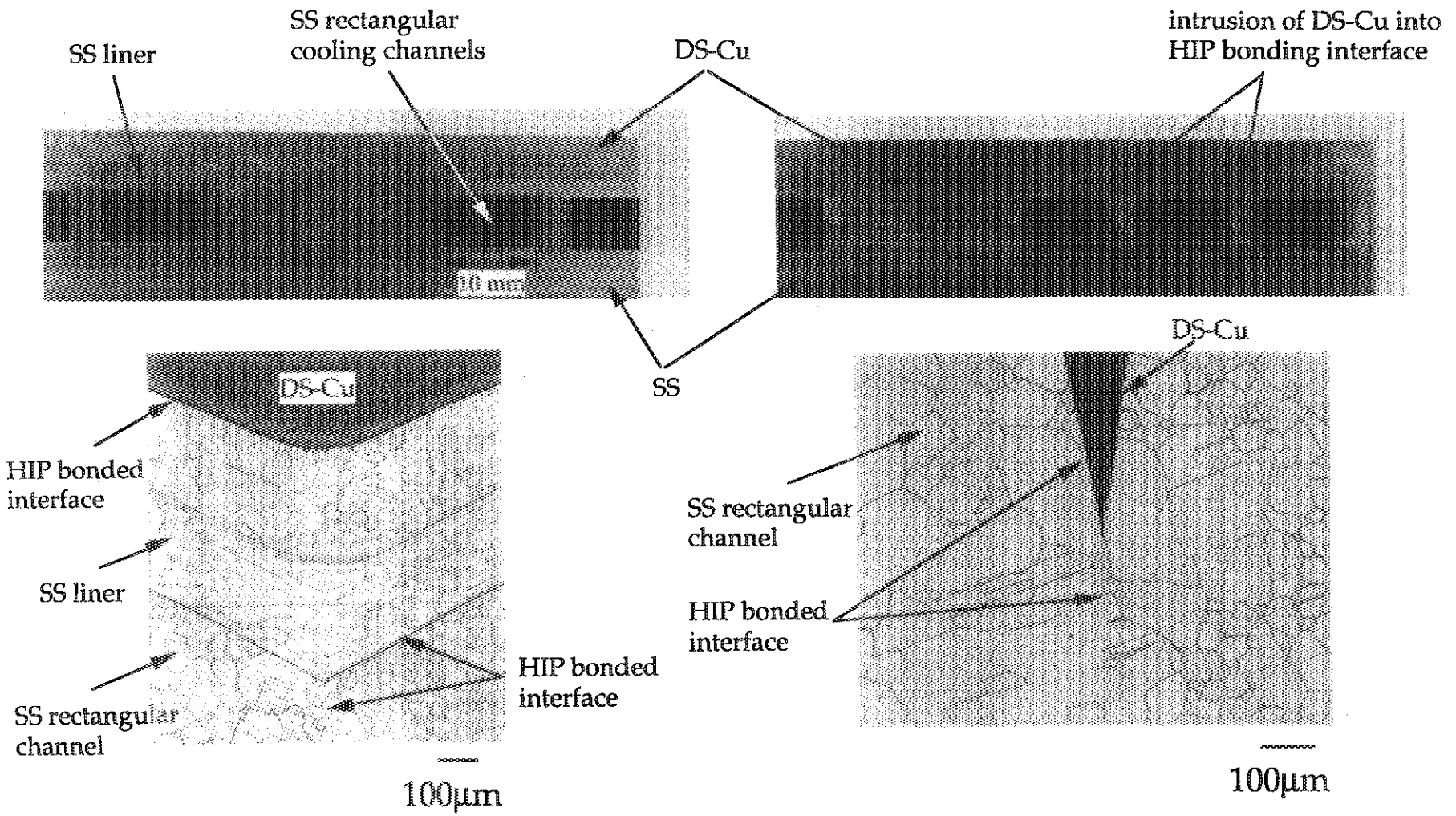

Fig. 4.2 Micro-photographs of trial HIPped fabrications

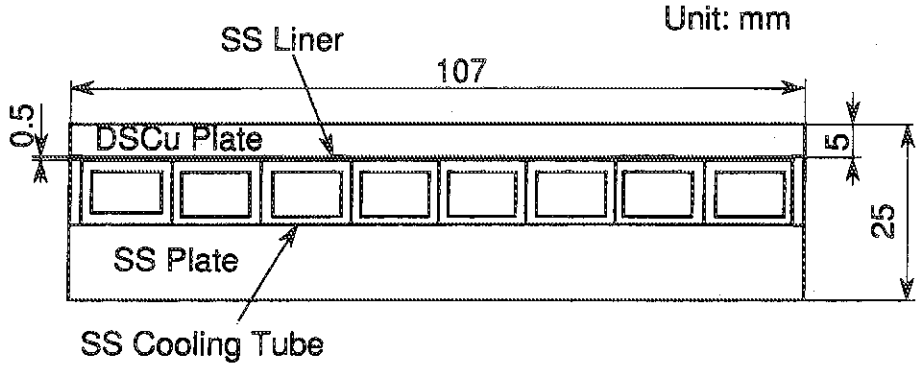

A-A cross section

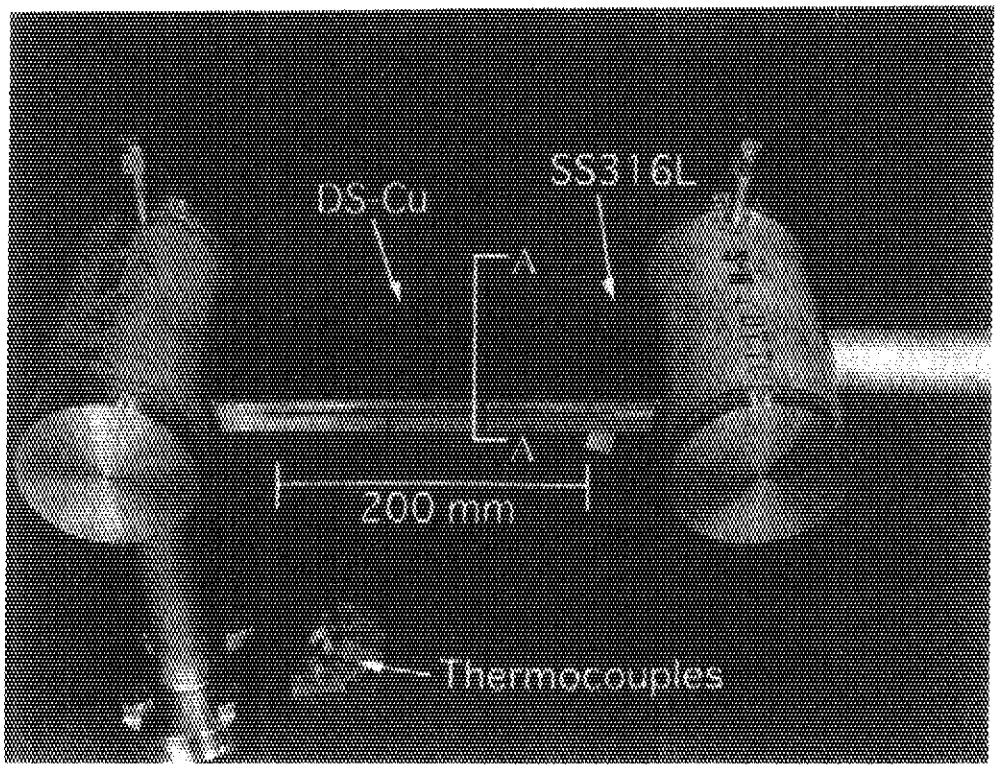

Fig. 4.3 300 mm long HIPped first wall mock-up

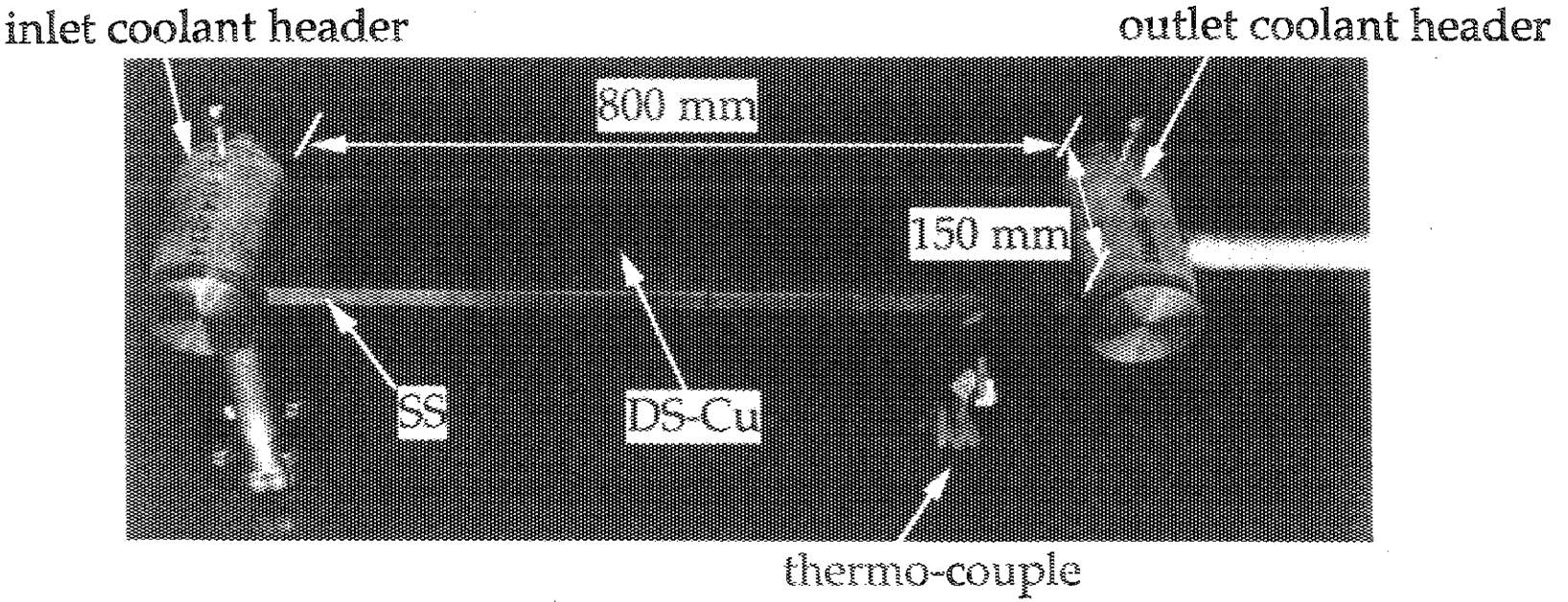

Fig. 4.4 Completed 800 mm longe mock-up of HIPped first wall

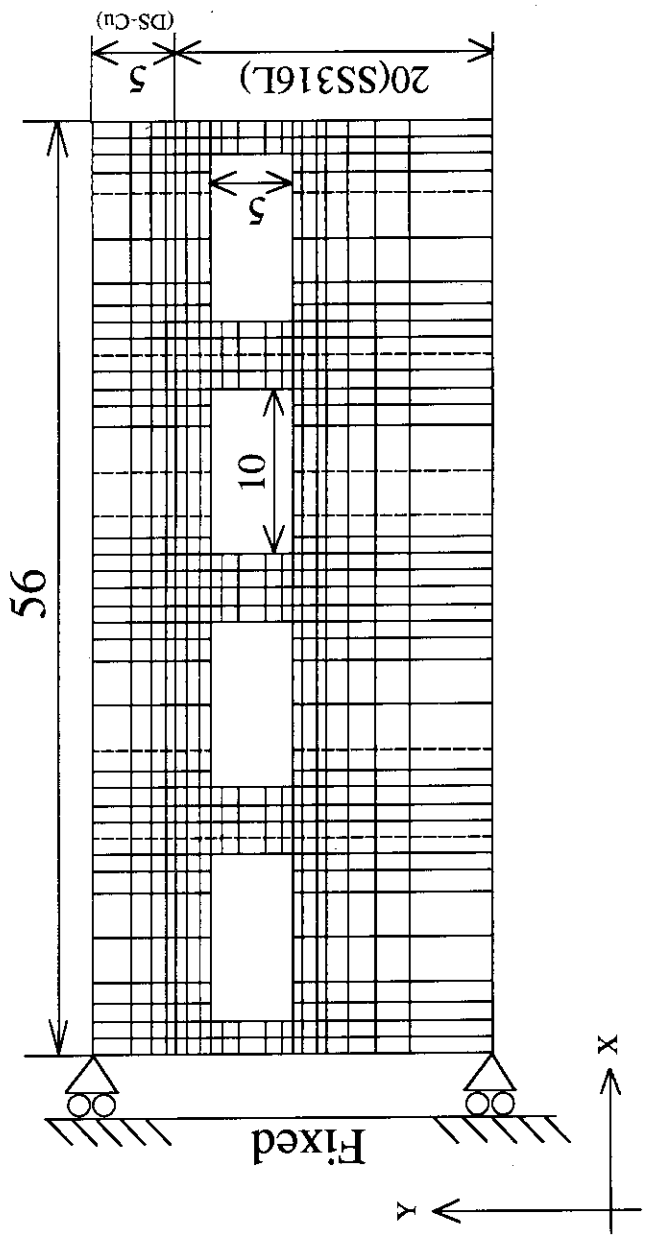

Fig. 5.1 Analysis model

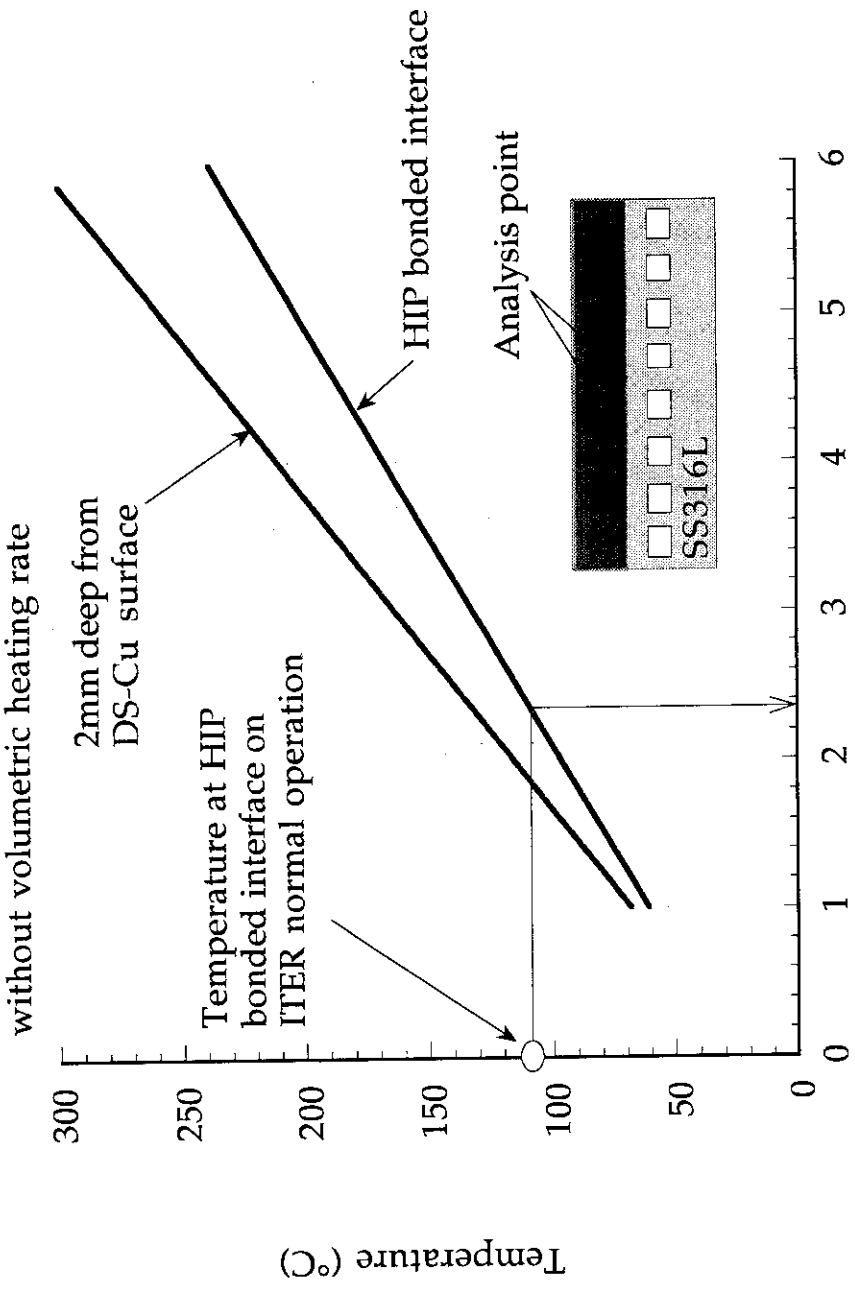

Fig. 5.2 Temperature analytical results

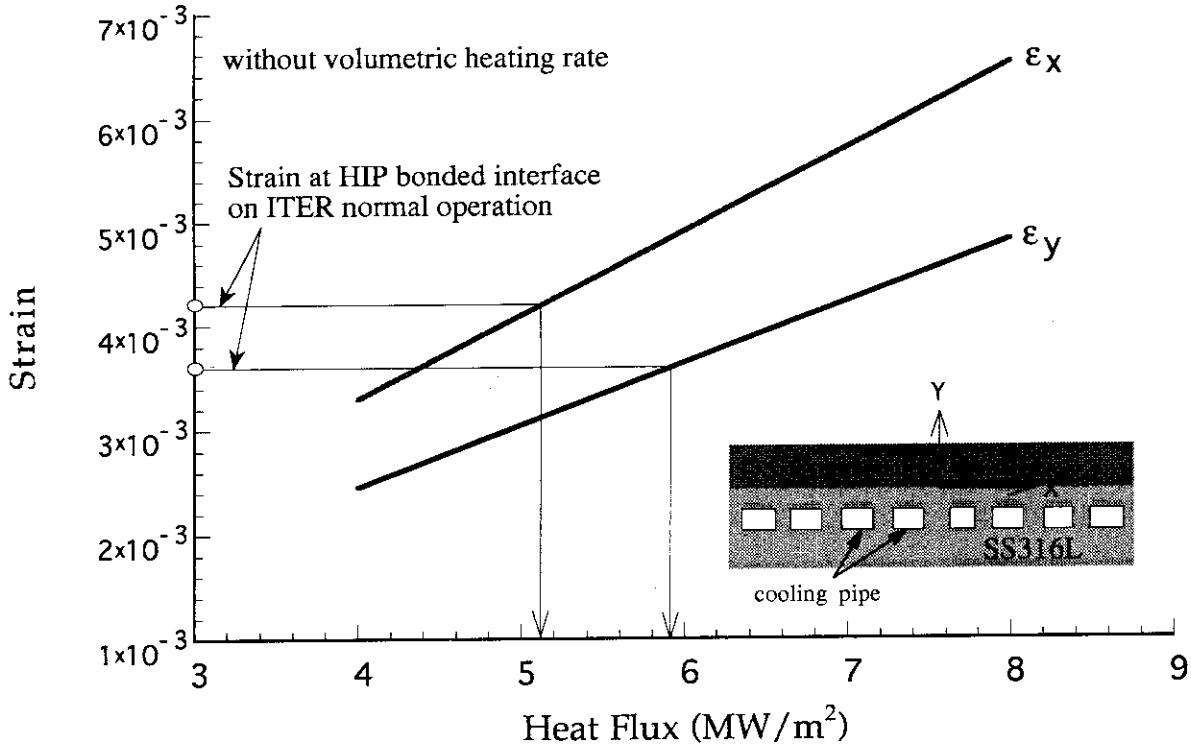

Fig. 5.3 Strain Analytical Result

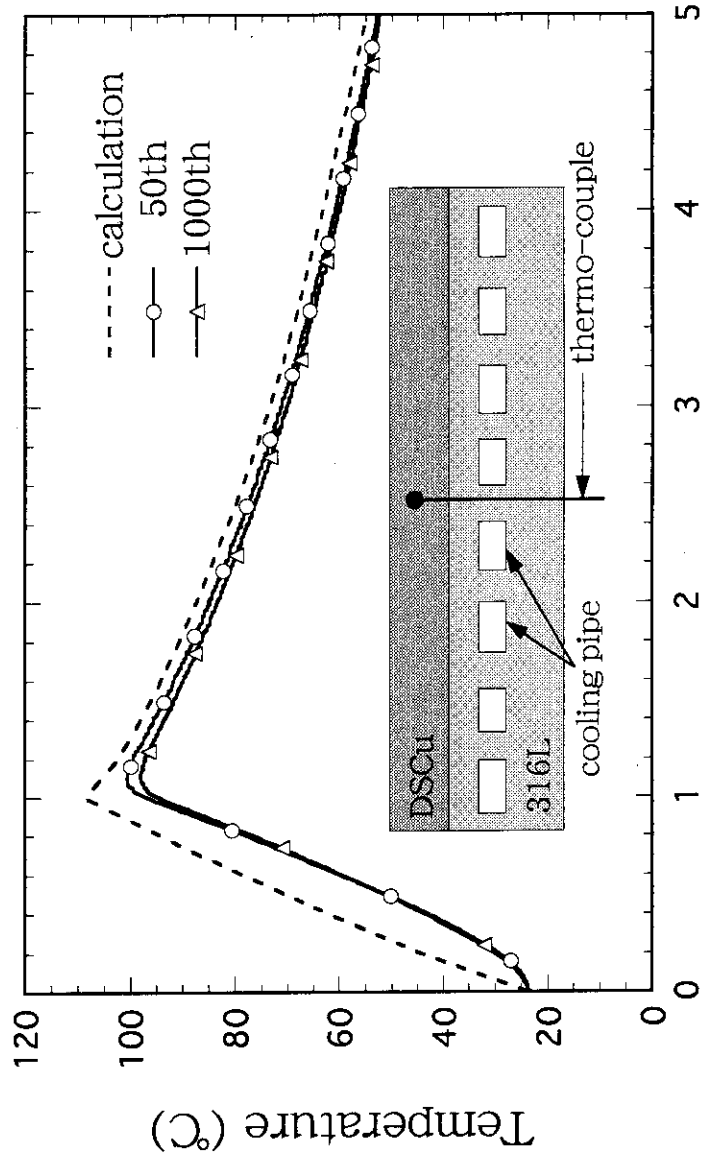

Fig. 5.4 Typical temperature responses under heat flux of 2.0MW/m^2

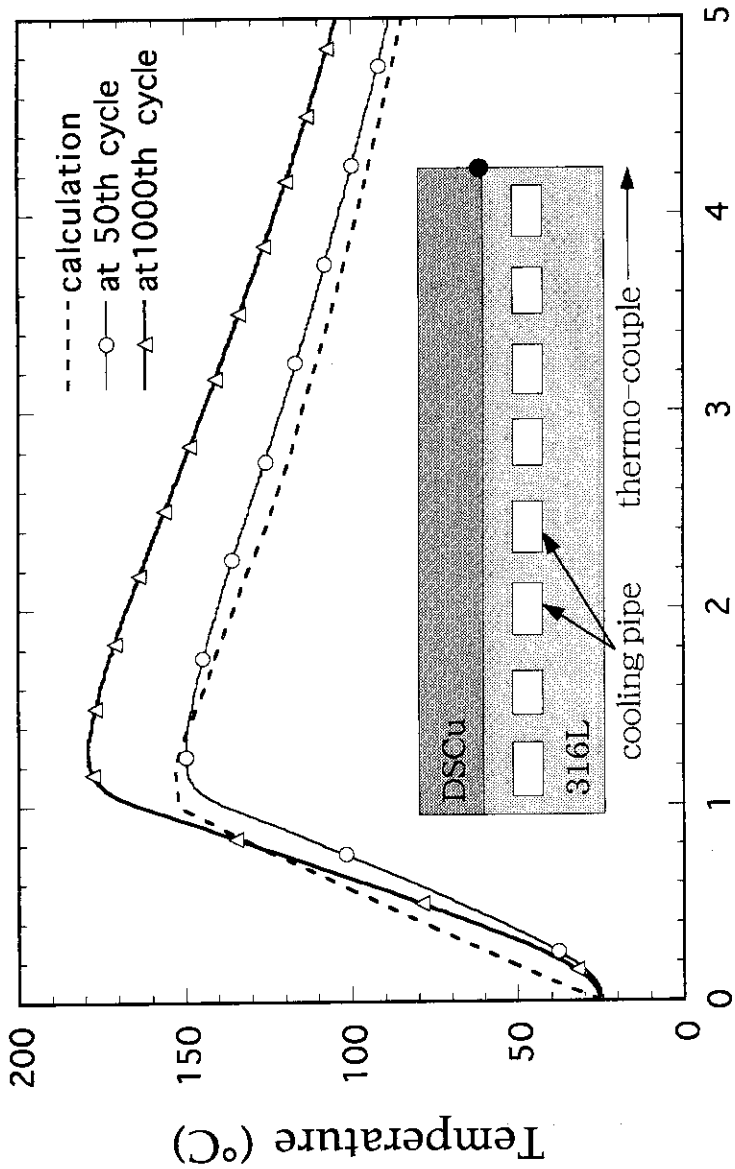

Fig. 5.5 Typical temperature responses under heat flux of 5.0 MW/m^2

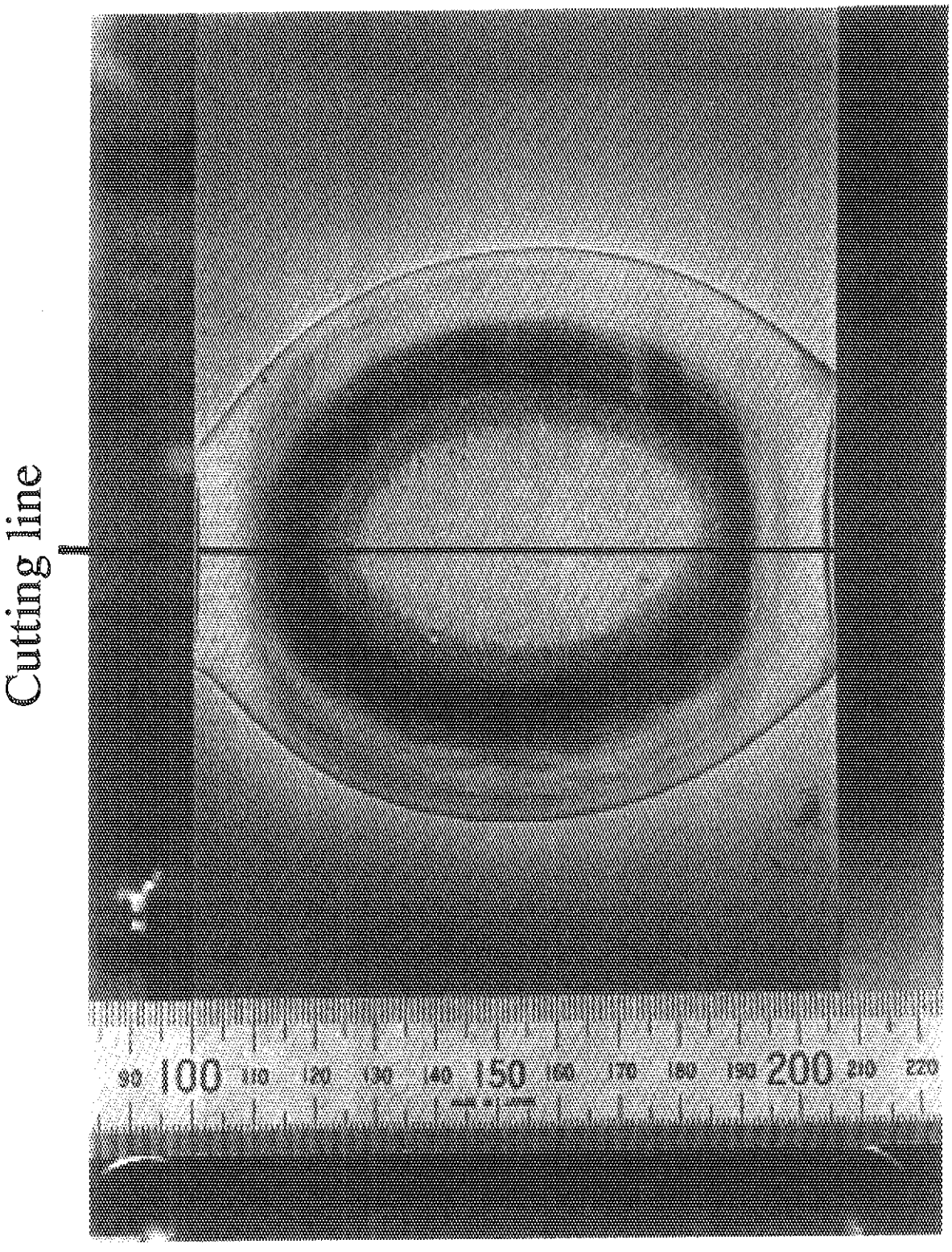

Fig. 5.6 Surface after high heat flux testing

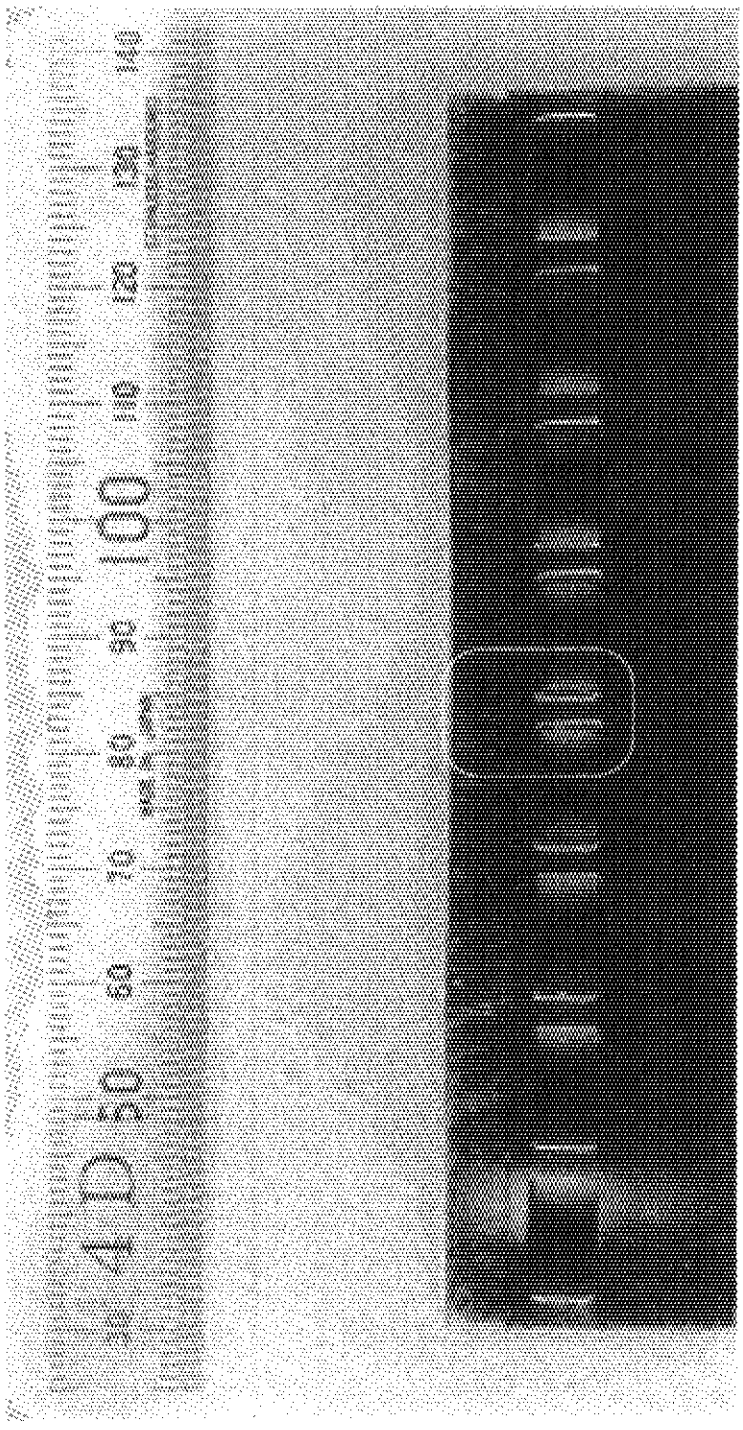

Fig. 5.7 Cross section under heat flux center

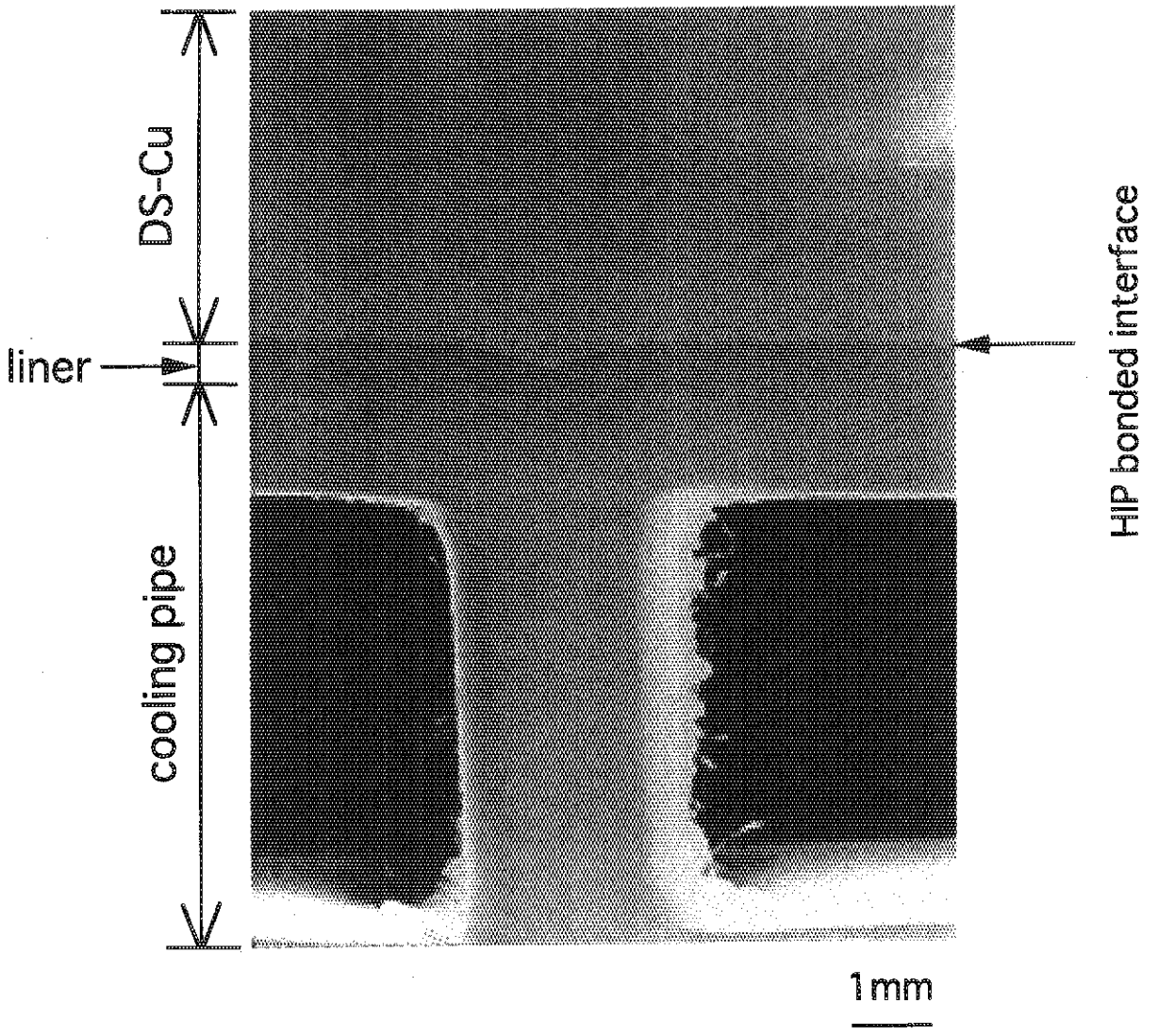

Fig. 5.8 HIP bonded DS-Cu/SS316L interface by SEM

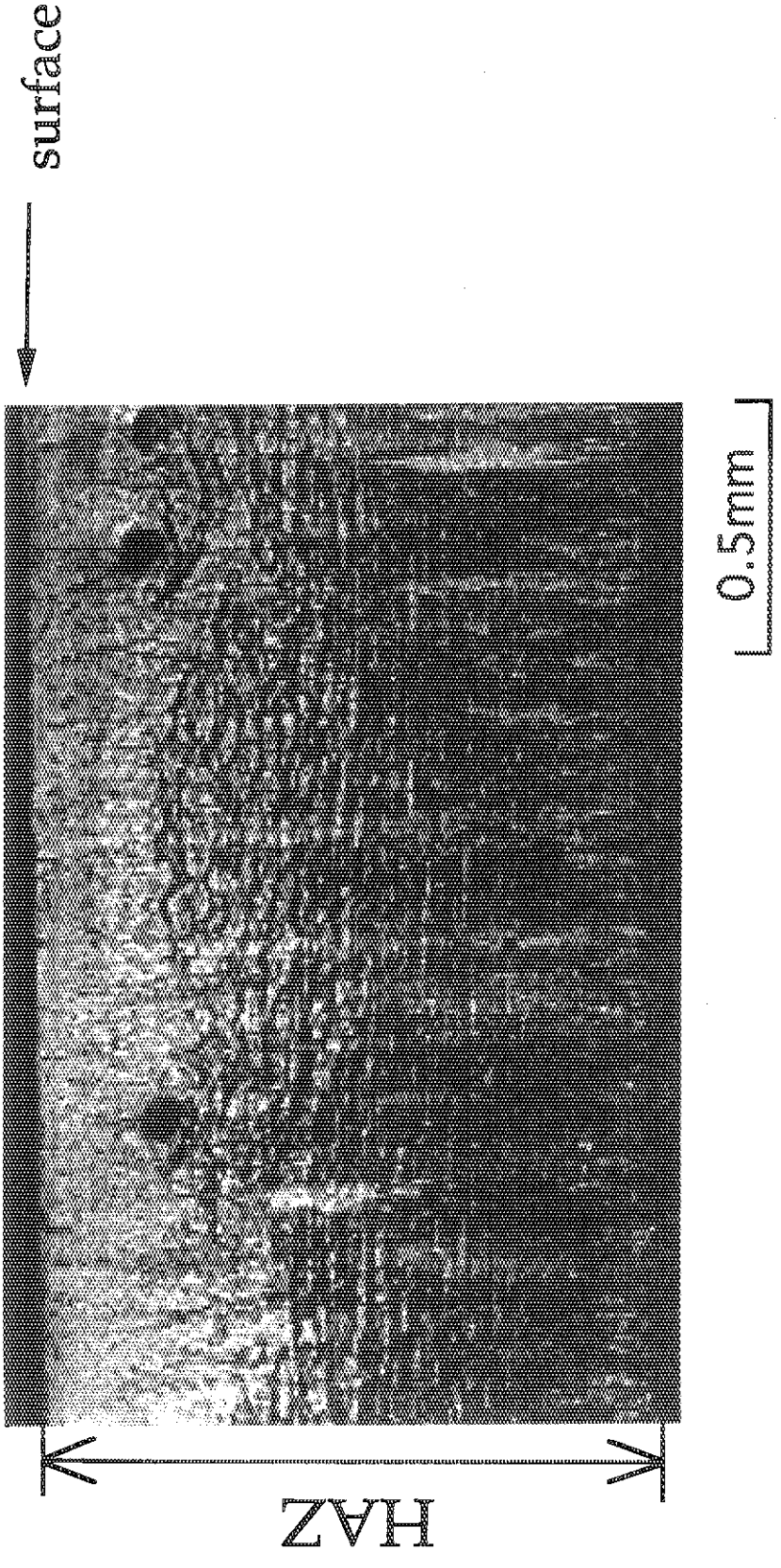

Fig. 5.9 DS-Cu under heat flux center

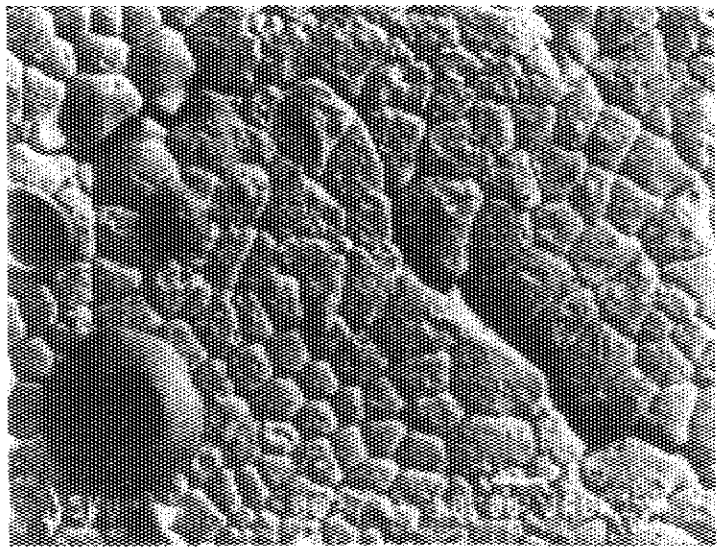

Fig. 5.10 SEM image of DSCu surface at the beam center

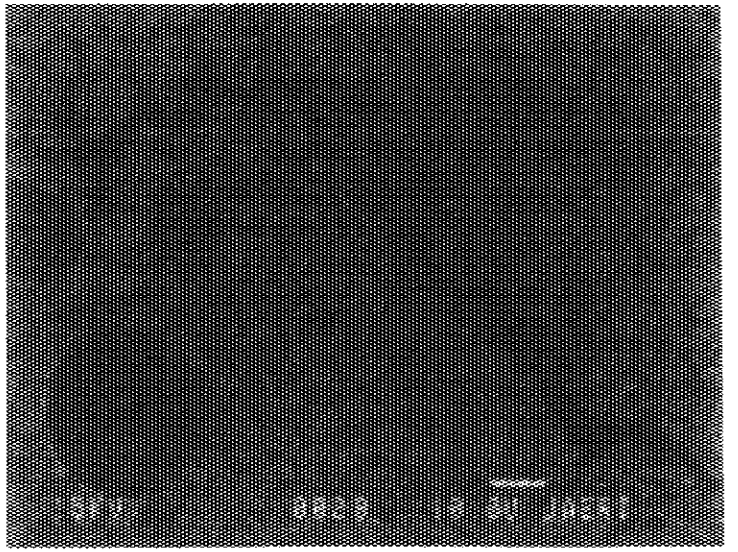

Fig. 5.11 COMP image of DSCu surface at the beam center

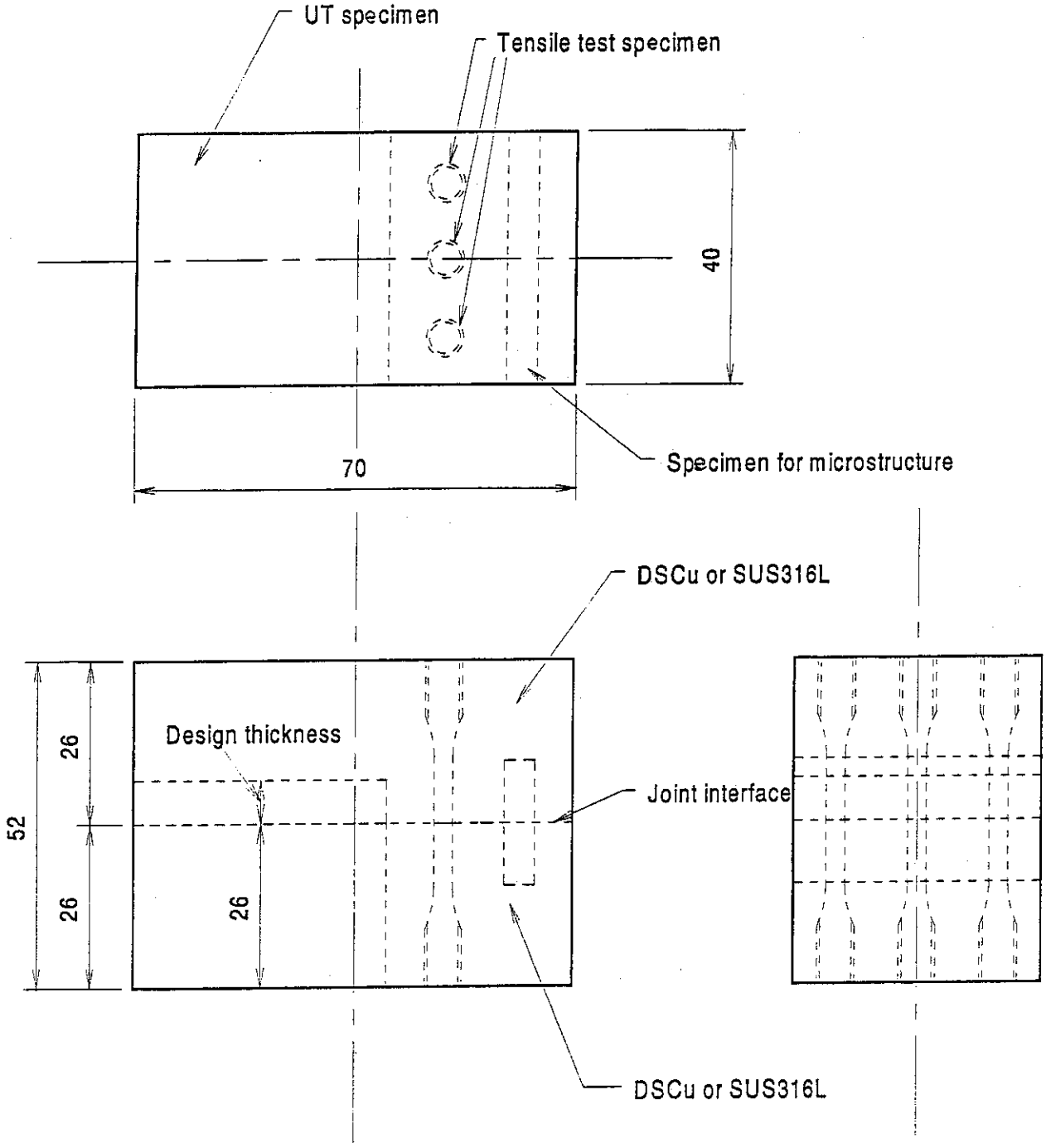

Fig. 6.1 Collected location of specimen used

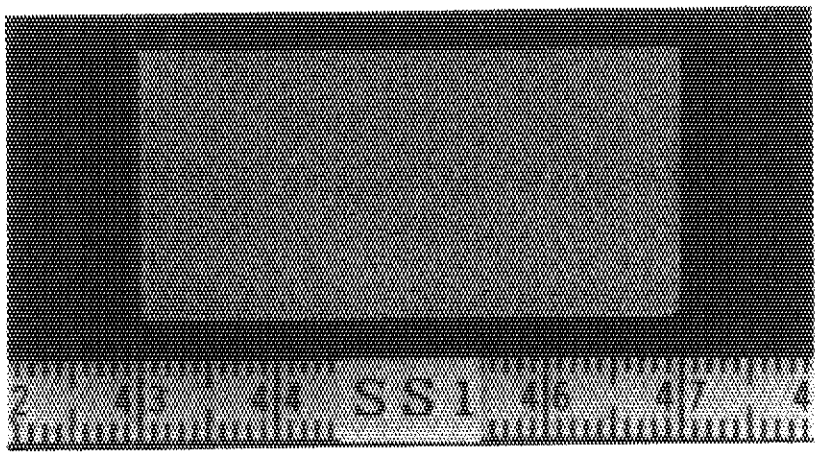

SS316L/SS316L (Rz : 41 μm)

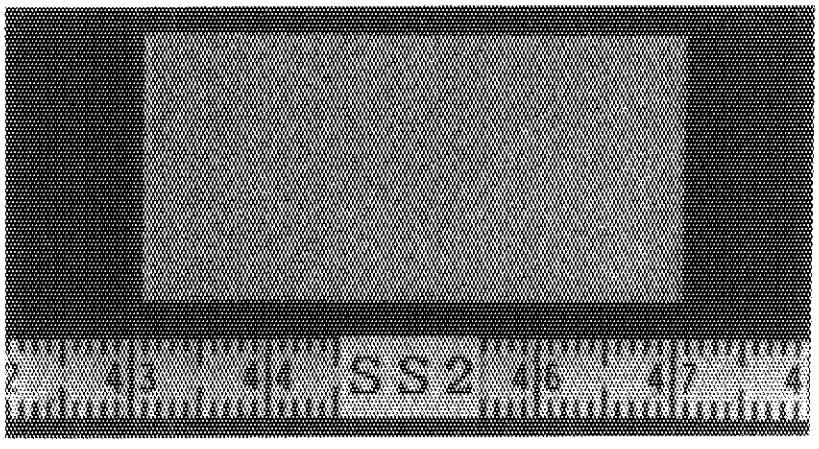

SS316L/SS316L (Rz : 11.4 μm)

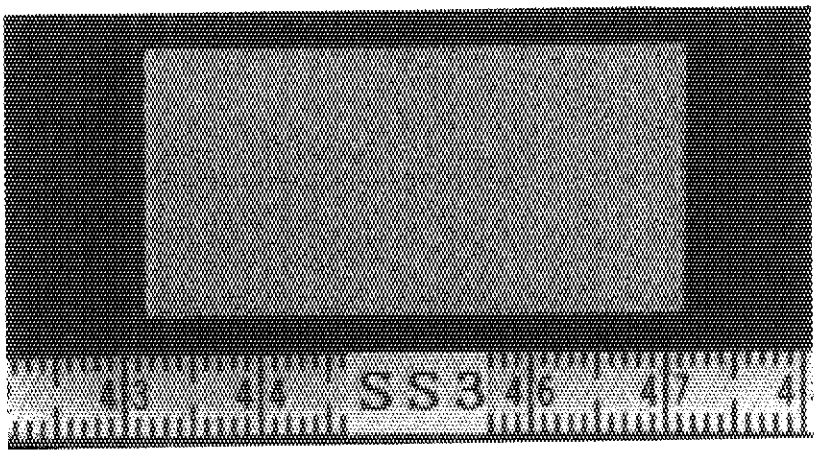

SS316L/SS316L (Rz : 1.3 μm)

Fig. 6.2 Macrostructure of joint (SS316L/SS316L)

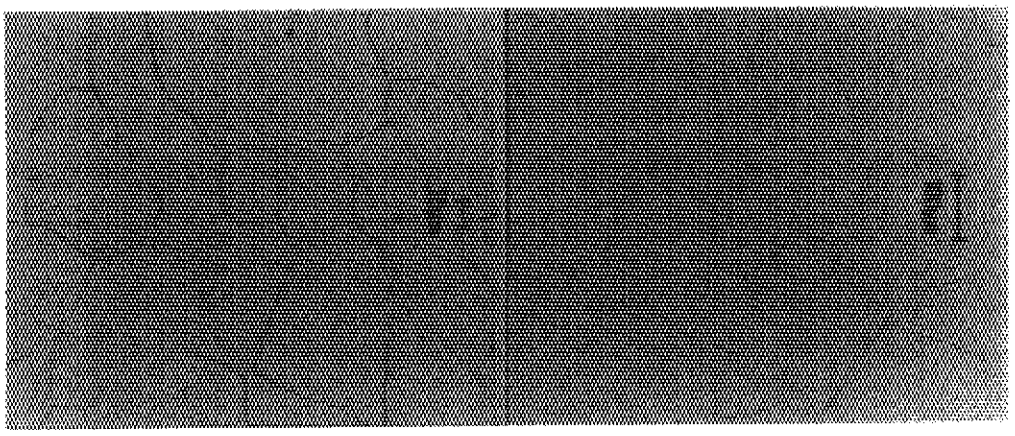

SS316L/SS316L (Rz : 41 μm)

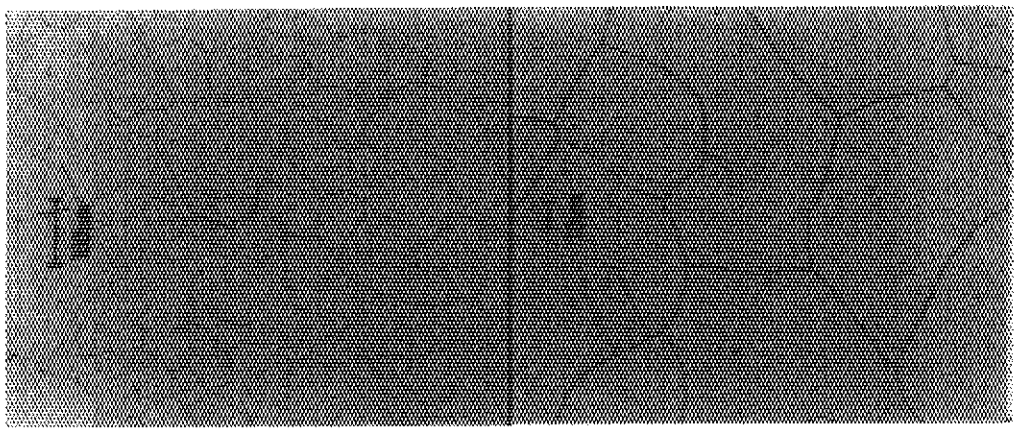

SS316L/SS316L (Rz : 11.4 μm)

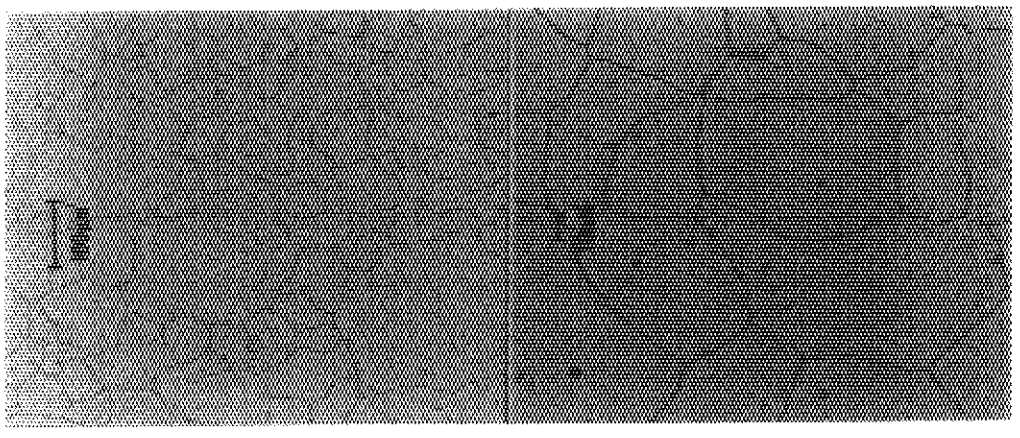

SS316L/SS316L (Rz : 1.3 μm)

Fig. 6.3 Microstructure of joint (SS316L/SS316L)

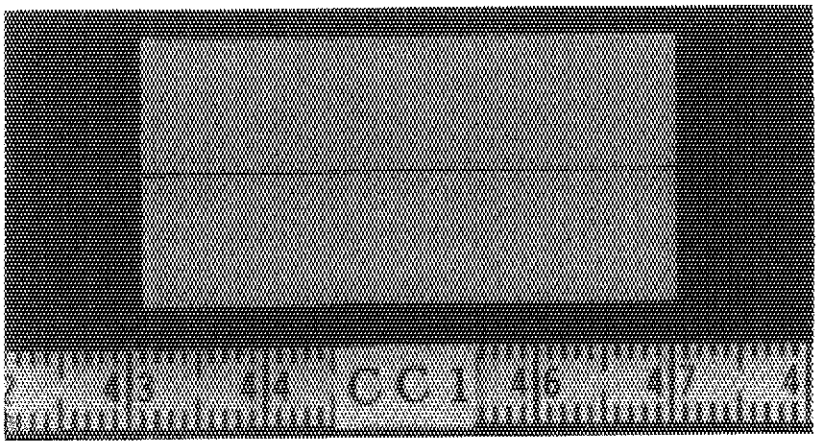

DSCu/DSCu (Rz : 43 μm)

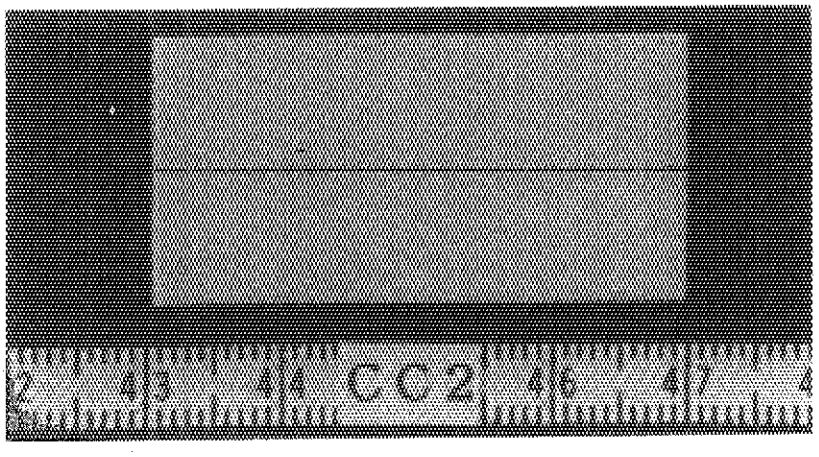

DSCu/DSCu (Rz : 11.9 μm)

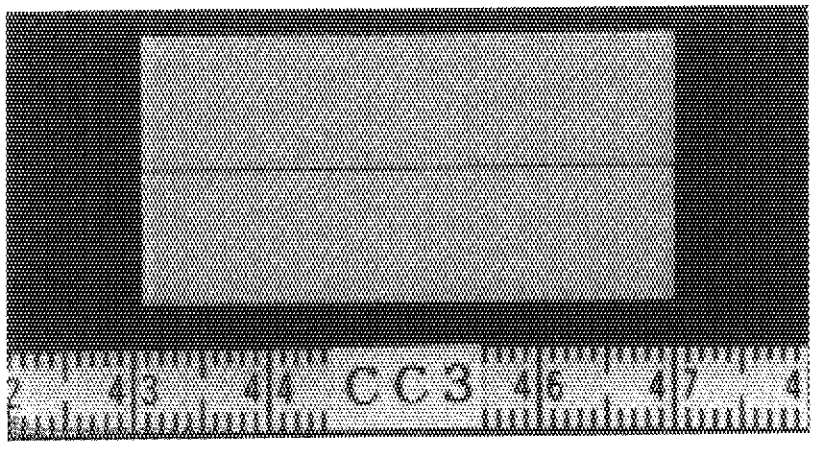

DSCu/DSCu (Rz : 1.5 μm)

Fig. 6.4 Macrostructure of joint (DSCu/DSCu)

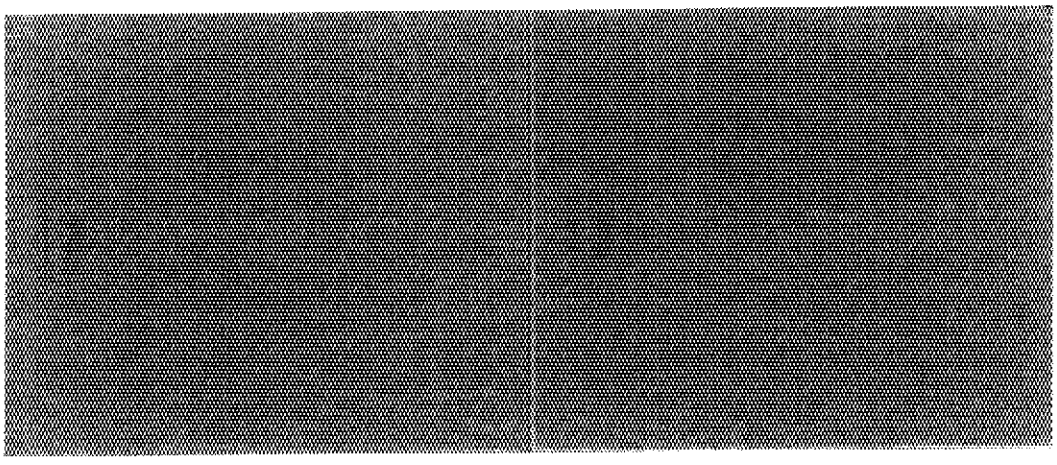

DSCu/DSCu (Rz : 43 μm)

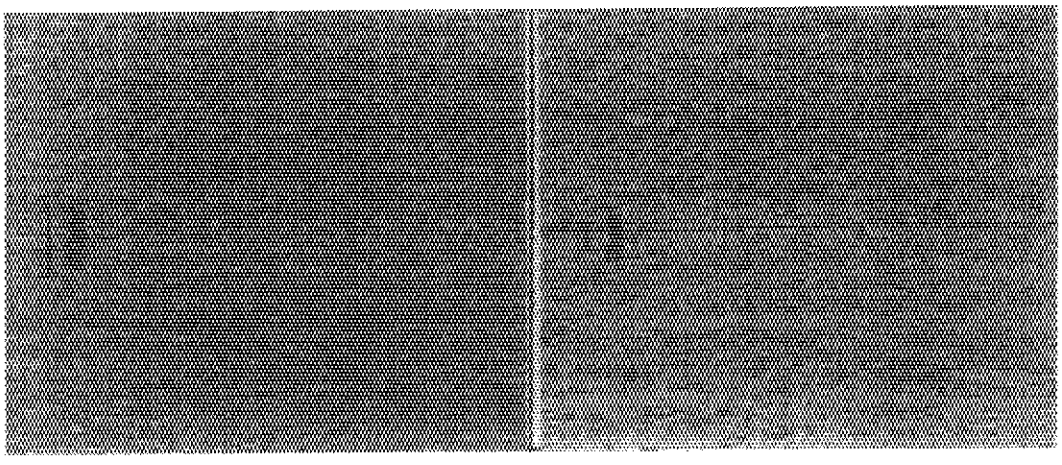

DSCu/DSCu (Rz : 11.9 μm)

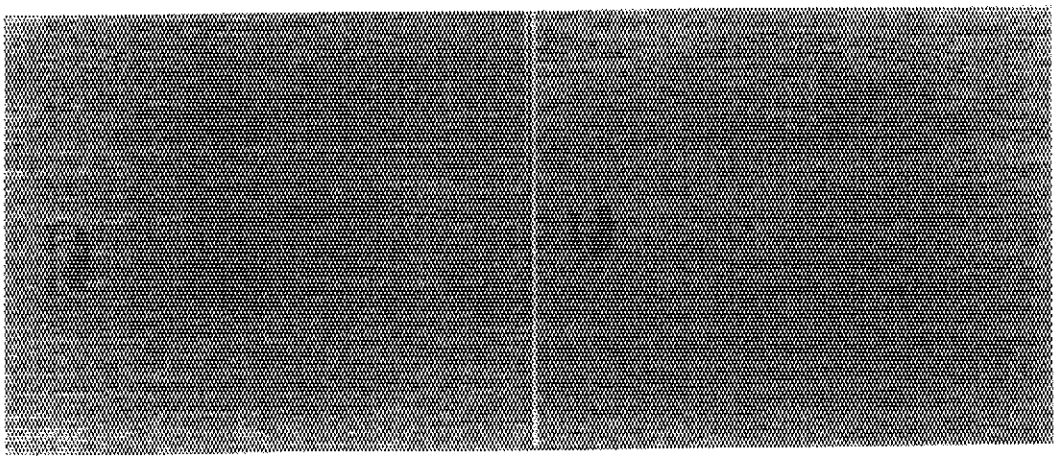

DSCu/DSCu (Rz : 1.5 μm)

Fig. 6.5 Microstructure of joint (DSCu/DSCu)

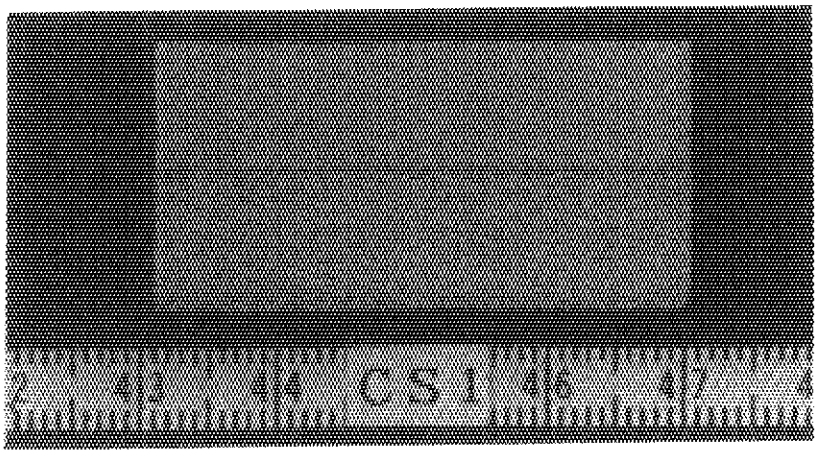

DSCu/SS316L (Rz : 41 μm)

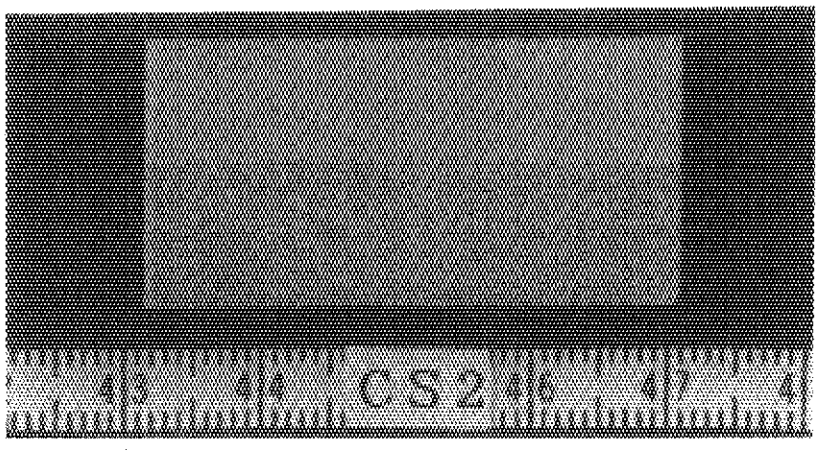

DSCu/SS316L (Rz : 11.7 μm)

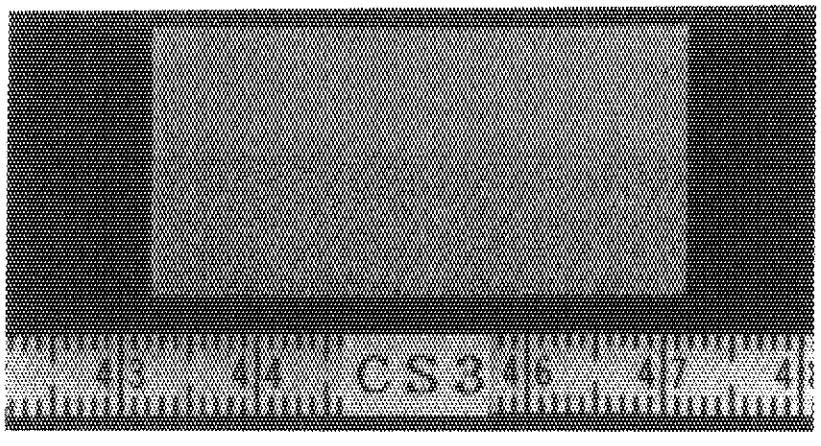

DSCu/SS316L (Rz : 1.5 μm)

Fig. 6.6 Macrostructure of joint (DSCu/SS316L)

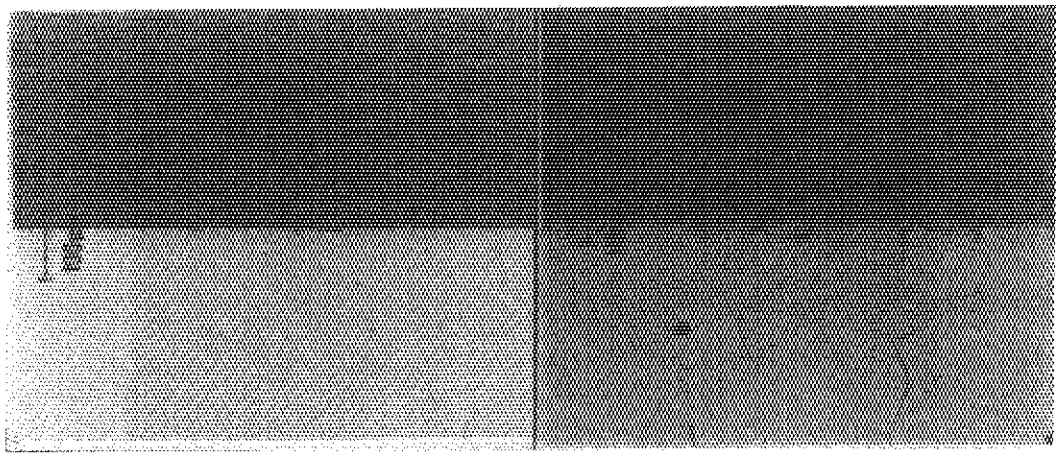

DSCu/SS316L (Rz : 41 μm)

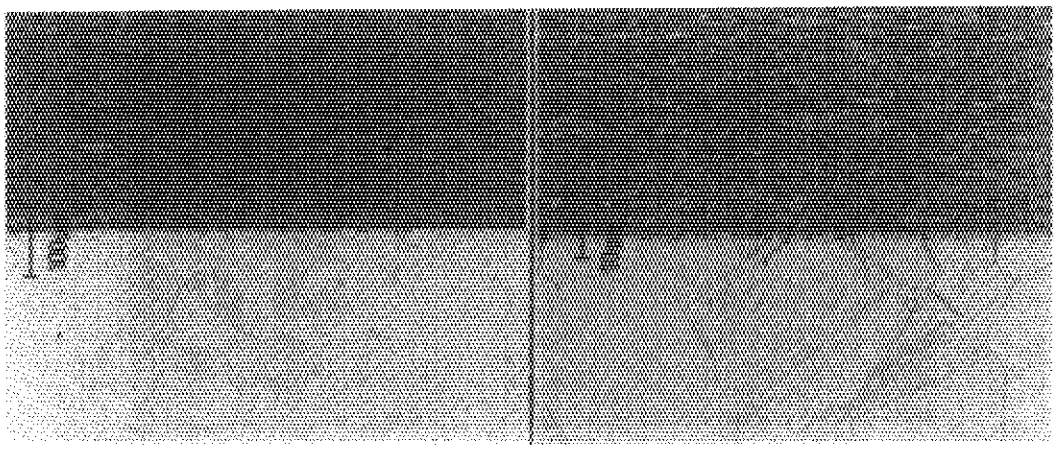

DSCu/SS316L (Rz : 11.7 μm)

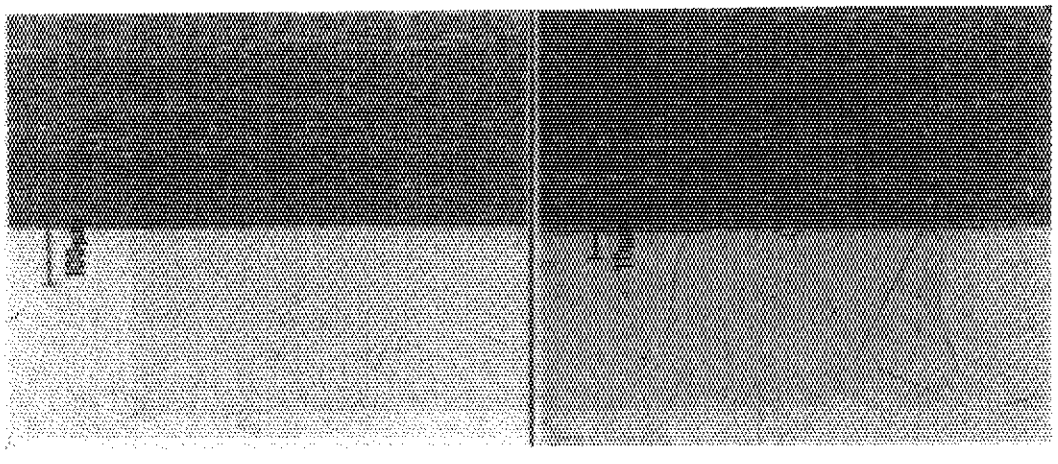

DSCu/SS316L (Rz : 1.5 μm)

Fig. 6.7 Microstructure of joint (DSCu/SS316L)

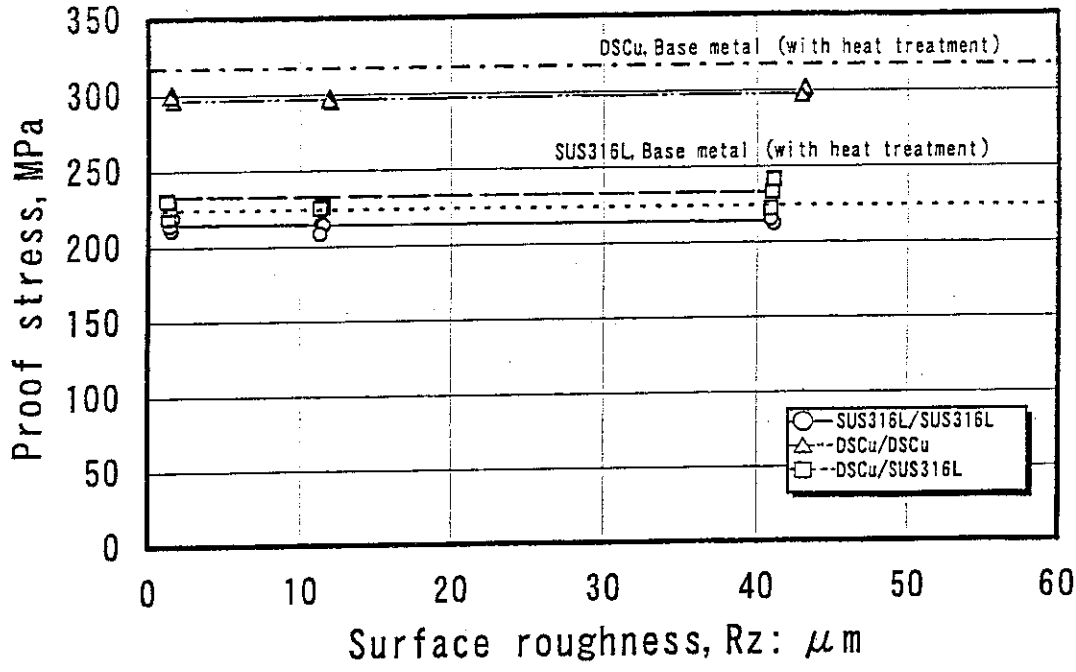

Fig. 6.8 Relationship between surface roughness and proof stress

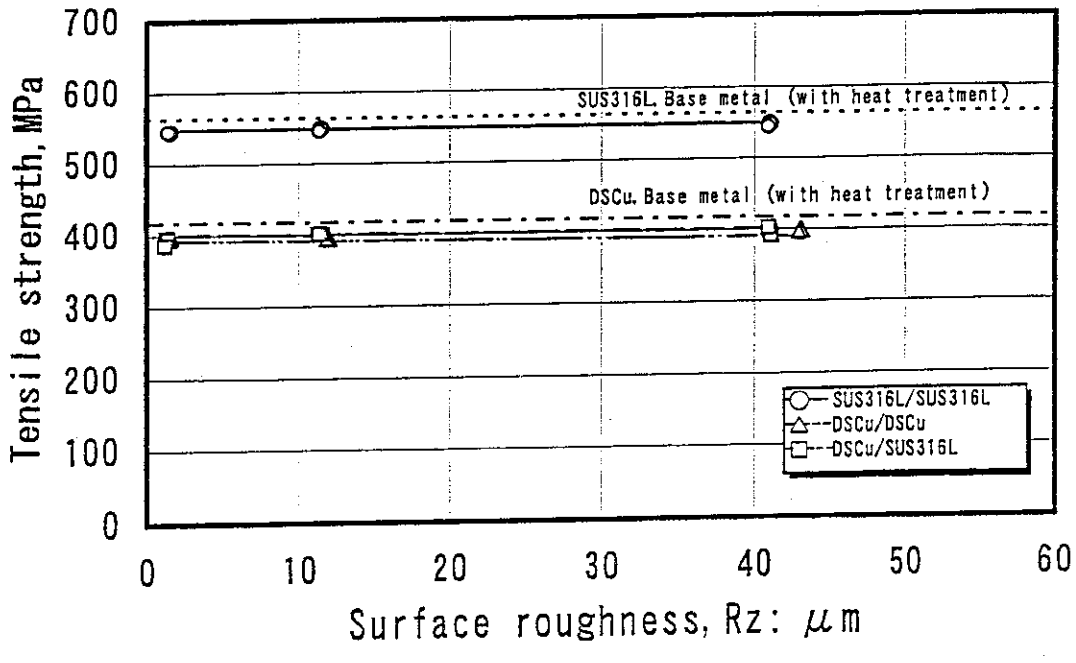

Fig. 6.9 Relationship between surface roughness and tensile stength

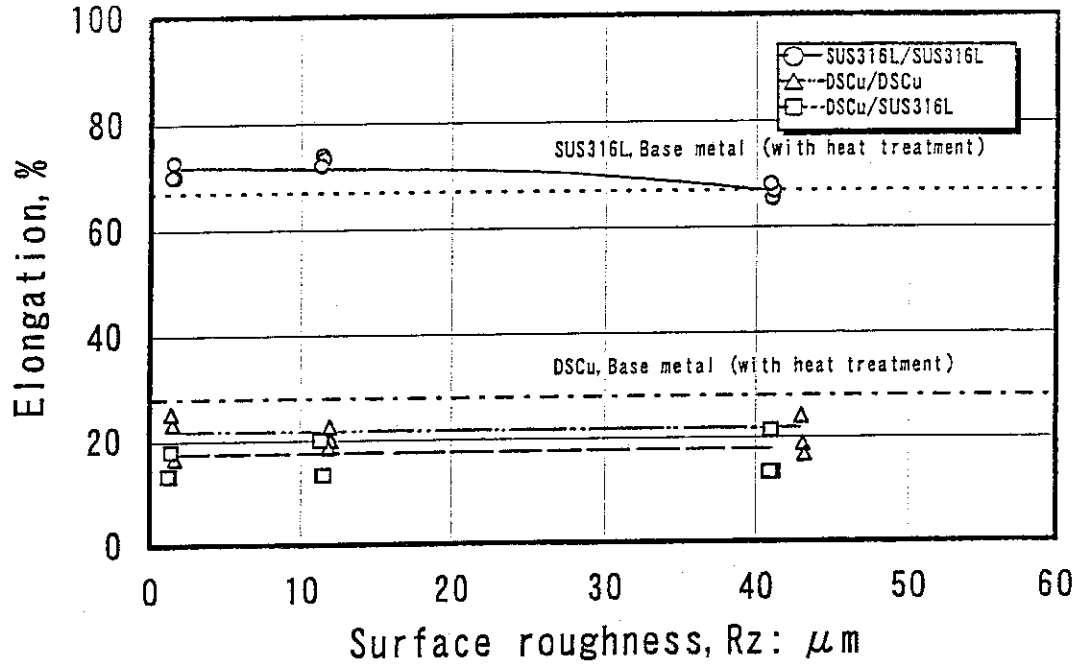

Fig. 6.10 Relationship between surface roughness and elongation

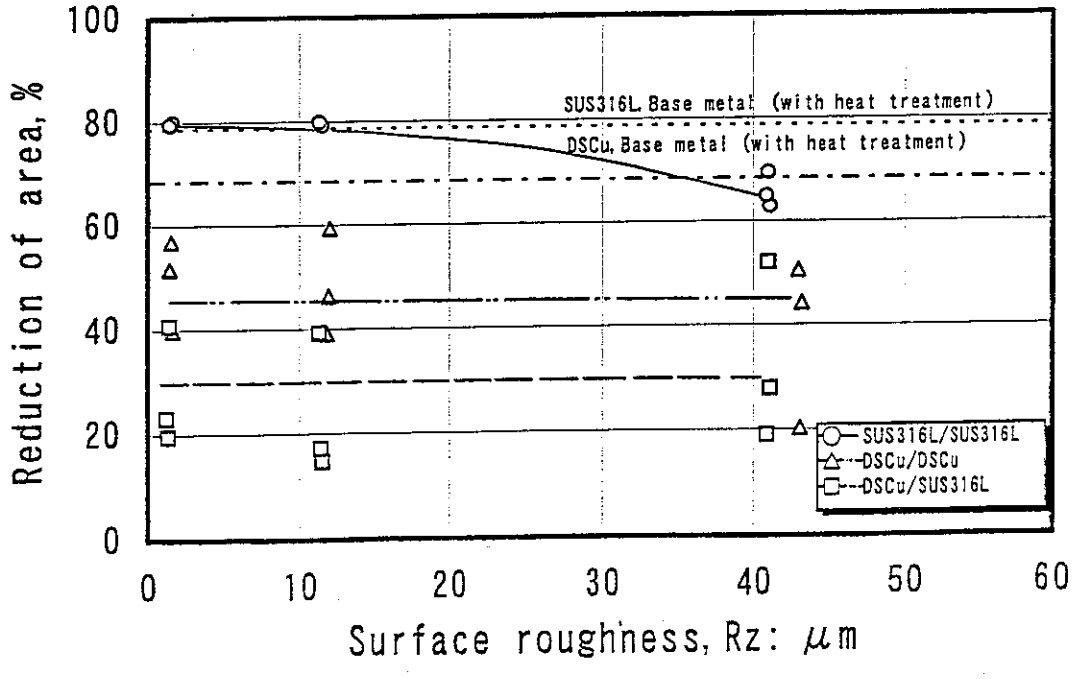

Fig. 6.11 Relationship between surface roughness and reduction of area

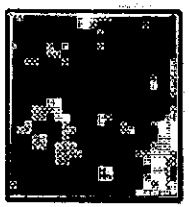

SS316L/SS316L
Rz : 41 μm

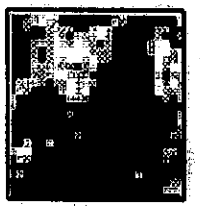

SS316L/SS316L
Rz : 11.4 μm

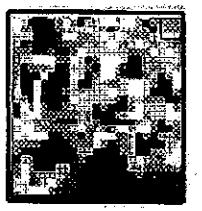

SS316L/SS316L
Rz : 1.3 μm

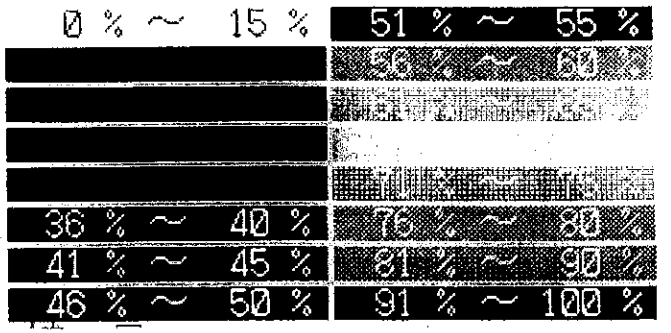

Sensitivity : wide plane + 48 dB

Fig. 6.12 Example of UT result (SS316L/SS316L) [5 MHz]

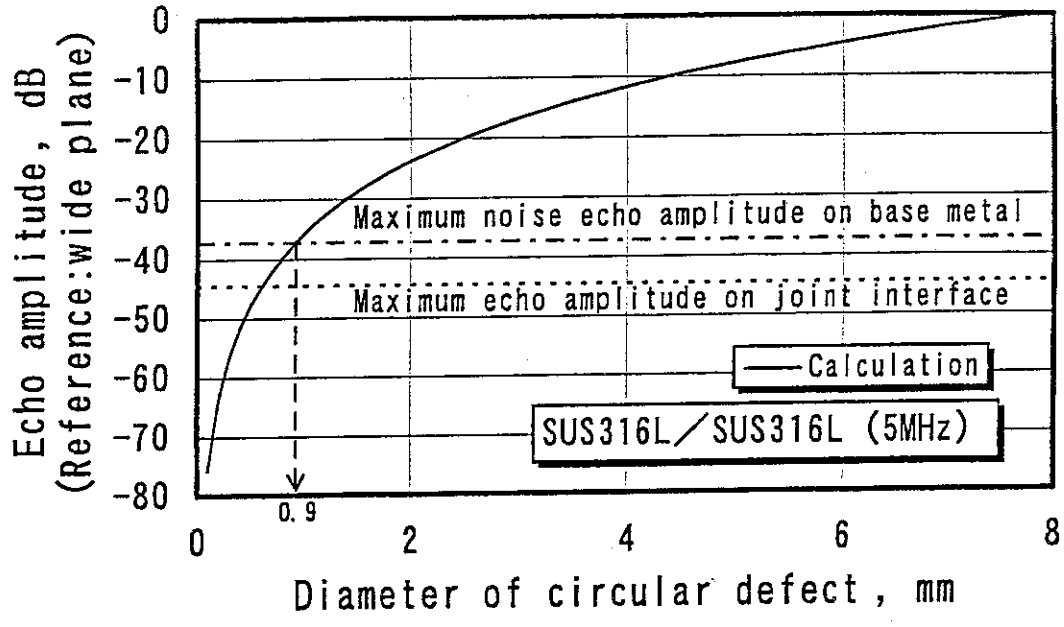

Fig. 6.13 Estimationof detectable defect size (SS316L/SS316L, 5 Mhz)

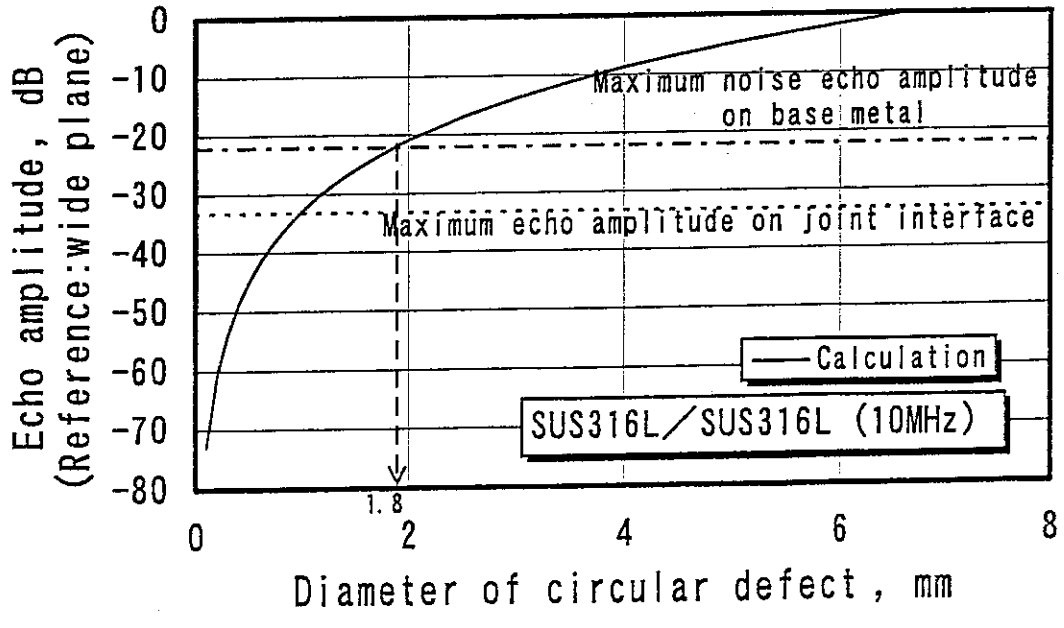

Fig. 6.14 Estimationof detectable defect size (SS316L/SS316L, 10 Mhz)

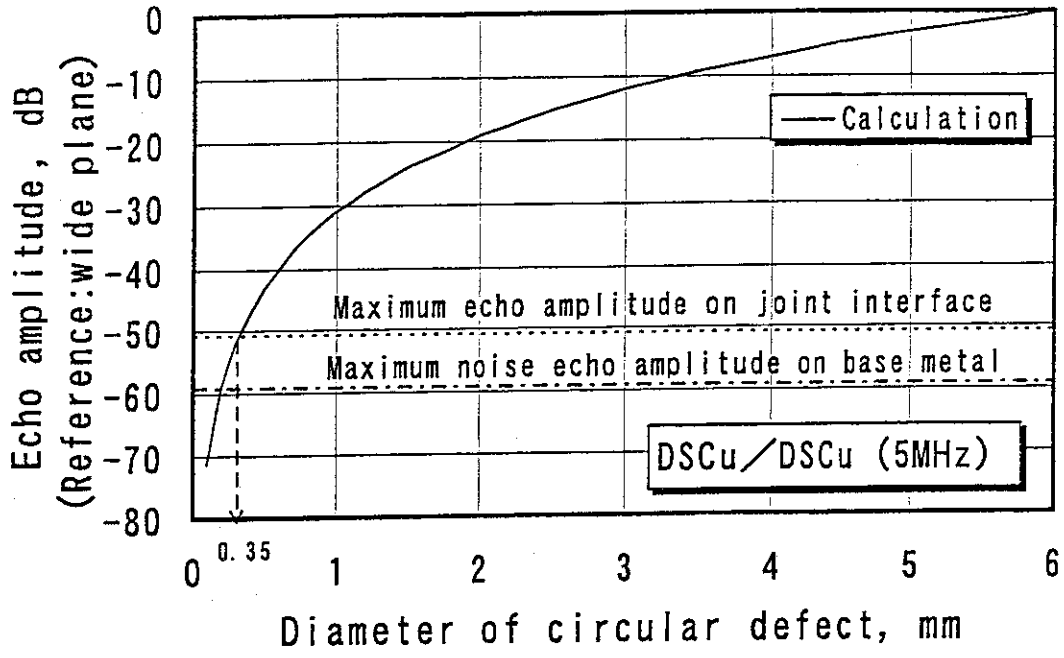

Fig. 6.15 Estimationof detectable defect size (DSCu/DSCu, 5 Mhz)

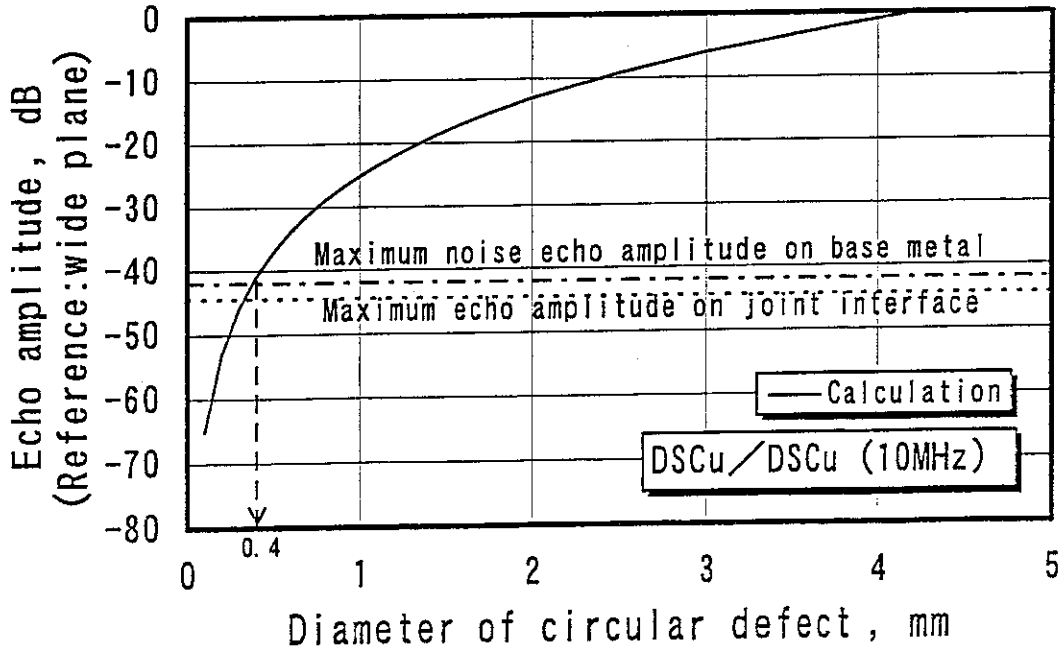

Fig. 6.16 Estimationof detectable defect size (DSCu/DSCu, 10 Mhz)

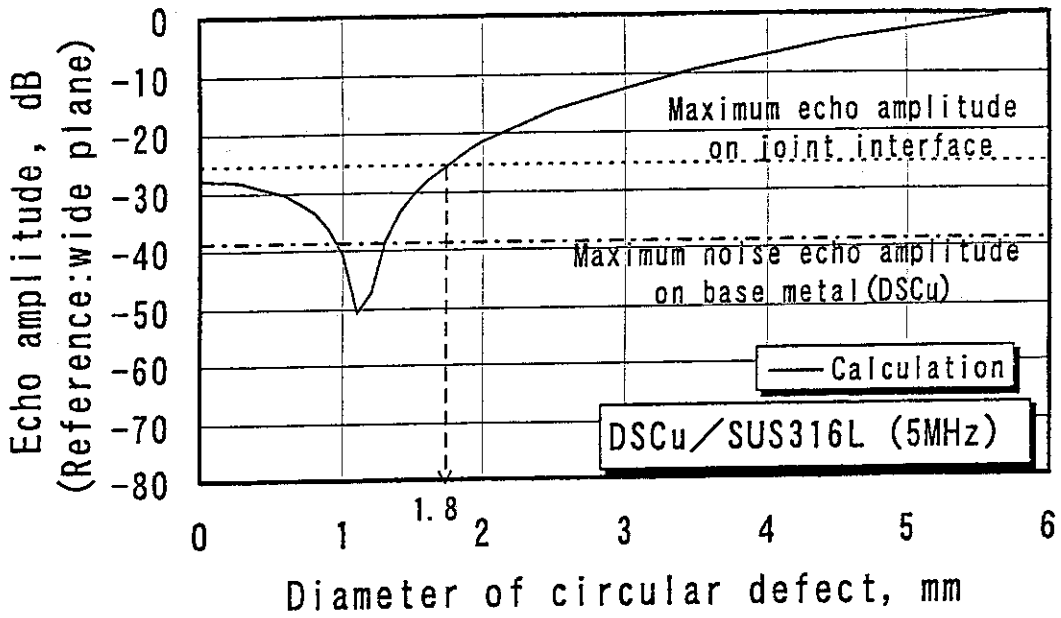

Fig. 6.17 Estimationof detectable defect size (DSCu/SS316L, 5 Mhz)

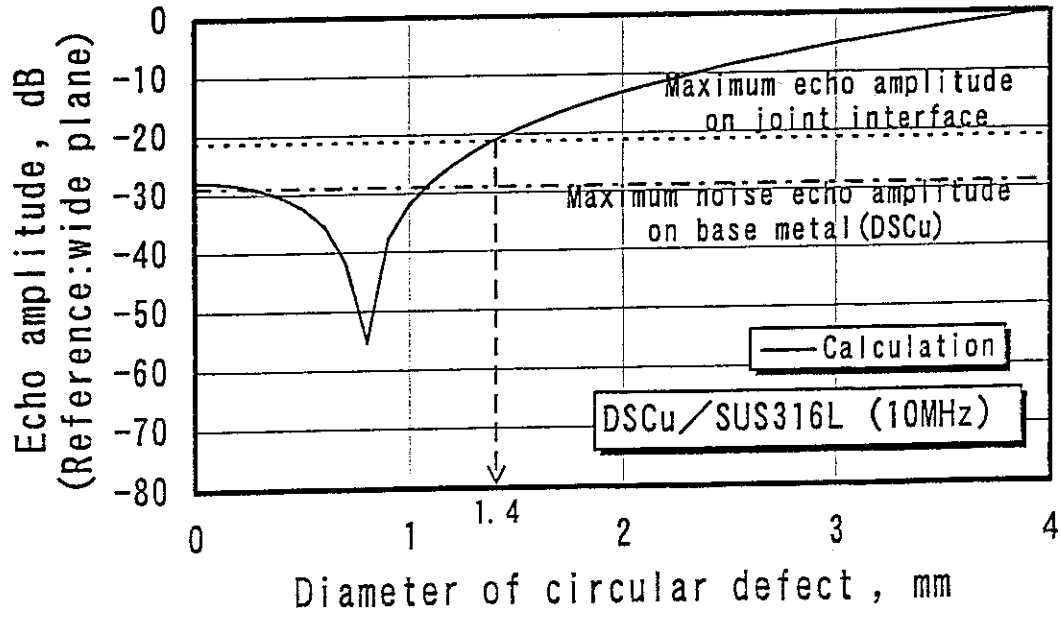

Fig. 6.18 Estimationof detectable defect size (DSCu/SS316L, 10 Mhz)

Table 6.1 Surface roughness

Joint	No.	Material	Surface roughness Rz, μ m	
			Each value	Mean
SUS316L/ SUS316L	1	SUS316L	42	41
		SUS316L	40	
	2	SUS316L	11.6	11.4
		SUS316L	11.2	
	3	SUS316L	1.2	1.3
		SUS316L	1.4	
DSCu/ DSCu	1	DSCu	44	43
		DSCu	42	
	2	DSCu	11.8	11.9
		DSCu	12.0	
	3	DSCu	1.4	1.5
		DSCu	1.6	
DSCu/ SUS316L	1	DSCu	42	41
		SUS316L	40	
	2	DSCu	12.2	11.7
		SUS316L	11.2	
	3	DSCu	1.4	1.5
		SUS316L	1.6	